BJBS

June 2025

# Dermatopathology and Associated Laboratory Investigations in the Study of Skin Disease


Issue Editor

Guy Edward Orchard

Synnovis Analytics,
United Kingdom


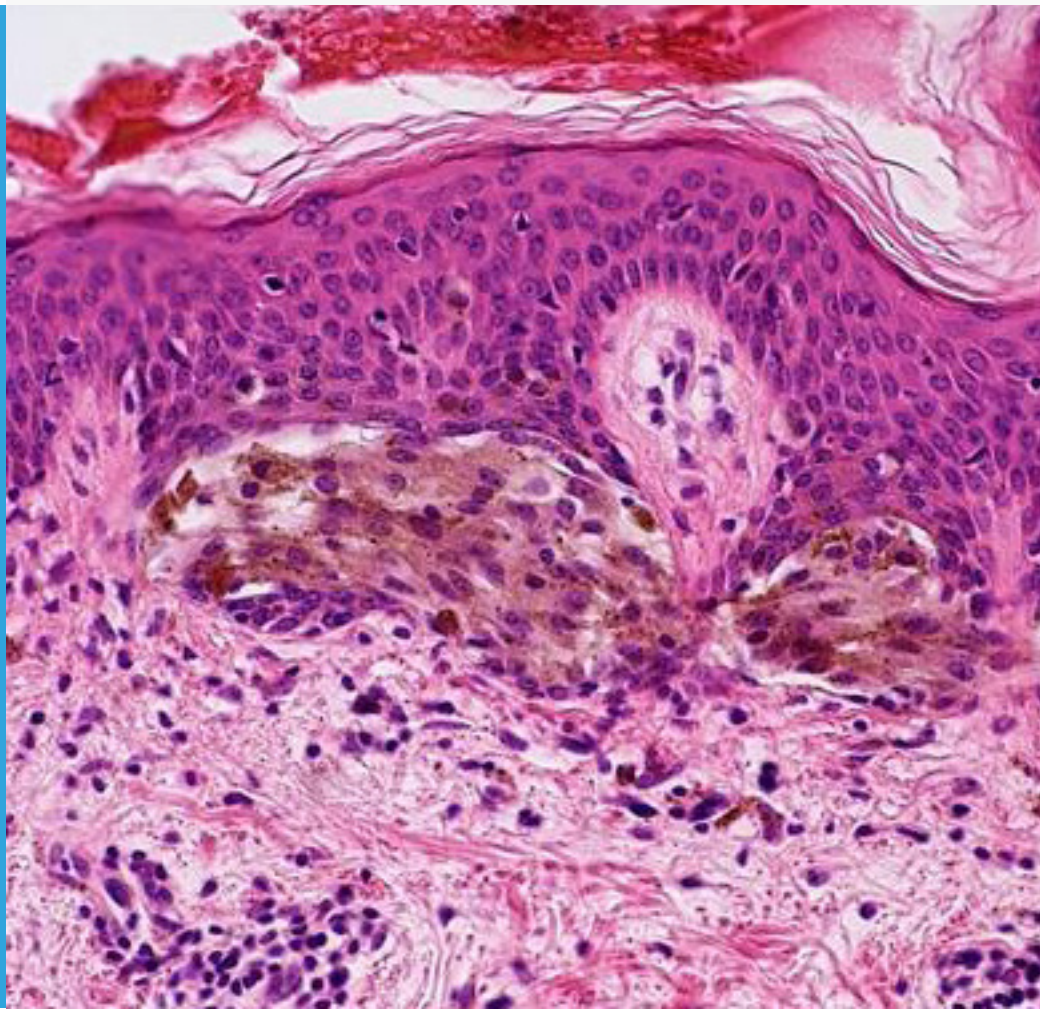


frontiers | Publishing Partnerships

BJBS

# Dermatopathology and Associated Laboratory Investigations in the Study of Skin Disease



ISSN 2474-0896
ISBN 978-2-8325-6524-7
DOI 10.3389/978-2-8325-6524-7

The diagnosis of skin disease requires both clinical and pathological expertise, which subsequently define the laboratory tests required. Central to these investigations is the biopsy, allowing key architectural features of the skin disease to be analysed, emphasizing the importance of dermatopathology to the treatment of skin disorders. In addition, and frequently of vital importance, is a range of laboratory procedures and tests that sit outside the realms of routine dermatopathology and which assist in the diagnosis and aid in the patient management of skin disease.

This Special Issue includes a number of review papers, original articles and short innovation communications. These articles explore why dermatopathology is often key in the diagnosis of skin disease and also explain its relationship and important links to other specialised laboratory services that help define and classify cutaneous disorders.

BJBS

# Table of contents


03 Editorial: Dermatopathology and Associated Laboratory Investigations in the Study of Skin Disease
DOI: 10.3389/bjbs.2025.14810
Guy Edward Orchard

06 A Narrative Review of Molecular, Immunohistochemical and In-Situ Techniques in Dermatopathology
DOI: 10.3389/bjbs.2024.13437
J. A. Gabriel, N. Weerasinghe, P. Balachandran, R. Salih and G. E. Orchard

23 Double Immunohistochemical Labelling of PRAME and Melan A in Slow Mohs Biopsy Margin Assessment of Lentigo Maligna and Lentigo Maligna Melanoma
DOI: 10.3389/bjbs.2024.12319
R. Salih, F. Ismail and G. E. Orchard

34 Diagnostic Techniques in Autoimmune Blistering Diseases
DOI: 10.3389/bjbs.2023.11809
John B. Mee

45 Evaluation of a New Mordant Based Haematoxylin Dye (Haematoxylin X) for Use in Clinical Pathology
DOI: 10.3389/bjbs.2023.11591
J. A. Gabriel, C. D'Amico, U. Kosgodage, J. Satoc, N. Haine, S. Willis and G. E. Orchard

57 Gout With Associated Cutaneous AA Amyloidosis: A Case Report and Review of the Literature
DOI: 10.3389/bjbs.2023.11442
G. E. Orchard

63 Dermatopathology and the Diagnosis of Fungal Infections
DOI: 10.3389/bjbs.2023.11314
S. A. Howell

BJBS

SPECIAL ISSUE EDITORIAL
published: 13 June 2025
doi: 10.3389/bjbs.2025.14810

# Editorial: Dermatopathology and Associated Laboratory Investigations in the Study of Skin Disease

*Guy Edward Orchard* *†

*St John's Dermatopathology, Synnovis Analytics, St. Thomas' Hospital, London, United Kingdom*

**Keywords: dermatopathology, mycology, fungus, gout, immunofluorescence**

## Editorial on the Special Issue

## Dermatopathology and Associated Laboratory Investigations in the Study of Skin Disease

In this Special Issue for the *British Journal of Biomedical Science* we see a mixture of papers, some original articles, some case studies and some reviews. All of these articles seek to contribute to the understanding and advancement in knowledge acquisition into the subject of dermatopathology and associated laboratory-based investigations in the study of skin disease. Each paper in this Special Issue deals with particular aspects on laboratory-based investigations into a wide range of skin diseases dealing with both inflammatory and cancerous conditions. Each of these papers in turn discusses current practice and techniques and shows how these can help define and identify a myriad of differing conditions. This Special Issue shows the importance of clinic-pathological correlation which is so well entrenched in the discipline of dermatopathology.

Howell presents an overview of dermatopathology and the identification of fungal infections employing mycological techniques and explains how they are so closely linked. In the study of subcutaneous skin infectious fungal disease, the histological techniques evaluate a skin biopsy, which defines the inflammatory process and may highlight and direct mycological culture investigations into an infectious cause or foreign body type reaction. This demonstrates the importance of how these two disciplines interact to confirm a definite cause of a fungal infection's states. Howell's review goes on to explain the value of histopathological special stains such as periodic acid–Schiff (PAS) and Grocott and Gomori Methanamine Silver (GMS)which greatly improve the detection of fungal elements. Although, careful morphological examination of the tissue in combination with the relevant clinical history can indicate the type of fungal infection, it cannot indicate the causative species. Culture techniques are still vital to define fungal species and through this approach determine the course of treatment needed. Howell's review also introduces the growing development of new molecular based diagnostic approaches to deliver faster diagnostic outcomes.

A case report and subsequent review by Orchard deals with a common inflammatory state involving Gout in a 73-year-old man, but, as in this case, unusually associated with AA amyloidosis. The paper explains the common dermatological findings of a cutaneous episode of a gout tophus and describes the classical macroscopic and dermatopathological features found. The identification of AA amyloid is described. AA amyloid is associated with chronic inflammatory changes and is often associated with deposits in the urine as well as tissue involvement. A review of only 16 previously reported cases in the literature of gout associated with AA is discussed investigating possible associations between the pathophysiology of these two processes. The paper also explores the evidence of the early use of anti-inflammatory drugs like colchicine before gout tophi formation as a mechanism to prevent the formation of AA amyloidosis.



***Correspondence**
Guy Edward Orchard,
guy.orchard@synnovis.co.uk

**†ORCID:**
Guy Edward Orchard
orcid.org/0000-0002-4757-0022

**Received:** 23 April 2025
**Accepted:** 15 May 2025
**Published:** 13 June 2025

**Citation:**
Orchard GE (2025) Editorial: Dermatopathology and Associated Laboratory Investigations in the Study of Skin Disease.
Br. J. Biomed. Sci. 82:14810.
doi: 10.3389/bjbs.2025.14810

Gabriel et al.'s original investigative paper evaluates the introduction of a new mordant based haematoxylin dye (Haematoxylin X) for use in clinical pathology. In this comparative study conventionally used alum based haematoxylins (Carazzi's, Harris' and Mayer's) are compared to the new chromium based mordant Haematoxylin X on formalin fixed paraffin embedded tissue (FFPE) sections taken from a selection of normal and pathological skin tissue types, along with tissue sampled from a wide host of other organ sites. The new Haematoxylin X was also compared with use as a counterstain in both special stains and immunohistochemistry and in cases of frozen section Mohs procedures. In terms of sensitivity and specificity scores on FFPE Haematoxylin X was rated second behind Harris haematoxylin. However, assessments of frozen Mohs section staining demonstrated that Haematoxylin X scored the highest in terms of both sensitivity and specificity and was an effective counterstain in some special staining techniques and also as a counterstain haematoxylin for immunohistochemical techniques.

Following on from the use of conventional haematoxylin staining we have Mee's review on the use of immunoflourescent (IMF) techniques in the study of autoimmune blistering diseases. In the review Mee highlights the fact that there is often significant overlap in clinical appearances in patients with cutaneous autoimmune states affecting the basement membrane zone (BMZ), with diagnosis often dependent on the identification and the detection and characterisation of specific autoantibodies. IMF provides the "gold standard" diagnostic approach in such scenario's identifying either tissue bound autoantibodies investigated from biopsies taken from lesion and perilesional sites of blistered affected skin, termed direct IMF or from circulating antibodies found within the patient's serum termed indirect IMF. Following on from this the characterisation of numerous antigenic targets in these group of diseases has involved the development of antigen specific tests most notably those based on enzyme-linked immunosorbent assays on serum from affected patients. Mee explains that by the use of all three of these approaches to the study of affected skin tissue and patient serum provides, evidence to define the autoimmune blistering disease process and thus establish the opitmal treatment regime to follow can be defined, as some of these conditions do also have an association and increased risk of malignancy.

Continuing on the theme of malignancy Salih et al.'s original paper on the use of a double labelling technique involving Prame and MelanA in cases of FFPE tissue sections in cutaneous slow Mohs tissue to assess cases of Lentigo Maligna (LM) and Lentigo Maligna Melanoma (LMM) highlights a novel and useful adjunct technique to assist in the evaluation of margin clearance in such cases. Morphological examination of surgical margin clearance is key to determining successful treatment in LM/LMM in slow Mohs cases. The use of preferentially expressed antigen in melanoma (Prame) to assist in such assessments is gaining in popularity. A total of 51 slow Mohs cases of LM/LMM were evaluated using the double labelling technique and compared to single labelling techniques. The results indicated that there was a high concordance between double labelling and single labelling techniques across the samples assessed. The Prame single labelling technique exhibited a sensitivity of 91.3% in slow Mohs cases with a 67.9% concordance in histologically confirmed positive margins. The study highlights the utility for the use of Prame immunohistochemistry and also Prame double labelling techniques as an adjunct to the assessment of LM/LMM in staged slow Mohs cases.

Finally, to finish off this special issue, Gabriel et al. have a narrative review of molecular, immunohistochemical and *in situ* techniques in dermatopathology. The review highlights the significant impact of skin disorders generally within the wider global population, highlighting how it can affect millions of individuals across diverse demographics. More recent advancements in molecular techniques have improved our understanding of the underlying mechanisms of skin disorders generally along with significant improvements in the application of molecular diagnostic testing in clinical practice. Immunohistochemistry and fluorescence *in situ* hybridisation have also played their part in determining protein expression patterns and in detecting chromosomal abnormalities, which in turn help characterise skin lesions in conjunction with the molecular data. This review explores the scope and range of these techniques, it highlights the combined approaches within dermatopathology, with a clear focus on cutaneous malignancies, autoimmune diseases, infectious diseases and neonatal screening approaches, which can be employed in both a diagnostic setting and also to aid in the improvement of patient treatment regimes. Gabriel et al explain the steady rise in molecular technology applications within the field of dermatopathology, but emphasises the importance of international collaboration to test the application of these technologies thoroughly before they become widely accepted in clinical use. This in conjunction with the requirement to comply with *in vitro* diagnostic regulations throughout Europe plus the constant need in investment in novel equipment which will assist in the evaluation of increasing numbers of molecular biomarkers remain key challenges for the future. Gabriel et al concludes by stating that molecular techniques represent a vital tool in the clinicopathological correlation of skin disease states generally and will enhance the information acquired from conventional light microscopic studies.

These six papers, covering a wide range of differing subject matter, technological advances and varied methodologies highlight the scope and importance of why dermatopathology is often key in the diagnosis of skin disease and also explain its relationship and importance to links with other specialised laboratory services that help define and characterise cutaneous disorders.

## AUTHOR CONTRIBUTIONS

This has been solely drafted by the Special Issue guest editor, GO.

## FUNDING

The author(s) declare that no financial support was received for the research and/or publication of this article.

## CONFLICT OF INTEREST

The author declares that the research was conducted in the absence of any commercial or financial relationships that could be construed as a potential conflict of interest.

## GENERATIVE AI STATEMENT

The author(s) declare that no Generative AI was used in the creation of this manuscript.

IBMS Institute of Biomedical Science | BJBS

REVIEW
published: 17 December 2024
doi: 10.3389/bjbs.2024.13437

# A Narrative Review of Molecular, Immunohistochemical and In-Situ Techniques in Dermatopathology

*J. A. Gabriel*[1†], *N. Weerasinghe*[2†], *P. Balachandran*[1†], *R. Salih*[1†] *and G. E. Orchard*[1*†]

[1]*St. John's Dermatopathology Laboratory, Synnovis Analytics, St. Thomas' Hospital, London, United Kingdom,* [2]*School of Health, Sports and Biosciences, University of East London, London, United Kingdom*

Skin disorders pose a significant health burden globally, affecting millions of individuals across diverse demographics. Advancements in molecular techniques have revolutionised our understanding of the underlying mechanisms of skin disorders, offering insights into their pathogenesis, diagnosis, and potential targeted treatment. Furthermore, the integration of molecular diagnostics into clinical practice has enhanced the accuracy of skin disorder diagnoses. Polymerase chain reaction (PCR), next-generation sequencing (NGS), and other molecular assays have allowed for the detection of infectious agents, assessment of genetic mutations, and profile gene expression patterns with unequalled precision. These techniques have proven instrumental in distinguishing between subtypes of skin cancers, aiding treatment strategies and prognostic assessments. Moreover, molecular profiling is increasingly guiding the selection of therapeutic agents, ensuring a personalised and effective approach to managing skin disorders. The application of PCR has revolutionised the field by enabling the identification of microbial DNA (i.e., *Mycobacterium tuberculosis* and Epstein-Barr Virus) in skin infections and detecting specific genetic mutations associated with dermatological disorders (e.g., BRAF). DNA sequencing technologies, such as next-generation sequencing, have facilitated the elucidation of genetic variations and mutations in skin diseases (i.e., bullous disorders), paving the way for personalised treatment approaches. Gene expression profiling techniques, such as microarrays and RNA sequencing, have provided insights into dysregulated pathways and molecular signatures associated with conditions ranging from inflammatory skin disorders to cutaneous malignancies. Immunohistochemistry and fluorescence *in situ* hybridization have proven invaluable in determining protein expression patterns and detecting chromosomal abnormalities, respectively, aiding in the characterization of skin lesions in conjunction with the molecular data. Proteomic studies have contributed to understanding the intricate protein networks involved in dermatological conditions (i.e., psoriasis), while epigenetic analyses have shed light on the role of epigenetic modifications in gene regulation within skin cancer (i.e., Malignant Melanoma). Together, these molecular techniques have laid the groundwork for targeted therapies and precision medicine in dermatology, with implications for improved diagnostics and treatment outcomes. This review focuses on the routinely employed molecular techniques within dermatopathology, with a focus on

OPEN ACCESS

***Correspondence**
G. E. Orchard,
guy.orchard@gstt.nhs.uk

**†ORCID:**
*J. A. Gabriel*
orcid.org/0000-0003-4492-5200
*N. Weerasinghe*
orcid.org/0009-0001-7506-9286
*P. Balachandran*
orcid.org/0009-0007-8924-9054
*R. Salih*
orcid.org/0009-0000-6253-5113
*G. E. Orchard*
orcid.org/0000-0002-4757-0022

**Received:** 24 June 2024
**Accepted:** 15 November 2024
**Published:** 17 December 2024

**Citation:**
*Gabriel JA, Weerasinghe N, Balachandran P, Salih R and Orchard GE (2024) A Narrative Review of Molecular, Immunohistochemical and In-Situ Techniques in Dermatopathology. Br J Biomed Sci 81:13437. doi: 10.3389/bjbs.2024.13437*

cutaneous malignancies, autoimmune diseases, infectious diseases, and neonatal screening which can be implemented in the diagnosis and contribute to improved patient care.

**Keywords: dermatopathology, PCR, NGS, molecular techniques, cutaneous disorders**

## INTRODUCTION

Good clinico-pathological correlation is the basis for the study of skin diseases. There are few clinical investigations that are primarily based around the information acquired through the clinical appearance of a dermatological process often only employing naked eye assessments. However the information gained can be highly informative and directs differential diagnoses when correlated with morphological characteristics and patterns discerned through microscopic assessments. These subsequent microscopic assessments often utilise sophisticated techniques that inform on protein or RNA/DNA expression.

Molecular techniques progress this level of information and have steadily increased in terms of their applications within dermatopathology as they are often a prerequisite for any personalised medicine approach to patient treatment and management. Molecular techniques are based on the assessment of DNA, RNA and proteins to identify and classify disease states. But they also have a predictive and prognostic significance, ultimately playing a key role in the development of personalised medicine and patient management therapies. As the consistency and reliability of molecular assays are expanding in diagnostic settings, it is no longer a technology that is solely employed in large referral centres, but more appropriately utilised in most medical institutions. It is also the case that molecular techniques are now increasingly automated, increasingly reliable and accurate, coupled with a general affordability resulting in an increase in their application in point of care testing strategies [1].

In this review on molecular techniques in dermatopathology we discuss the key emerging technologies and discuss their applications within the context of cutaneous malignancies, autoimmune diseases, infectious diseases [2] as well as neonatal screening.

## MELANOCYTIC LESIONS (MALIGNANT MELANOMA)

Cutaneous melanoma is a malignant neoplasm that arises in the cells of the epidermis referred to as melanocytes. Melanocytes are responsible for producing melanin pigment and are predominately found in skin but are also found in the ears, eyes (Uvea), gastrointestinal tract, leptomeninges, genital, oral and sinonasal mucosal membranes [3]. The majority of melanoma cases are due to cutaneous malignancies (>90% diagnoses), with mucosal and uveal melanomas occurring less frequently (<15% diagnoses with country specific variation) [3]. The vast majority of cutaneous melanomas arise due to molecular changes induced by exposure to ultra-violet radiation, there are several rarer subtypes that are not [4]. The incidence of melanoma has increased in the recent decades with approximately 25 new cases per 100,000 in Europe and 30 cases per 100,000 in the USA [3]. The gold standard for the diagnosis of melanoma is through the morphological assessment of histological sections. However, with the development of molecular diagnostics techniques which assess and highlight genetic and epigenetic alterations, they have provided adjunctive diagnostic information for risk stratifying melanocytic lesions of uncertain malignant potential. Some good examples of this include fluorescent *in-situ* hybridisation (FISH), comparative genomic hybridisation (CGH), gene expression profiling, as well as targeted immunohistochemical assays.

### Comparative Genomic Hybridisation

CGH is utilised to detect chromosomal copy number variation (gains and loses) throughout the genome [5]. There are two main variations to this technique; classic and array-based CGH [5].

Classic CHG involves the analysis of lesional neoplastic tissue extracted from paraffin embedded histological sections [5, 6]. The tumour and normal human reference tissue samples are labelled using differently labelled fluorochromes, mixed in a 1: 1 ratio [5–7]. The samples are then denatured and hybridised onto a substrate of normal metaphase chromosomes [5–7]. Following these steps the samples are visualised using fluorescent microscopy and analysed using computer software to compare the differential signal expression along the length of each chromosome [5, 6]. The relative wavelength observed is reflective of the proportion of tumour compared to normal DNA and can be used to detect gains and losses of DNA material [5, 8, 9].

Array-based CHG utilises arrayed artificial genomic clones as a substrate instead of normal metaphase chromosomes. This resulted in improved resolution, assay robustness and reproducibility compared to the classic CGH [5, 6]. On the array the dots correlate to genomic DNA from a specific locus and the number dots relates to the resolution [5, 6]. This assay depending on the platform can either be co-hybridizing the tumour and normal DNA onto the assay (like the classic CHG) or by hybridising only tumour DNA [5, 6]. With the latter method the copy number for a certain locus is determined by comparing the signal intensity of the tumour against a reference from a control series of non-tumour tissue [5, 6].

Single -nucleotide polymorphism (SNP) arrays is an alternative to CGH. SNP arrays utilises probed loci to bind to known SNPs and each genomic locus is represented by two spots on the array corresponding to the two alleles [5]. The SNP arrays provide an advantage due to its ability to detect loss of heterozygosity and detect allelic ratio [5]. As well as that SNP can also detect selected point mutations [5]. Recent protocol

developments utilising molecular inversion probes (MIP) that require low quantities of tumour DNA from formalin fixed paraffin embedded (FFPE) tissue have been developed [5]. MIP are 40 bp in size, which allows for the evaluation of degraded DNA [5].

Although initial applications of CGH to melanoma primarily focused on metastatic tissue, subsequent literature has shown that CGH can also be beneficial in distinguishing benign melanocytic naevi and from primary cutaneous melanoma. Bastian et al were among the first to demonstrate this, showing that CGH had a sensitivity of 94.8% and a specificity of 90.4% in differentiating unequivocally benign melanocytic variants, including congenital, blue, and spitz naevi, from malignant melanoma [10]. They found that chromosomal aberrations were detected at a higher rate in melanoma compared to naevi [6].

## Fluorescence *In Situ* Hybridization (FISH)

Fluorescence *in situ* hybridization (FISH) is a technique used to detect alterations in chromosomal copy numbers at predetermined genomic loci [5]. This technique allows for the identification of various chromosomal changes, such as entire chromosome gains or losses, targeted loci alterations, loss of heterozygosity, and homozygous deletions [5]. The FISH methodology involves the generation and hybridisation of single stranded fluorescently labelled DNA probes which contain the gene of interest onto formalin fixed paraffin embedded, fresh or frozen tissue sections [5]. After the completion of several processing steps the results are examined and quantified microscopically [5]. FISH offers many advantages including less tissue requirement, faster turnaround times and direct visualisation of cells of interest [5]. However, the technique is limited to only targeted genes, potentially missing relevant alterations in genes not included in the assay [6].

A study by Gerami et al identified a panel of probes for 6p25 (RREB1), 6q23 (MYB), 11q13 (CCND1) and centromere 6 (CEP6) when used in combination assisted in differentiating between melanomas and naevi with a sensitivity of 86.7% and specificity of 95.4% [11]. In melanomas this probe set panel identified interchromsomal rearrangement in chromosome 6 with gains in 6p25 (RREB1) and loses in 6q23 (MYB), as well as common gains in 11q13 (CCND1) [11]. The FISH analysis is performed by evaluating 30 adjacent cell nuclei and calculating the percentage of nuclei where there is a gain in 6p25, 11q13 and a loss of 6q23 compared with CEP6 relative to validated cut-off values and the test result is considered positive if this is observed [11]. Although FISH exhibits high sensitivity and specificity in differentiating primary cutaneous melanomas from benign naevi [12, 13], its reliability in histologically ambiguous melanocytic tumours is variable [14].

## Gene Expression Profiling

Several innovative quantitative gene expression profiling platforms have emerged as supplementary diagnostic tools for evaluating melanocytic tumours. Examples of these technologies include the DecisionDx-Melanoma (Castle Biosciences, Friendswood, Texas), myPath Melanoma (Castle Biosciences, Friendswood, Texas) and Pigmented Lesion assay (DermTech, Inc., La Jolla, California) which utilises algorithmic analysis of RNA based gene expression profiles using tape stiped or biopsied patient tissue samples.

DecisionDx-Melanoma (Castle Biosciences, Friendswood, Texas) is a test produced by Castle Bioscience which is utilised for assessing the risk of metastatic disease in patients who have already been diagnosed with melanoma [15]. The test employs a messenger RNA based gene expression profile using reverse transcription polymer chain reaction [15]. The DecisionDx-Melanoma 31 GEP assay is made up of 28 genes that provides insight into prognostic potential and 3 control genes [15]. The gene panel was devised by identifying genes that over expressed and under expressed from publicly available dataset on metastatic melanoma [15]. The assay aims to provide insight into the likelihood of regional lymph node spread and overall disease survival [15]. By stratifying patients, it allows the identification of low risk patient groups that may not have to undergo invasive lymph node biopsies [15]. The assay classifies the patient results into two main groups, either as low risk (class 1) or high risk (class 2) [15].

The myPath Melanoma (Castle Biosciences, Friendswood, Texas) assay is a test that utilises a quantitative polymer chain reaction to aid in differentiating malignant melanoma from benign naevus in histologically ambiguous lesions [16]. The assay measures the expression of 23 genes (14 melanoma signature and 9 reference genes) and the level of signature genes and reference genes is evaluated [16]. The final result generated is a quantitative result ranging from −16.7 to 11.1 with a range between 16.7 and -2.1 classified as benign, −2.0 to −0.1 classified as intermediate and 0.0 to +11.1 classified as likely malignant [16]. Studies evaluating the myPath test have validated the GEP 23 as reliably differentiating ambiguous melanocytic lesions [16]. Clarke et al evaluated 1,400 melanocytic lesions as part of a prospectively submitted sample study [16]. The samples were evaluated histologically by three dermatopathologists and only samples which had diagnostic concordance of benign or malignant were included [16]. Results for sensitivity and specificity were generated to assess the score generated and the pathological diagnosis [16]. The gene expression signature differentiated benign naevi from malignant melanoma with a sensitivity of 91.5% and a specificity of 92.5% [16].

The Pigmented Lesion assay (DermTech, Inc., La Jolla, California) is a non-invasive gene expression test which utilises tape stripping of lesions to obtain stratum corneum from which RNA is then isolated [17]. From the isolated RNA the expression level of PRAME (preferentially expressed antigen in melanoma) and LINC 518 (long intergenic non-coding RNA 518) are evaluated [17]. Lesions expressing high levels of both PRAME and LINC518, either PRAME or LINC518 or neither correlates with high, moderate, or low risk of the lesions being malignant melanoma [17]. A study conducted by Gerami et al validating the PLA analysed 398 pigmented lesions (87 melanomas and 311 nonmelanomas), PLA was able to accurately differentiate with a sensitivity of 91% and a specificity score of 69% [18].

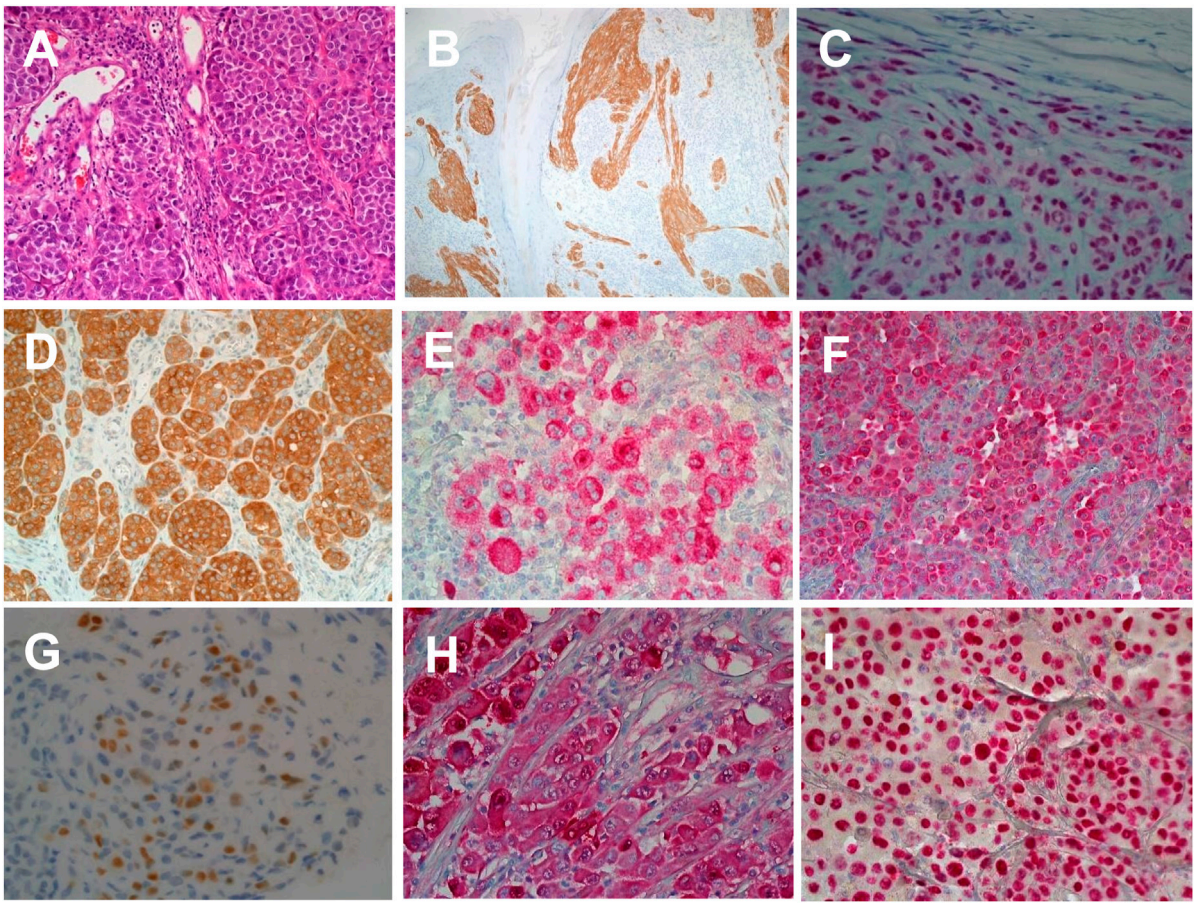


**FIGURE 1 |** Immunohistochemical labelling of malignant melanoma in histological sections. **(A)** Haematoxylin and Eosin staining of skin section showing malignant melanoma (×20 magnification). **(B)** Anti-ALK1 expression in a melanocytic spitzoid tumour (×20 magnification). **(C)** Ant-BAP1 expression in in BAP1 inactivated melanocytic tumour (×20 magnification). **(D)** Anti-BRAFV600E expression in nodular malignant melanoma (×20 magnification). **(E)** Anti-HMB45 expression in superficial spreading melanoma (×20 magnification). **(F)** Anti-Melan A/MART1 expression in superficial spreading melanoma (×20 magnification). **(G)** Anti-PRAME expression in superficial spreading melanoma (×40 magnification). **(H)** Anti-S100 expression in superficial spreading melanoma (×20 magnification). **(I)** Anti-SOX10 expression in superficial spreading melanoma (×20 magnification).

Molecular tests are used to predict response to immunotherapeutic drugs are usually utilised for patients with high stage tumour. Currently there are multiple therapeutic targets in melanoma with inhibitors which include the MAPK pathway, MEC and KIT [19–21].

The use of targeted therapies relies on the detection of an activation mutation on the *BRAF* gene [19, 20]. This is due to the fact that the use of these therapies without the genetic mutation can in turn lead to activation of the MAPK pathway [19, 20]. Another mutation encountered in melanoma is the NRAS-mutation which is found in 20% nonacral melanomas [22]. Currently, there are no effective targeted immunotherapy treatments for NRAS mutations, trials of MEK combined with cyclin dependent kinase 4/6 (CDK4/6) are be conducted to determine efficacy with this mutation [21]. A mutation encountered more commonly in acral and mucosal melanoma is the KIT mutation and these patients may benefit from the use of KIT inhibitors [21]. The detection of the *BRAF, NRAS and KIT* gene mutations are usually determined using next-generation sequencing and the positive detection is required for the consideration of inhibitory therapy [19–21].

## Immunohistochemistry

The histological morphology of Melanomas can mimic a wide range of tumours including poorly differentiated carcinomas, lymphomas, sarcomas and germ cell tumours [23]. Melanoma cell morphologically can appear spindled or epithelioid with diverse cytoplasmic morphologies as rhabdoid, signet ring, clear cell, plasmacytoid and balling in appearance [23]. Immunohistochemistry (IHC) remains a very important adjunct tool in differentiating melanoma from other tumour types that they mimic. Commonly utilised markers for assessing melanocytic lesions include S100, PRAME, MART-1/Melan A, HMB45, Sox-10, MITF and Tyrosinase [23] (See **Figure 1**). Furthermore, IHC remains a useful tool in identifying genomic events that can aid in differentiating

**TABLE 1 |** Immunohistochemistry tests used in identifying the subtype of melanocytic tumours [7].

| IHC Marker | Genetic alteration detected | Diagnostic uses |
|---|---|---|
| ALK (Anaplastic Lymphoma Kinase) | Fusions | ALK rearranged Spitz tumours |
| BAP1 (BRCA1-Associated Protein 1) | Loss of function mutation and Loss of heterozygosity | Lost in BAP1 inactivated melanocytic tumours VS retained in Spitz tumours |
| β -catenin | *CTNNB1* activating mutation | Deep penetrating Naevus |
| BRAFV600E | *BRAFV600E* activating mutation | Negative in low risk spitz lesions VS positive in superficial spreading melanoma with spitzoid morphology |
| NRAS61R | *NRASQ61R* activating mutation | Negative in low risk spitz lesion VS positive in superficial spreading melanoma with spitzoid morphology |
| Pan-TRK | *NTRK1* and *NTRK3* fusions | NTRK-rearranged Spitz tumours |
| PRKR1A1 | Loss of function mutation and Loss of heterozygosity | Pigmented epithelioid melanocytoma |

between tumour subtypes, these markers include BRAFV600E, Beta Catenin, PRKAR1, BAP1, ALK, PAN-TRK, NRASQ61R [24, 25]. The use of these markers is shown in **Table 1**.

## CUTANEOUS LYMPHOMA (INCLUDES DISCUSSIONS ON LIQUID BIOPSY AND NGS)

Lymphomas encompass a heterogeneous array of malignancies originating from the clonal proliferation of B-cell, T-cell, and natural killer (NK) cell populations within lymphocytes at different developmental stages. These malignancies collectively represent approximately 4.3% of all cancer cases in the UK; on average between 2016–2018 [26]. Lymphoma is classified into two main types; Hodgkin's lymphoma (HL) and non-Hodgkin's lymphoma (NHL). The estimated overall survival rate of 10 or more years for patients diagnosed with HL stands at 75% and NHL at 55% [26].

Up to 95% of Hodgkin's lymphoma are classic Hodgkin's lymphoma (CHL) and the rest are subdivided into four categories, each characterized by the presence of atypical cells known as Reed-Sternberg cells. These cells originate from B lymphocytes that undergo malignant transformation [27].

Although recent years have seen advancements in understanding the genetic makeup of CHL and nodular lymphocyte-predominant Hodgkin/B-cell lymphoma, mutational profiling currently lacks practical diagnostic significance [28]. Notably, modern protocols allow for the detection of B-cell clonality in a considerable subset of cases, rendering clonality studies ineffective in distinguishing Hodgkin lymphoma from other B-cell lymphomas with CHL-like morphology [28]. In contrast, identifying T-cell clonality and mutations characteristic of Follicular helper T-cell lymphoma may assist in distinguishing T-cell lymphomas with Reed-Sternberg cells from CHL [29].

Non-Hodgkin lymphoma (NHL) is a cancer of the lymphatic system. Diffuse large Bcell lymphoma and follicular lymphoma are among the most common subtypes in non- Hodgkin's lymphoma, additionally there are more than 60 different types of nonHodgkin lymphoma [26].

T-cell and natural killer (NK)-cell neoplasms are relatively uncommon, comprising approximately 12% of non-Hodgkin lymphomas (NHL) collectively [30]. Despite their rarity, molecular assessment is commonly employed in clinical practice for most T-cell lymphoproliferations. This diagnostic necessity arises because T cells lack a definitive immunophenotypic marker of clonality, comparable to the kappa and lambda antigen receptor immunophenotyping in B cells, thereby necessitating the use of molecular techniques [31]. Specifically, clinical testing of T-cell lymphomas (TCL) typically involves two main categories of molecular changes: T-cell receptor (TCR) gene rearrangements and chromosomal alterations such as translocations, insertions, or deletions [32].

Additionally, as biopsies become smaller in size, distinguishing between neoplastic and reactive T-cell infiltrates based on immunomorphological criteria is becoming increasingly challenging [31]. To address this issue, molecular techniques such as multiplex polymerase chain reaction (PCR) assays to evaluate T-cell receptor (TCR) gene rearrangements have become widely adopted in daily clinical practice [31].

Multiplex PCR refers to a method employed to amplify numerous distinct genetic loci using multiple PCR primer pairs within a single reaction [28]. This technique enables the simultaneous addressing of various related inquiries about a specimen, eliminating the necessity for multiple individual PCR steps [28]. These individual PCR steps typically involve preparing separate reactions for each target sequence, each with its own set of primers and optimized conditions [28]. It is frequently utilized to confirm the presence of amplifiable nucleic acid in the sample [28].

Most T lymphocytes possess α: β heterodimeric T-cell receptors (**Figure 2**); however, a subset expresses a unique γ: δ T-cell receptor comprised of distinct antigen-recognition chains, γ and δ, which are arranged in a γ: δ heterodimer [32]. These cells, characterized by such receptors, are referred to as γ: δ T cells. The TCR gene rearrangements occurs in these loci, and commonly analysed in dermatopathology using PCR [32] (**Figure 3**). **Table 2** outlines the classification of Cutaneous TCell and B-Cell lymphomas, along with the known genetic abnormalities in each subset of cutaneous lymphoma. Additionally, clinical features and diagnostic immunohistochemical markers used in

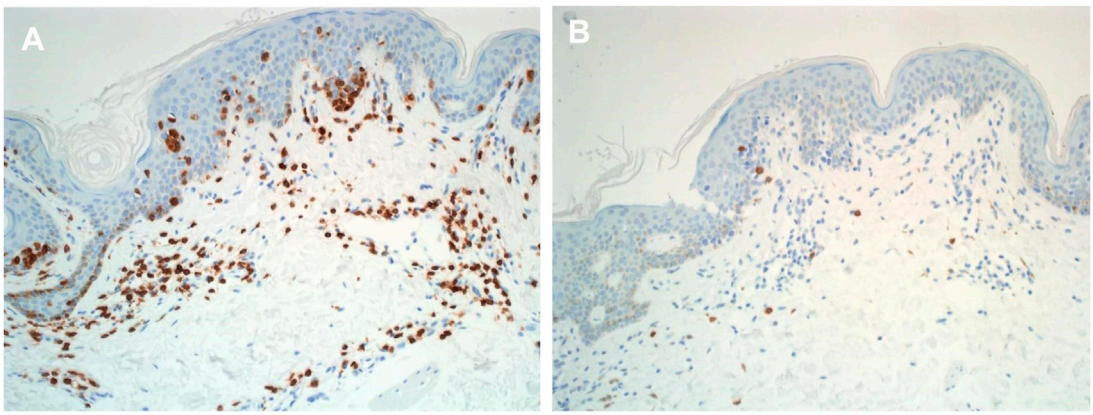


**FIGURE 2 |** Immunohistochemical labelling of cutaneous lymphoma in histological sections. **(A)** Anti - Alpha Beta TCR expression in mycosis fungoides tissue section (X20) **(B)** Anti - Gama Delta TCR expression in mycosis fungoides tissue section (X20).

conjunction with molecular testing to confirm the diagnosis are provided. In most cases, immunohistochemistry (IHC) plays a crucial role in refining the diagnosis before molecular testing is conducted to pinpoint the specific diagnosis.

Liquid biopsy has the advantage of overcoming tumour heterogeneity compared to contemporary testing methods. Traditional tissue biopsies may only capture a snapshot of the tumour's genetic profile at a specific location, which may not fully represent the genetic diversity present throughout the tumour or across metastatic sites [47]. In contrast, liquid biopsy allows for the sampling of circulating tumour DNA shed from various tumour sites, providing a more comprehensive and dynamic view of the tumour's genetic landscape [48]. This ability to capture genetic information from different tumour regions helps overcome the limitations of tumour heterogeneity seen with traditional tissue biopsies, ultimately leading to more accurate diagnosis and treatment selection [48].

Liquid biopsy samples are commonly analysed using Next-Generation Sequencing (NGS) technology; this allows for the comprehensive analysis of circulating tumour DNA (ctDNA) or other nucleic acids present in the liquid biopsy sample [49].

While ctDNA shedding can vary and may not capture every mutation, numerous studies validate its utility [47–55]. Research indicates that ctDNA often reflects a broad spectrum of genetic alterations present in different tumour regions and metastatic sites, offering a dynamic snapshot of tumour evolution [49]. Advances in Next-Generation Sequencing (NGS) and other technologies enhance the sensitivity and accuracy of ctDNA analysis, making it a reliable tool for providing a comprehensive and dynamic view of the tumour's genetic makeup and informing on treatment decisions [49].

In the context of liquid biopsy analysis, NGS enables the detection and characterization of genetic alterations such as point mutations, insertions and deletions, copy number variations, and gene fusions in the circulating tumour DNA. This information can provide insights into the genetic makeup of the tumour, including its mutational profile, heterogeneity, and potential therapeutic targets [50, 51].

NGS-based liquid biopsy analysis offers several advantages, including high sensitivity and specificity, the ability to detect rare mutations, and the capacity for multiplexed analysis of multiple genes simultaneously [52]. Additionally, NGS allows for the monitoring of disease progression, treatment response, and the emergence of resistance mutations over time [52, 53].

Despite the advantages of liquid biopsies, there are several limitations. Liquid biopsies can experience issues such as inconsistent ctDNA shedding, leading to variability in detection and potential false negatives, particularly in early-stage cancers with low ctDNA concentrations [49]. Additionally, ctDNA assays may not capture all genetic mutations, potentially missing important alterations [48]. Overall, liquid biopsy has emerged as a powerful tool in precision oncology, enabling non-invasive monitoring of cancer dynamics and informing personalized treatment decisions [47–55]. These limitations highlight the need for ongoing research and technological improvements to enhance the reliability and availability of these diagnostic tools.

## AUTOIMMUNE AND GENETIC SKIN DISORDERS

Conducting a thorough physical examination is a vital part of diagnosing blistering diseases, as it allows clinicians to evaluate the precise location, dispersion, and characteristics of the blisters themselves [56]. Additionally, dermatologists will examine a biopsy of the affected skin to analyse it under a microscope. Examining the skin sample enables detection of specific antibodies and other important indicators that provide evidence to support an accurate diagnosis [56, 57].

The diagnosis of autoimmune and genetic skin conditions has been advanced considerably in recent decades through the application of molecular biology techniques [56]. By enabling analysis at the DNA, RNA, and protein levels, modern molecular methods provide objective biological insight beyond visual symptoms. Techniques like PCR, DNA sequencing,

**TABLE 2 |** WHO-EORTC Classification 2018 of Cutaneous lymphomas, involved genetic abnormalities and diagnostic immunohistochemical Markers [27–46].

| WHO-EORTC Classification 2018 | Gene/Translocation | Target/gene | Diagnostic immunohistochemical Markers |
|---|---|---|---|
| Cutaneous T-cell lymphomas | | | |
| Mycosis fungoides | CNV involve the 17p, 9p21 and 10q deletions and 17q amplification<br>Somatic mutation in JAK/STAT | e.g. of some gene are: DNMT3A, ARID1A, CTCF, NCOR1, KDM6A, SMARCB1, ZEB1, PRKCB, PTPRN2, and RLTPR | CD3+, CD4+, CD8–, Cytotoxic proteins–, CD56–, αβ T cell lineage and EBV– |
| Mycosis fungoides variants<br>• Folliculotropic MF<br>• Pagetoid reticulosis<br>• Granulomatous slack skin | Copy number variations (CNV)<br>Somatic mutation in JAK/STAT | | FMF: CD3+, CD4+, CD8-, with an elevated CD4: CD8 ratio (6–10:1); CD30 may be positive in large cell transformation<br>PR: variable CD4, CD8, and CD30 expression; Ki-67/MIB1 may show active proliferation but is not specific<br>GSS: CD4+/45RO+/30+; multinucleated giant cells, often CD68+, and may have surrounding CD1a+ cells |
| Sézary syndrome | CNVs<br>Somatic mutation in JAK/STAT | | CD3+, CD4+, CD5+/–, CD7–, CD25+/–, CD30+/–, CD56-, CCR4+ |
| Adult T-cell leukemia/lymphoma | PLCG1,PRKCB,CARD11 and VAV1 | CTLA4-CD28 and ICOSCD28 fusions | CD3+, CD5+, CD45RO+, CD8+/–, CD25+/–, CD30+/–, CD7–, CD20–,<br>CD79a-; elevated Ki-67 may be present in more aggressive forms of ATL |
| *Primary cutaneous CD30-positive lymphoproliferative disorders* | | | |
| • Primary cutaneous anaplastic large cell lymphoma | t(2;5)(p23;q35)<br>6p25.3<br>3q28<br>NPM1-TYK2<br>IL6-JAK-STAT mutation<br>DNMT3A, TP53 mutation | ALK/NPM (ALK+ systemic)<br>DUSP22/IRF4 TP63<br>JAK/STAT | CD3+/–, CD4–, CD8–, CD30+, Cytotoxic proteins+, CD56–, αβ T cell lineage and EBV– |
| • Lymphomatoid papulosis | IRF4/DUSP22 locus alteration | | CD3+, CD4+, CD25+, CD30+, CD45RO+, CD56+/–, CD2–, CD3–, CD5–,<br>CD7–. CD8 positivity, as opposed to CD4, is more frequently seen in Type D and Type E |
| Subcutaneous panniculitislike T-cell lymphoma | | | CD3+, CD4–, CD8+, Cytotoxic proteins+, CD56–, αβ T cell lineage and EBV– |
| Extranodal NK/T-cell lymphoma, nasal type<br>Chronic active EBV infection | JAK-STAT mutation Gains in 8q24 [MYC]<br>mutations in *DDX3X* | | CD3+, CD4-, CD8+ (surface CD3–), Cytotoxic proteins+, CD56+, NK or γδ T cell lineage and EBV+ |
| *Primary cutaneous peripheral T-cell lymphoma, rare subtypes* | | | |
| • Primary cutaneous γ/δ T-cell lymphoma | STAT5B mutation SETD2 mutation | JAK/STAT | CD3+, CD4–, CD8–/+, Cytotoxic proteins+, CD56+, γδ T cell lineage and EBV– |
| • Primary cutaneous aggressive epidermotropic CD8-positive T-cell lymphoma (provisional) | CAPRIN1-JAK2 SELENOI-ABL1 | JAK/STAT | CD3+, CD4–, CD8+, Cytotoxic proteins+, CD56–, αβ T cell lineage and EBV– |
| • Primary cutaneous CD4+ small/medium T-cell LPD (provisional) | Clonally rearranged TCR genes | Specific genetic abnormalities have not been described | CD3+, CD4+, CD8–, CD279/PD-1+, Cytotoxic proteins-, CD56–, αβ T cell lineage and EBV-. |
| • Primary cutaneous acral CD8+ T-cell lymphoma (provisional) | Clonally rearranged TCR genes | Specific genetic abnormalities have not been described | CD3+, CD4–, CD8+, Cytotoxic proteins- but TIA-1+, CD56–, αβ T cell lineage and EBV– |
| Primary cutaneous peripheral T-cell lymphoma, NOS | Clonally rearranged TCR genes | Specific genetic abnormalities have not been described | |
| Cutaneous B-cell lymphomas | | | |
| Primary cutaneous marginal zone lymphoma | T (14;18) (q32;q21) t (3;14) (p14.1;q32)<br>18q trisomy | IgH/MALT FOXP1/IGH FAS mutations | CD20+, CD79a+, BCL2+, BCL6–, CD5–, CD10–, CD16- |
| Primary cutaneous follicle center lymphoma | t(14;18)(q32;q21) 2p16.31 (amp REL<br>14q32.32 del<br>1p36 del | IgH/BCL2 (rare in cutaneous counterpart)<br>TNFRS14 mutations | CD19+, CD20+, CD22+, CD79a+, PAX5+, BCL6+, CD10+/-, BCL2 |
| Primary cutaneous diffuse large B-cell lymphoma, leg type | 9p21<br>3p.14.1<br>6q del<br>8q24<br>3q27.3, 14q32<br>PDL1/PDL2-transl.<br>18q21.31–q21 ampl. | CDKN2A (or hypermethytation)<br>FOXP1<br>BIMP1<br>MYC<br>BCL6, IgH<br>MYD88-mut, CD79B,<br>CARD11, TNFAIP3/A20 (NF-κB)<br>BCL2 | CD19+, CD20+, CD22+, CD79a+, PAX-5+, BCL2+, IRF4/MUM-1+, FOXP1+ |

(Continued on following page)

**TABLE 2 |** (*Continued*) WHO-EORTC Classification 2018 of Cutaneous lymphomas, involved genetic abnormalities and diagnostic immunohistochemical Markers [27–46].

| WHO-EORTC Classification 2018 | Gene/Translocation | Target/gene | Diagnostic immunohistochemical Markers |
|---|---|---|---|
| EBV-positive mucocutaneous ulcer (provisional) | Clonally rearranged IG and TCR genes | | CD15+, CD30+, CD19+, CD22+, CD79a+, PAX-5+, EBV+, IRF4/MUM-1+, CD20+/–, CD10–, BCL6– |
| Intravascular large B-cell lymphoma | Mutations in MYD88, CD79B, SETD1B, and HLA-B and PD-L1/PD-L2 involving the 3' untranslated region | | CD79a+, CD20+, IRF4/MUM-1+, CD5+/–, CD10+/–, CD29–, CD54– |

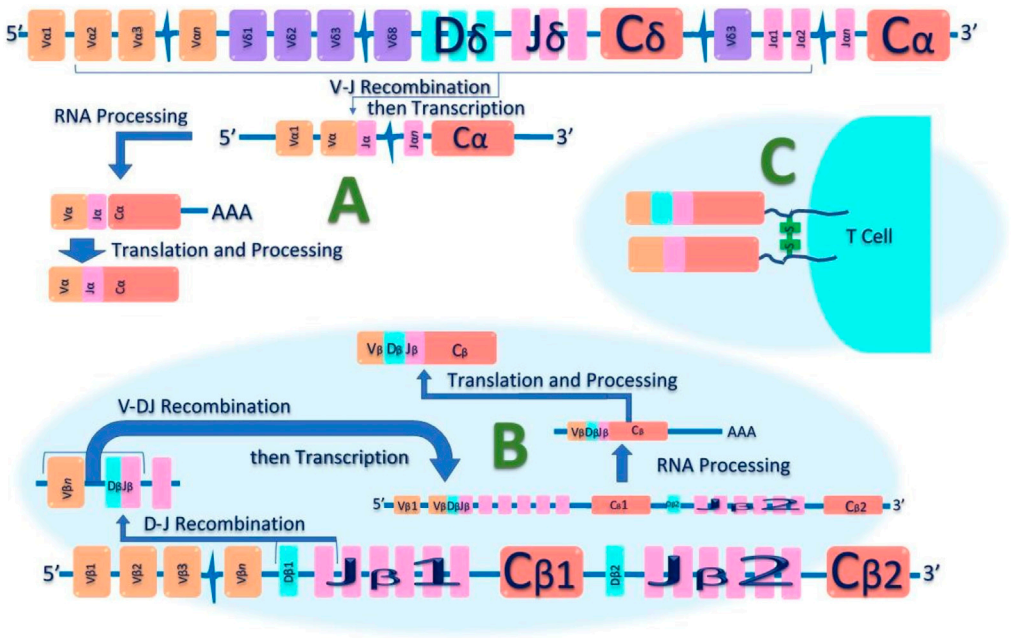


**FIGURE 3 |** Schematic diagram of T-cell receptor (TCR) Alpha Beta Gene Rearrangement. Initially, in the undeveloped genome, the TCR's genetic components are separated and unassembled. During T-cell development, these distinct genetic segments—variable (V), diversity (D), and joining (J)—are combined in various ways. Additionally, nucleotides at the junctions between these segments can be added or removed. This random assembly process, particularly in the complimentary determining region 3 (CDR3), creates such a vast array of possibilities that it's extremely unlikely for two T cells to have identical TCR nucleotide sequences. **(A)**: shows V-J recombination of the TCR-α chain DNA. **(B)**: Shows V-D-J recombination of the TCR-β chain DNA. **(C)**: shows heterodimer structure of αβ-TCR on the surface of T lymphocytes, that can serve as a unique molecular identifier for each T cell.

microarrays, and mass spectrometry have illuminated causes and mechanisms in complex dermatological diseases [56].

In autoimmune disorders such as psoriasis, bullous pemphigoid, and lupus, molecular techniques assist in determining auto-antibodies involved in aberrant immune attacks on skin cells [56]. ELISA assays detect circulating autoantibodies in serum, while immunofluorescence microscopy localises autoantibody binding on skin biopsies. Identifying autoantibody profiles verifies diagnoses, reveals antigen targets, and guides treatment. PCR also measures inflammatory markers like cytokines to monitor disease severity [56, 57].

Beyond DNA, other developing molecular techniques further elucidate biological underpinnings [57]. RNA microarrays and sequencing reveal gene expression changes in diseased skin compared to healthy skin while mass spectrometry analyses the skin proteome (the entire complement of proteins) pinpoint dysregulated proteins [57]. Microbiome analysis examines microbial residents on skin that are related to autoimmune disorders [57].

These approaches provide precise, unbiased data about biological factors contributing to skin pathology [57]. Incorporating molecular biomarkers into diagnosis yields objective information that complements symptom-based observation. Molecular techniques also enable personalised medicine by matching treatments to an individual's molecular profile [56, 57].

Epidermolysis bullosa (EB) refers to a group of rare genetic skin disorders that cause blistering and damaging of the skin in response to minor mechanical friction or trauma. There are four main types of inherited EB – EB simplex, junctional EB, dystrophic EB, and Kindler syndrome – with over 30 specific

**TABLE 3 |** Classification and molecular characteristics of epidermolysis bullosa (EB) [52, 53].

| Gene | Level of skin cleavage and ultrastructural anomalies | Relative protein expression | Types of pathogenic sequence variants | Protein | Inheritance |
|---|---|---|---|---|---|
| KRT5 | Cleavage: basal keratinocyte cytoplasm; tonofilament clumping in EBS generalized severe; lack of tonofilaments in basal keratinocytes in AR EBS | Unchanged | Missense, nonsense, splice site, frameshift, in-frame (large) deletions or insertions | Keratin 5 | AD |
| KRT14 | Cleavage: basal keratinocyte cytoplasm; tonofilament clumping in EBS generalized severe; lack of tonofilaments in basal keratinocytes in AR EBS | Unchanged or absent | Missense, nonsense, splice site, frameshift, in-frame deletion or duplications | Keratin 14 | AD, AR |
| PLEC | Cleavage: basal keratinocyte cytoplasm just above hemidesmosome s; diminutive hemidesmosome s | Plectin unchanged, absent or reduced with domain-specific antibodies | Missense, nonsense, frameshift, splice site | Plectin | AD, AR |
| KLHL24 | Cleavage: basal keratinocyte cytoplasm; reduced tonofilaments in basal keratinocytes | Keratin 14 reduced or unchanged | Pathogenic variants in the translation initiation codon | Kelch-like protein 24 | AD |
| DST | Cleavage: basal keratinocyte cytoplasm; diminutive hemidesmosome s lacking tonofilament attachment | BPAG1 (isoform e) absent | Nonsense, missense, frameshift, splice site | BPAG1 | AR |
| EXPH5 | Cleavage: basal keratinocyte cytoplasm; tonofilament aggregation in basal keratinocytes | Exophilin 5 absent | Nonsense, frameshift | Exophilin 5 | AR |
| CD151 | Cleavage: lower epidermis | CD151 absent | Frameshift, splice site | Tetraspanin 24 | AR |
| TGM5 | Cleavage: between stratum granulosum and corneum | Absent or reduced activity and expression of transglutamina se 5 | Missense, nonsense, frameshift, splice site | Transglutam inase 5 | AR |
| PKP1 | Cleavage: suprabasal epidermal layers; hypoplastic desmosomes | Plakophilin 1 absent | Nonsense, frameshift, splice site | Plakophilin 1 | AR |
| DSP | Cleavage: suprabasal epidermal layers; hypoplastic desmosomes | Desmoplakin reduced or absent | Nonsense, frameshift | Desmoplaki n | AR |
| JUP | Cleavage: suprabasal epidermal layers; hypoplastic desmosomes | Plakoglobin absent | Nonsense | Plakoglobin | AR |

*AD, autosomal dominant; AR, autosomal recessive.*

clinical subtypes [58]. EB displays substantial heterogeneity in symptoms, ranging from severe congenital blistering of the skin and mucous membranes that can impact lifespan, to very mild localised blistering such as nail dystrophy that begins later in life. In babies and adults, the blistering pattern and location may be distinctive enough to allow clinical diagnosis of the EB subtype. However, in newborns and milder cases, laboratory diagnostic testing is required to definitively determine the EB classification. Additionally, when EB occurs for the first time in a family, with no prior history, genetic testing is necessary to establish whether the inheritance pattern is autosomal dominant or recessive [58].

The four primary types of epidermolysis bullosa (EB) are categorised based on the ultrastructural level within the skin at which blistering, and separation occur. In EB simplex, splitting happens within the layers of the epidermis [59]. In junctional EB, it occurs in the lamina lucida layer. In dystrophic EB, cleavage takes place beneath the basement membrane zone in the uppermost dermis. Finally, in Kindler syndrome there is mixed-level blistering. An "onion skin" classification scheme for EB has been developed which sequentially considers the skin cleavage plane corresponding to EB type, clinical severity, inheritance pattern, and the specific molecular defect involved, including both the protein expression and disease-causing genetic mutations present [59].

In some subtypes of epidermolysis bullosa (EB), known as syndromic forms, the affected genes are expressed in tissues outside the skin, leading to involvement of other body systems and organs [60]. For example, muscular dystrophy can occur in EB simplex caused by plectin deficiency; pyloric atresia is seen in EB simplex with plectin deficiency and junctional EB with integrin α6β4 deficiency; cardiomyopathy is associated with KLHL24 or PLEC gene variants in EB simplex and with DSP and JUP variants in skin fragility disorders; lung fibrosis and nephrotic syndrome arise in junctional EB with integrin α3 subunit deficiency; connective tissue abnormalities occur with PLOD3 mutations; and nephrotic syndrome is seen with CD151 deficiency (**Table 3**). In these syndromic subtypes, the extracutaneous effects reflect expression of the defective genes in additional tissues, beyond simply the skin [59, 60].

For new-borns presenting with congenital skin absence, fragility, or blistering that could indicate epidermolysis bullosa (EB), prompt referral to a specialised EB diagnostic centre is recommended to establish a diagnosis [61]. The diagnostic workup should include acquiring a blood sample for DNA extraction, as well as a skin biopsy. Confirming the diagnosis can be achieved through immunofluorescence mapping (IFM) of skin samples using fluorescence-labelled antibodies, transmission electron microscopy (TEM) to examine skin ultrastructure, and/or direct genetic testing, depending on the centre's capabilities. While genetic testing can provide a definitive result, IFM can yield a diagnosis within hours to guide urgent neonatal care [61]. Thus, IFM remains the preferred first-line approach currently, though genetic testing is increasingly accessible. In some complex cases, all three diagnostic modalities may be utilised to reach a conclusion. The goal is to leverage available resources to determine the EB subtype quickly and accurately [61].

For paediatric or adult patients who exhibit skin fragility and blistering consistent with epidermolysis bullosa (EB) subtypes, direct referral to a diagnostic centre for genetic testing can be appropriate once characteristic manifestations develop [61, 62]. The testing methodology chosen may involve next-generation sequencing (NGS) or Sanger sequencing (SS) depending on the circumstances. If both sequencing approaches fail to determine a genetic diagnosis, immunofluorescence mapping (IFM) and transmission electron microscopy (TEM) of skin samples may provide supplementary molecular and ultrastructural insights to elucidate the underlying basis for the skin fragility phenotype. In patients with clearer EB manifestations, proceeding straight to genetic analysis allows subtype classification, while IFM and TEM remain additional options when sequencing is inconclusive [61, 62].

Benign familial pemphigus (BFP) is an autosomal dominant skin disorder characterised by blistering and there are two main subtypes: BFP type I (Hailey-Hailey disease/HHD) and BFP type II (Gabriel's disease) [63]. BFP type I is caused by mutations in the ATP2C1 gene which encodes a calcium ATPase and these mutations disrupt calcium homeostasis in keratinocytes leading to acantholysis (loss of cell adhesion). Approximately, 90% of HHD patients have ATP2C1 mutations while BFP type II is caused by mutations in M1S1 which encodes a desmosomal glycoprotein and these mutations impair keratinocyte adhesion through defective desmosome formation. The diagnosis of BFP's include mutation screening of ATP2C1 and M1S1 genes by sequencing and immunofluorescence that shows loss of desmosomal proteins which is also visible on histology. Therefore, identifying causative mutations in adhesion proteins like ATP2C1 and M1S1 allows definitive diagnosis and classification of benign familial pemphigus subtypes [63].

Mucous membrane pemphigoid (MMP) refers to a group of chronic autoimmune blistering diseases primarily affecting the mucous membranes and skin. These diseases lead to progressive scarring and impairment [64, 65]. Laminin-332 is a key component of epithelial basement membranes, synthesised by keratinocytes. It plays an important role in dermal-epidermal adhesion and wound healing. Laminin-332 has a cross-like structure with three chains - α3, β3 and γ2 [64].

Patients with MMP have autoantibodies against the α3, β3 or γ2 subunits of laminin332. Immunoprecipitation of radiolabelled cultured keratinocytes has been the gold standard for detecting these autoantibodies [64, 66]. Alternatively, immunoblotting using keratinocyte extracellular matrix or purified laminin-332 can identify antibodies.

However, these techniques are time-consuming, labour-intensive, and restricted to specialised labs. Radio-immunoassays are highly sensitive and specific but cumbersome, expensive, and tightly regulated. ELISA systems using purified laminin332 or keratinocyte extracellular matrix have been developed as more accessible antibody detection methods [64, 67, 68].

However, significant barriers exist regarding cost, access, and practical integration into clinical dermatology. Much research has yet to translate out of specialised labs into widespread use. Additionally, the complexity of results requires collaboration between clinicians, researchers, and bioinformaticians to determine appropriate interpretation and application [69]. Therefore, histopathological analysis of these autoimmune diseases still remains to the gold standard technique.

## INFECTIOUS DISEASES

Dermatopathology occupies a central position in the comprehensive diagnosis and management of skin conditions, extending to those with infectious aetiology. Whilst conventional culture-dependent methodologies and microscopic analyses have

**TABLE 4 |** Key pathogens commonly found or relevant within dermatopathology 651 investigations with both conventional and molecular methods outlined [70–82].

| Pathogen / Infection | Conventional diagnostic methods | Molecular diagnostic methods |
|---|---|---|
| Bacterial - Mycobacterium | | |
| *Mycobacterium tuberculosis* | Histopathology & special staining by Ziehl-Neelsen (acid-fast). Tissue culture for M. *tuberculosis* with sensitivity testing. | PCR on fresh samples is recommended with further sequencing for antimicrobial resistance genes. |
| *Mycobacterium leprae* | Histopathology & special staining by Wade-Fite (modified acidfast). | PCR is a viable option on FFPE samples due to lack of culturing M. *Leprae* |
| Atypical *Mycobacteria* | Tissue Culture. Special staining by acid-fast stains are less useful during microscopy | PCR on fresh samples is recommended with sequencing for species differentiation |
| Bacterial - Spirochetes | | |
| *Borrelia burgdorferi* | Serological studies | PCR on fresh (serologic) samples |
| *Treponema pallidum* | Serological studies. Histopathology with Anti-*Treponema pallidum* IHC is recommended and is more sensitive than special staining by Warthin-Starry. | PCR on fresh (serologic) samples. FFPE samples may also be used if fresh specimens cannot be obtained. |
| Bacterial - Other | | |
| *Bartonella henselae* | Serological studies preferred. Tissue culture, although requires prolonged culturing time. | PCR on fresh (serologic) or. FFPE samples, with the latter to be used if suspected during histopathology work-up. |
| *Rickettsia rickettsii* | Serological studies. | PCR on fresh (eschar) skin sample. PCR on FFPE can also be useful |
| Viral | | |
| Human Papilloma Virus, Human Herpesvirus-8, Herpes Simplex Virus 1 & 2, Merkel cell polyomavirus, Epstein–Barr virus. | Histopathology with adjunct IHC for viral proteins. | HPV, EBV – In-situ hybridisation (typically chromogenic) on FFPE sections would be suitable within the routine diagnostic setting. PCR may also be useful and can be used on FFPE tissues. |
| Fungal | | |
| *Candida albicans, Histoplasmosis capsulatum,* Dermatophytes, *Aspergillus* species | Fungal culture & microscopy. In addition, IHC and special staining: periodic acid-Schiff (PAS) and Gömöri methenamine silver (GMS). | Pan-fungal PCR with subsequent sequencing, or species-specific PCR can be used on FFPE samples - ideally when fungal structures are observed histologically. Alternatively, in-situ hybridisation (alongside IHC) with species specific probes may also be useful in PAS/GMS positive sections. |
| Parasite | | |
| *Leishmania spp.* | Histology with Giemsa special staining or in addition, anti-*Leishmania* IHC | PCR - broad-range or *Leishmania* genus PCR on Cultured samples which can then be followed by subspecies differentiation via restriction fragment length polymorphism (RFLP) or sequencing. PCR can also be carried out directly on fresh tissue samples and FFPE. |

historically underpinned the diagnostic framework for most cutaneous infections, their effectiveness is circumscribed by inherent limitations. Specifically, microscopic examination through histochemical staining, exhibits diminished sensitivity and specificity, while culture-based strategies are characterised by prolonged turnaround times and are unsuitable for nonviable pathogens [70, 71]. The last few decades have seen the increased use of molecular techniques in the diagnosis of skin infections within the clinical and laboratory setting, through nucleic acid-based detection methods including PCR, *in-situ* hybridisation and sequencing of target pathogen DNA or RNA, detecting a wide range of infectious agents spanning, bacteria, viruses, fungi, and parasites in skin specimens [70, 71]. More importantly, these techniques have been particularly useful in the definitive diagnosis of often challenging and ambiguous infectious skin lesions, including tuberculosis, leishmaniasis, leprosy, lyme disease, and fungal infections [72–74]. Furthermore, the supplementary use of these molecular detection methods can also be applied to both fresh and formalin fixed paraffin embedded (FFPE) tissues, the latter of which relating to dermatopathology specimens [70, 72, 73, 75]. As a result, molecular techniques have become increasingly employed within the dermatopathology laboratory setting, having found use within the diagnosis of infectious or infection-related skin conditions.

In most cases, the conclusive diagnosis of cutaneous infections necessitates a comprehensive and interdisciplinary methodology. This combines clinical assessment with microbiological and microscopic investigations, alongside the established application of molecular assays aimed at identifying infectious pathogens from freshly obtained serological and tissue specimens [75, 76]. Specifically within dermatopathology, using routine histopathological techniques not only allows for the direct visualisation of infectious agents (histochemical stains) and infectious morphological hallmarks in tissues, but they also provide important context for differentiating between

**TABLE 5 |** An overview of the main immunohistochemical, *in-situ* hybridisation and molecular methodologies available, highlighting they key benefits and restrictions [83–87].

| Name of technique | Benefits | Restrictions |
|---|---|---|
| Immunohistochemistry (IHC) | Detects at the light microscope level cellular compartment localisation of protein(s) expression<br>Has application to both frozen tissue (i.e. immunofluorescence) and formalin fixed paraffin embedded tissue<br>Cost effective<br>Rapid turnaround times<br>Reproducible and widely employed and can be fully automated<br>Pivotal in certain tumour cancer pathologies for typing and classification of entities i.e. lymphoma typing. | Can lack high resolution imaging<br>Limited options on multicolour chromogenic staining<br>Prone to section detachment issues from slides, due to tissue or section preparation<br>IHC slides will photo bleach over time<br>Stringent controls needed to avoid false positives and false negative signal interpretation. Due to a number of factors i.e. tissue processing, antigen retrieval or antibody concentration issues |
| In-situ hybridization (ISH) | Application on complex tissue types i.e. embryos.<br>Higher resolution than IHC<br>Useful to identify gene losses and duplications employing one chromogenic colour and gene splits and fusions (two colour chromogenic colours)<br>Effective on formalin fixed paraffin embedded tissue and can be fully automated on IHC platforms<br>Highly effective when employed in combination with IHC techniques i.e. Epstein Barr virus detection employing ISH in combination with lymphoma panel IHC or HPV detection employing ISH HPV high and low risk in conjunction with P16 expression in head and neck tumour pathology. | The procedures for in situ hybridization (ISH) are generally more complex and time-consuming compared to immunohistochemistry.<br>ISH provides only semiquantitative results, allowing for the detection of relative changes in nucleic acid levels.<br>Evaluating and identifying targets with low-copy number DNA or RNA can be challenging. |
| Polymerase Chain Reaction (PCR) DNA sequencing | High sensitivity and resolution technique can detect single genome copy changes i.e. base pair substitutions within fewer than 100 cells.<br>Largely automated process<br>Can be employed on material taken from formalin fixed paraffin embedded tissue blocks.<br>Archival assessments employing PCR can be performed.<br>Can be utilised as a technique to assess antimicrobial resistance | Relatively expensive compared to both IHC and ISH; thus, limited to small regions (target specific)<br>Cannot distinguish between viable and nonviable cells: PCR can detect nucleic acids from both infectious and noninfectious pathogens, making it difficult to assess how harmful a sample is.<br>PCR requires specific primers for each microorganism, which can be difficult for identifying mixtures of microorganisms.<br>PCR can be inhibited by substances like metals found in environmental samples.<br>Turnaround times are longer than IHC and ISH.<br>Results need to be interpreted and assessed in the context of clinical symptoms. |
| PCR RNA sequencing | Gene Expression: RNA sequencing can identify changes in gene expression, including allelespecific variations, and can quantify significant differences in expression levels.<br>Non-Coding Variants: RNA sequencing can reveal noncoding variants that may not be identified in traditional DNA sequencing methods.<br>Fusion Genes: RNA sequencing is capable of detecting fusion genes without the limitations of predefined probe sequences.<br>RNA Types: RNA sequencing allows for the characterization of various RNA types, such as mRNA and small regulatory RNAs.<br>Reduced Noise: RNA sequencing generates data with less noise compared to microarray-based assays.<br>New Transcripts: RNA sequencing can uncover new transcripts and coding regions that might not be detected through DNA sequencing. | RNA sequencing generally has a longer turnaround time compared to most DNA sequencing methods.<br>Choice of sampling methods can affect gene expression estimates and may also influence the sensitivity and specificity in detecting low-abundance transcripts. |
| Restriction fragment length polymorphism (RFLP) | Creates unique DNA profiles for individuals, making it especially effective for identifying common base pair variations.<br>It is widely used and standardized across various applications.<br>This method is reliable and relatively straightforward compared to other techniques.<br>It is also less susceptible to contamination from other DNA sources. | More challenging to automate.<br>Longer turnaround time compared to DNA sequencing.<br>Results are gene-specific, requiring knowledge of common mutations associated with that gene.<br>DNA degradation can lead to a higher likelihood of inconclusive results.<br>Requires computer analysis and significant data storage capacity.<br>Read lengths are short, typically between 50 and 300 base pairs.<br>Next-generation sequencing can identify various molecular abnormalities, though the clinical significance of many of these anomalies remains unclear. |

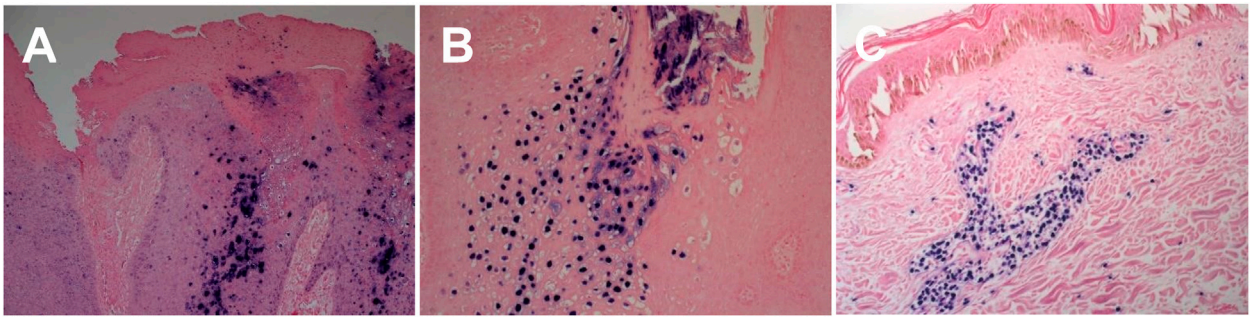


**FIGURE 4 |** Chromogenic In - situ hybridisation labelling in histological sections. **(A)** HPV High risk expression in cutaneous genital wart lesion (X20) **(B)** HPV Low risk expression in cutaneous genital wart lesion (X20) **(C)** EBV expression in cutaneous EBV positive lymphoma tissue section (X20).

noninfectious and infectious aetiology, localisation of infectious agents within tissues, host response to infection, and also infectious disease progression [75]. In addition to H&E sections, a variety of ancillary tests in the form of special stains and IHC can be employed to directly demonstrate infectious agents within skin biopsies, aiding in diagnosis (**Table 4**). These ancillary tests offer a relatively inexpensive and quick method towards the microscopic demonstration of pathogens within tissues and are used routinely within dermatopathology. However, many of these ancillary tests often exhibit several limitations, namely a low sensitivity, arising due to low bacterial load within tissues, poor staining, as well as other technical considerations leading to required further testing [70, 71]. Whilst the examination of histopathological preparations forms the basis of dermatopathology, it alone, is not always sufficient towards the definitive diagnosis of skin infections [76]. It does however, at the very least, provide initial guidance and infectious work-up, correlating with other concurrent laboratory tests such as microbiological cultures and prompting for molecular testing [75].

## Molecular Approaches for Infections in Dermatopathology

All pathogenic organisms have nucleic acid genomes which can be targeted by highly sensitive and specific molecular assays. Nucleic-acid-based amplification technologies (NAATs) such as PCR, along with several PCR-based variations, are some of the most widely used molecular methods for the detection of infectious pathogens and have seen much use over the last few decades [70–77]. The primary advantage of PCR-based methods is in the high level of sensitivity and specificity it provides, in a fast turnaround time, relative to other conventional methods relating to both microscopy and microbiological culturing. In addition to PCR, *in-situ* hybridisation (ISH) techniques can also be a viable alternative, particularly for viral infections [70, 77]. These ISH techniques utilise pathogen specific nucleic acid probes that can detect target pathogen DNA or RNA, in order to visualise infectious agents and their localisation within tissue sections, using chromogenic (CISH) or fluorescent labelling. Furthermore, CISH has the added advantage of being easily incorporated within the dermatopathology laboratory setting, utilising the same IHC platforms that are used routinely (**Figure 4**).

Sequencing technologies can also be employed on pathogen specific PCR amplicons, allowing for the simultaneous identification of pathogens at the species level in addition to the identification of drug resistant organisms [70, 75, 78, 79].

## Limitations of Molecular Techniques for Infections in Dermatopathology

Serology and fresh tissue cultures have traditionally served as the gold standard sample types for employing NAATs in pathogen detection. Whilst FFPE derived samples can be used for pathogen detection, it is associated with limitations that require further consideration for its appropriate use [70]. Molecular techniques such as PCR are not infallible and can be prone to false-positive findings when using FFPE derived samples, as a result of contamination during the numerous histological processing steps [70, 75]. Most importantly, FFPE derived samples are associated with false-negative findings that are a consequence of poor nucleic acid quality and lower yield. This is due to the degradation and alteration of nucleic acids due to resultant fixation and tissue processing leading to DNA fragmentation and formalin-induced sequence artefact [70, 75, 78, 79]. Furthermore, low presence of pathogens within FFPE tissues can also contribute to false-negative PCR results despite suggestive morphological features. As a result of these aforementioned limitations, a consensus review by Sunderkötter et al. outline the various indications, contraindications and key infectious scenarios to which NAATs should be appropriately requested as an adjunctive tool within the diagnostic workup, in order to prevent misinterpretation of results [70, 75]. In general, FFPE derived samples should be reserved for use as a "diagnostic rescue method" for NAATs, a scenario in which non-fixed samples can no longer be obtained from the patient, and or when slow growing or non-viable pathogens are suspected [70, 73, 74]. In these instances, adjunctive NAATs on FFPE sections can be vital to the diagnosis and worth conducting especially when infection is

suspected at a later stage by the pathologist. Examples of infections that have clear indications for NAATs on FFPE tissues include; *Mycobacterium leprae*, cutaneous leishmaniasis, *bartonella spp*., rickettsiosis and *treponema pallidum* [70, 71, 73, 75, 80] Other key encountered infections within the dermatopathology setting such as cutaneous tuberculosis, atypical *mycobacterium*, *borrelia* and other fungal and viral skin infections, may benefit from NAATs when requested on FFPE tissues, albeit with greater reservation [70, 71, 73, 75, 81]. However, close histological and clinical correlation is vital when requesting NAATs on FFPE samples to minimise the impact of these aforementioned limitations and subsequent misinterpretation of results and misdiagnosis [70, 75, 81]. **Table 4** provides a summary of relevant pathogens encountered in dermatopathology in which molecular techniques can be used to aid in diagnosis.

## Conclusion

There has been a steady rise in the application of molecular technologies within the field of dermatopathology. However there remains a requirement for extensive international collaboration to test applications and establish a broader base for clinical use generally [88–90]. The current literature is not robust enough in terms of large cohort studies to substantiated evidence for the application of most of these molecular biomarkers in a wider clinical setting [89, 90]. There is also a growing need to comply to *in vitro* diagnostic regulations (VDR) throughout Europe and this will increase the degree of rules and regulations on the use of these methodologies in diagnostic settings [82, 88].

The investment in novel equipment which can assist in the assessment of new molecular biomarkers is also constantly evolving with the development of innovative technology and near patient testing approaches [88]. Although these remain mainly applicable to the evaluation of infectious diseases currently [88]. The introduction of image analysis and the use of artificial intelligence, will accompany the rise in automation of complex molecular diagnostic assays. It will also improve the efficiency and enable faster assessment of patient material [91, 92].

The development of new and improved sampling techniques that are less invasive i.e., skin tapes, compared to conventionally employed tissue biopsies, are also set to expand [89]. It is also the case that these techniques will enable improved sensitivity and will rely on less patient DNA/ RNA being required for testing [89].

Of great interest will be the continual identification of new molecular biomarkers that are linked to prognostic outcomes, especially those associated with rare and unusual skin diseases such as epidermolysis bullosa (EB) [90]. These will expand our understanding of the disease processes still further.

Currently, many omics technologies have been utilised in the research setting to better understand cell populations in healthy and diseased states [88, 89]. Techniques such as spatial transcriptomics is a state-of-the-art technology with immense potential for future applications in various domains, such as medical research, cancer diagnostics, and therapeutic development [93, 94]. One of the most exciting uses is in cancer research, where it can analyse the intricate tumour microenvironment, revealing spatially distinct gene expression patterns that contribute to tumour growth and resistance to treatments [93, 94]. This insight can help identify new biomarkers for early detection and pave the way for highly targeted therapies, ultimately improving patient outcomes. This is particular key in many cancer and non-cancerous dermatological diseases [95, 96].

Moreover, spatial transcriptomics can enhance precision medicine by combining spatial gene expression data with other omics data, facilitating the creation of highly personalised treatment plans tailored to the unique spatial gene expression profiles of individual patients. This approach also has the potential to shed light on disease mechanisms, leading to more accurate therapeutic interventions. The potential integration of this techniques in routine practice could be a potential future development in dermatology.

Within the field of dermatology and more specifically dermatopathology there is a need to inform, educate and expand the repertoire of reliable and significantly validated tests that can be utilised within the diagnostic setting. There also needs to be clearer guidance and evidence-based research into potential biomarkers which will support the further development of new tests beyond the realm of research settings and into diagnostic prognostic and therapeutic applications. A number of new tests are yet to be validated in a diagnostic setting and as such remain academically interesting developments but as of yet not fully accepted in diagnostic practice. Ideally going forward there will be improved development in terms of new tests offering advanced sensitivity and specificity with the ultimate gain of improved patient care [97].

Molecular techniques represent a vital tool in the clinico-pathological correlation of skin disease states. The techniques and advances will enhance the information gleaned from conventional light microscope procedures that for so long have provided us with so much information on morphological criteria and disease processes and as a result will together continue to mould our diagnostic understanding (**Table 5**).

## AUTHOR CONTRIBUTIONS

All authors listed have made a substantial, direct, and intellectual contribution to the work and approved it for publication.

## FUNDING

The author(s) declare that no financial support was received for the research, authorship, and/or publication of this article.

## CONFLICT OF INTEREST

The authors declare that the research was conducted in the absence of any commercial or financial relationships that could be construed as a potential conflict of interest.

## REFERENCES


1. Kim H, Huh HJ, Park E, Chung D-R, Kang M. Multiplex Molecular Point of Care Test for Syndromic Infectious Diseases. *Biochip J* (2021) 15:14–22. doi:10.1007//s13206-021-00004-5
2. Kim H, Huh HJ, Park E, Chung DR, Kang M. Multiplex Molecular Point-of-Care Test for Syndromic Infectious Diseases. *Biochip J* (2021) 15(1):14–22. doi:10.1007/s13206021-00004-5
3. Long GV, Swetter SM, Menzies AM, Gershenwald JE, Scolyer RA. Cutaneous Melanoma. *Lancet* (2023) 402(10400):485–502. doi:10.1016/S01406736(23)00821-8
4. Elder DE, Bastian BC, Cree IA, Massi D, Scolyer RA. The 2018 World Health Organization Classification of Cutaneous, Mucosal, and Uveal Melanoma: Detailed Analysis of 9 Distinct Subtypes Defined by Their Evolutionary Pathway. *Arch Pathol Lab Med* (2020) 144(4):500–22. doi:10.5858/arpa.2019-0561-RA
5. Miedema J, Andea AA. Through the Looking Glass and What You Find There: Making Sense of Comparative Genomic Hybridization and Fluorescence In Situ Hybridization for Melanoma Diagnosis. *Mod Pathol* (2020) 33(7):1318–30. doi:10.1038/s41379020-0490-7
6. Bauer J, Bastian BC. Distinguishing Melanocytic Nevi from Melanoma by DNA Copy Number Changes: Comparative Genomic Hybridization as a Research and Diagnostic Tool. *Dermatol Ther* (2006) 19(1):40–9. doi:10.1111/j.15298019.2005.00055.x
7. Andea AA. Molecular Testing in Melanoma for the Surgical Pathologist. *Pathology* (2023) 55(2):245–57. doi:10.1016/j.pathol.2022.12.343
8. North JP, Vemula SS, Bastian BC. Chromosomal Copy Number Analysis in Melanoma Diagnostics. *Methods Mol Biol* (2014) 1102:199–226. doi:10.1007/978-162703-727-3_12
9. Kallioniemi A, Kallioniemi OP, Sudar D, Rutovitz D, Gray JW, Waldman F, et al. Comparative Genomic Hybridization for Molecular Cytogenetic Analysis of Solid Tumors. *Science* (1992) 258(5083):818–21. doi:10.1126/science.1359641
10. Bastian BC, Olshen AB, LeBoit PE, Pinkel D. Classifying Melanocytic Tumors Based on DNA Copy Number Changes. *Am J Pathol* (2003) 163(5):1765–70. doi:10.1016/S0002-9440(10)63536-5
11. Gerami P, Jewell SS, Morrison LE, Blondin B, Schulz J, Ruffalo T, et al. Fluorescence In Situ Hybridization (FISH) as an Ancillary Diagnostic Tool in the Diagnosis of Melanoma. *Am J Surg Pathol* (2009) 33(8):1146–56. doi:10.1097/PAS.0b013e3181a1ef36
12. Gerami P, Mafee M, Lurtsbarapa T, Guitart J, Haghighat Z, Newman M. Sensitivity of Fluorescence In Situ Hybridization for Melanoma Diagnosis Using RREB1, MYB, Cep6, and 11q13 Probes in Melanoma Subtypes. *Arch Dermatol* (2010) 146(3):273–8. doi:10.1001/archdermatol.2009.386
13. North JP, Vetto JT, Murali R, White KP, White CR, Jr, Bastian BC. Assessment of Copy Number Status of Chromosomes 6 and 11 by FISH Provides Independent Prognostic Information in Primary Melanoma. *Am J Surg Pathol* (2011) 35(8):1146–50. doi:10.1097/PAS.0b013e318222a634
14. Vergier B, Prochazkova-Carlotti M, de la Fouchardière A, Cerroni L, Massi D, De Giorgi V, et al. Fluorescence In Situ Hybridization, a Diagnostic Aid in Ambiguous Melanocytic Tumors: European Study of 113 Cases. *Mod Pathol* (2011) 24(5):613–23. doi:10.1038/modpathol.2010.228
15. Hsueh EC, DeBloom JR, Lee J, Sussman JJ, Covington KR, Middlebrook B, et al. Interim Analysis of Survival in a Prospective, Multi-Center Registry Cohort of Cutaneous Melanoma Tested With a Prognostic 31-gene Expression Profile Test. *J Hematol Oncol* (2017) 10(1):152. doi:10.1186/s13045-017-0520-1
16. Clarke LE, Flake DD2nd, Busam K, Cockerell C, Helm K, McNiff J, et al. An Independent Validation of a Gene Expression Signature to Differentiate Malignant Melanoma from Benign Melanocytic Nevi. *Cancer* (2017) 123(4):617–28. doi:10.1002/cncr.30385
17. Shah A, Hyngstrom J, Florell SR, Grossman D. Use of the Pigmented Lesion Assay to Rapidly Screen a Patient With Numerous Clinically Atypical Pigmented Lesions. *JAAD Case Rep* (2019) 5(12):1048–50. doi:10.1016/j.jdcr.2019.10.004
18. Gerami P, Yao Z, Polsky D, Jansen B, Busam K, Ho J, et al. Development and Validation of a Noninvasive 2-Gene Molecular Assay for Cutaneous Melanoma. *J Am Acad Dermatol* (2017) 76(1):114–20.e2. doi:10.1016/j.jaad.2016.07.038
19. Chapman PB, Hauschild A, Robert C, Haanen JB, Ascierto P, Larkin J, et al. Improved Survival with Vemurafenib in Melanoma With BRAF V600E Mutation. *N Engl J Med* (2011) 364(26):2507–16. doi:10.1056/NEJMoa1103782
20. Flaherty KT, Infante JR, Daud A, Gonzalez R, Kefford RF, Sosman J, et al. Combined BRAF and MEK Inhibition in Melanoma with BRAF V600 Mutations. *N Engl J Med* (2012) 367(18):1694–703. doi:10.1056/NEJMoa1210093
21. Delyon J, Lebbe C, Dumaz N. Targeted Therapies in Melanoma Beyond BRAF: Targeting NRAS-Mutated and KIT-Mutated Melanoma. *Curr Opin Oncol* (2020) 32(2):79–84. doi:10.1097/CCO.0000000000000606
22. Cancer Genome Atlas Network. Genomic Classification of Cutaneous Melanoma. *Cell.* (2015) 161(7):1681–96. doi:10.1016/j.cell.2015.05.044
23. Ohsie SJ, Sarantopoulos GP, Cochran AJ, Binder SW. Immunohistochemical Characteristics of Melanoma. *J Cutan Pathol* (2008) 35(5):433–44. doi:10.1111/j.1600-0560.2007.00891.x
24. Ho J, Collie CJ. What's New in Dermatopathology 2023: WHO 5th Edition Updates. *J Pathol Transl Med* (2023) 57(6):337–40. doi:10.4132/jptm.2023.09.22
25. Orchard GE, Wojcik K, Rickaby W, Martin B, Semkova K, Shams F, et al. Immunohistochemical Detection of V600E BRAF Mutation Is a Useful Primary Screening Tool for Malignant Melanoma. *Br J Biomed Sci* (2019) 76(2):77–82. doi:10.1080/09674845.2019.1592885
26. Cancer Intelligence Statistical Information Team. Cancer Incidence From Cancer Intelligence Statistical Information Team at Cancer Research UK (2016 - 2018 UK Average) (2023). Available from: https://www.cancerresearchuk.org/healthprofessional/cancer-statistics/statistics-by-cancer-type/non-hodgkin-lymphoma (Accessed February, 2024).
27. Sadaf H, Ambroziak M, Binkowski R, Kluebsoongnoen J, Paszkiewicz-Kozik E, Steciuk J, et al. New Molecular Targets in Hodgkin and Reed-Sternberg Cells. *Front Immunol* (2023) 14:1155468. doi:10.3389/fimmu.2023.1155468
28. Weniger MA, Küppers R. Molecular biology of Hodgkin lymphoma. *Leukemia* (2021) 35:968–981. doi:10.1038/s41375-021-01204-6
29. Tousseyn TA, King RL, Fend F, Feldman AL, Brousset P, Jaffe ES. Evolution in the Definition and Diagnosis of the Hodgkin Lymphomas and Related Entities. *Virchows Arch* (2023) 482(1):207–26. doi:10.1007/s00428-022-03427-z
30. Badheeb AM, Ahmed F, Elhadi M, Alyami N, Badheeb MA. Clinical and Therapeutic Profile of Non-hodgkin's Lymphoma: A Retrospective Study from a Najran Oncology Center. *Cureus* (2023) 15(6):e40125. doi:10.7759/cureus.40125
31. Glenn ST, Galbo PM, Jr, Luce JD, Miles KM, Singh PK, Glynias MJ, et al. Development and Implementation of an Automated and Highly Accurate Reporting Process for NGS-Based Clonality Testing. *Oncotarget* (2023) 14:450–61. doi:10.18632/oncotarget.28429
32. Seçme M, Dodurga Y, Çallı Demirkan N, Kaçar N, Günel NS, Açıkbaş İ, et al. Determination of T-Cell Clonality and Expression Profiles of Toll-Like Receptors Signaling Pathway Genes and Related miRNAs in Patients with Mycosis Fungoides. *Gene* (2024) 891:147825. doi:10.1016/j.gene.2023.147825
33. Tavarozzi R, Zacchi G, Pietrasanta D, Catania G, Castellino A, Monaco F, et al. Changing Trends in B-Cell Non-Hodgkin Lymphoma Treatment: The Role of Novel Monoclonal Antibodies in Clinical Practice. *Cancers (Basel)* (2023) 15(22):5397. doi:10.3390/cancers15225397
34. Willemze R, Cerroni L, Kempf W, Berti E, Facchetti F, Swerdlow SH, et al. The 2018 Update of the WHO-EORTC Classification for Primary Cutaneous Lymphomas. *Blood* (2019) 133:1703–14. doi:10.1182/blood-2018-11-881268
35. Kawada JI, Ito Y, Ohshima K, Yamada M, Kataoka S, Muramatsu H, et al. Updated Guidelines for Chronic Active Epstein-Barr Virus Disease. *Int J Hematol* (2023) 118(5):568–76. doi:10.1007/s12185-023-03660-5
36. Shimada K, Yoshida K, Suzuki Y, Iriyama C, Inoue Y, Sanada M, et al. Frequent Genetic Alterations in Immune Checkpoint-Related Genes in Intravascular Large B-Cell Lymphoma. *Blood* (2021) 137(11):1491–502. doi:10.1182/blood.2020007245

37. Sakihama S, Karube K. Genetic Alterations in Adult T-Cell Leukemia/lymphoma: Novel Discoveries with Clinical and Biological Significance. *Cancers (Basel)* (2022) 14(10):2394. doi:10.3390/cancers14102394
38. Gonzalez-Farre B, Ramis-Zaldivar JE, Castrejón de Anta N, Rivas-Delgado A, Nadeu F, Salmeron-Villalobos J, et al. Intravascular Large B-Cell Lymphoma Genomic Profile Is Characterized by Alterations in Genes Regulating NF-Kb and Immune Checkpoints. *Am J Surg Pathol* (2023) 47(2):202–11. doi:10.1097/PAS.0000000000001978
39. Xiao A, Beatty CJ, Choudhary S, Akilov OE. CD5+ Primary Cutaneous Diffuse Large B-Cell Lymphoma, Leg Type, Presenting as an Asymptomatic Nodule. *Hematol Rep* (2023) 15(3):513–7. doi:10.3390/hematolrep15030053
40. Alvarez G, Rodriguez-Homs L, Al-Rohil RN, Kheterpal M, Fresco A. Sequential Primary Cutaneous Follicle Center Lymphoma and Marginal Zone B-Cell Lymphoma Arising in the Same Patient. *JAAD Case Rep* (2023) 40:30–3. doi:10.1016/j.jdcr.2023.07.028
41. Miyagaki T. Diagnosis and Prognostic Stratification of Cutaneous Lymphoma. *J Dermatol* (2022) 49(2):210–22. doi:10.1111/1346-8138.16099
42. Trivedi N, Padhiyar J, Patel N, Gandhi S. A Case Report of Double Positive Peripheral T Cell Lymphoma Not Otherwise Specified in a Young Pregnant Female. *Indian Dermatol Online J* (2022) 13(1):98–101. doi:10.4103/idoj.IDOJ_78_21
43. Olsen EA, Whittaker S, Willemze R, Pinter-Brown L, Foss FM, Geskin LJ, et al. Primary Cutaneous Lymphoma: Recommendations for Clinical Trial Design and Staging Update From the ISCL, USCLC, and EORTC. *Blood* (2021) 140:419–37. doi:10.1182/blood.2021012057
44. Sánchez-Romero C, Bologna-Molina R, Paes de Almeida O, Santos-Silva AR, Prado-Ribeiro AC, Brandão TB, et al. Extranodal NK/T Cell Lymphoma, Nasal Type: An Updated Overview. *Crit Rev Oncol Hematol* (2021) 159:103237. doi:10.1016/j.critrevonc.2021.103237
45. Luo H, Yuan Z, Qin B. Case Report: Chronic Active Epstein-Barr Virus Infection With Subcutaneous Nodules and Systemic Damage. *Front Med (Lausanne)* (2022) 9:759834. doi:10.3389/fmed.2022.759834
46. Stein T, Robak T, Biernat W, Robak E. Primary Cutaneous CD30-Positive Lymphoproliferative Disorders-Current Therapeutic Approaches With a Focus on Brentuximab Vedotin. *J Clin Med* (2024) 13(3):823. doi:10.3390/jcm13030823
47. Yamashita Y, Wang X, Kawakami H, Haga H, Takimoto-Shimomura T, Sakata-Yanagimoto M. Liquid Biopsy Reveals a Case of Peripheral T-Cell Lymphoma, Not Otherwise Specified With a Novel Chromosomal Translocation, T (2; 8) P12; P21. *Int J Hematol* (2021) 113(6):912–6. doi:10.1007/s12185-021-03106-5
48. Scherer F. Capturing Tumor Heterogeneity and Clonal Evolution by Circulating Tumor DNA Profiling. *Cancer Res* (2020) 215:213–30. doi:10.1007/978-3030-26439-0_11
49. Nikanjam M, Kato S, Kurzrock R. Liquid Biopsy: Current Technology and Clinical Applications. *J Hematol Oncol* (2022) 15(1):131. doi:10.1186/s13045-02201351-y
50. Sardarabadi P, Kojabad AA, Jafari D, Liu CH. Liquid Biopsy-Based Biosensors for MRD Detection and Treatment Monitoring in Non-Small Cell Lung Cancer (NSCLC). *Biosensors (Basel).* (2021) 11(10):394. doi:10.3390/bios11100394
51. Omar U, Grover N, Tomar S, Bhalla K, Singh S. Liquid Biopsy and its Significance in Tumour Detection in the Field of Pathology. *J Oral Maxillofac Pathol* (2023) 27(1):195–200. doi:10.4103/jomfp.jomfp_251_22
52. Satam H, Joshi K, Mangrolia U, Waghoo S, Zaidi G, Rawool S, et al. Next-generation Sequencing Technology: Current Trends and Advancements. *Biology (Basel)* (2023) 12(7):997. doi:10.3390/biology12070997
53. Jia Q, Chu H, Jin Z, Long H, Zhu B. High-Throughput Single-Cell Sequencing in Cancer Research. *Signal Transduct Target Ther* (2022) 7:145. doi:10.1038/s41392-022-00990-4
54. Pham HT, Morrison AJ, Scholz J, Sweeney J, Nicolae A, Vierthaler M, et al. HER3-Receptor-Mediated STAT3 Activation Plays a Central Role in Adaptive Resistance toward Vemurafenib in Melanoma. *Cancers* (2020) 12(12):3761. doi:10.3390/cancers12123761
55. Song TL, Nairismägi ML, Carlson LE, Walker LM, Campbell TS. Potentially Modifiable Factors Associated with Adherence to Adjuvant Endocrine Therapy Among Breast Cancer Survivors: A Systematic Review. *Cancers* (2021) 13(1):107. doi:10.3390/cancers13010107
56. Gudjonsson JE, Kabashima K, Eyerich K. Mechanisms of Skin Autoimmunity: Cellular and Soluble Immune Components of the Skin. *J Allergy Clin Immunol* (2020) 146(1):8–16. doi:10.1016/j.jaci.2020.05.009
57. Abdallah HY, Faisal S, Tawfik NZ, Soliman NH, Kishk RM, Ellawindy A. Expression Signature of Immune-Related MicroRNAs in Autoimmune Skin Disease: Psoriasis and Vitiligo Insights. *Mol Diagn Ther* (2023) 27(3):405–23. doi:10.1007/s40291-023-00646-1
58. Has C, Liu L, Bolling MC, Charlesworth AV, Hachem E, Escámez M, et al. Clinical Practice Guidelines for Laboratory Diagnosis of Epidermolysis Bullosa. *The Br J Dermatol* (2022) 182(3):574–92. doi:10.1111/bjd.18128
59. Kotalevskaya YY, Stepanov VA. Molecular Genetic Basis of Epidermolysis Bullosa. *Vavilovskii Zhurnal Genet Selektsii* (2023) 27(1):18–27. doi:10.18699/VJGB-23-04
60. Mariath LM, Kiszewski AE, Frantz JA, Siebert M, Matte U, SchulerFaccini L. Gene Panel for the Diagnosis of Epidermolysis Bullosa: Proposal for a Viable and Efficient Approach. *An Bras Dermatol* (2021) 96(2):155–62. doi:10.1016/j.abd.2020.05.015
61. Fine JD, Mellerio JE. Extracutaneous Manifestations and Complications of Inherited Epidermolysis Bullosa: Part I. Epithelial Associated Tissues. *J Am Acad Dermatol* (2009) 61:367–86. doi:10.1016/j.jaad.2009.03.052
62. Feinstein JA, Jambal P, Peoples K, Lucky AW, Khuu P, Tang JY, et al. Assessment of the Timing of Milestone Clinical Events in Patients With Epidermolysis Bullosa From North America. *JAMA Dermatol* (2019) 155:196–203. doi:10.1001/jamadermatol.2018.4673
63. Porro AM, Arai Seque C, Miyamoto D, Vanderlei Medeiros da Nóbrega D, Simões E, Santi CG. Hailey-Hailey Disease: Clinical, Diagnostic and Therapeutic Update. *A Bras Dermatol* (2024) 99(5):651–61. doi:10.1016/j.abd.2023.12.003
64. Chiorean R, Danescu S, Virtic O, Mustafa MB, Baican A, Lischka A, et al. Molecular Diagnosis of Anti-laminin 332 (Epiligrin) Mucous Membrane Pemphigoid. *Orphanet J Rare Dis* (2018) 13:111. doi:10.1186/s13023-018-0855-x
65. Otten JV, Hashimoto T, Hertl M, Payne AS, Sitaru C. Molecular Diagnosis in Autoimmune Skin Blistering Conditions. *Curr Mol Med* (2014) 14:69–95. doi:10.2174/1566524013136660079
66. Tešanović Perković D, Bukvić Mokos Z, Marinović B. Epidermolysis Bullosa Acquisita-Current and Emerging Treatments. *J Clin Med* (2023) 12(3):1139. doi:10.3390/jcm12031139
67. Egan CA, Lazarova Z, Darling TN, Yee C, Coté T, Yancey KB. Antiepiligrin Cicatricial Pemphigoid and Relative Risk for Cancer. *Lancet*. (2001) 357:1850–1. doi:10.1016/S0140-6736(00)04971-0
68. Yilmaz K, Goletz S, Pas HH, van den Bos RR, Blauvelt A, White WL, et al. Clinical and Serological Characterization of Orf-Induced Immunobullous Disease. *JAMA Dermatol* (2022) 158(6):670–4. doi:10.1001/jamadermatol.2022.0290
69. Mao X, Yamagami J, Pan M. Editorial: Mechanism and Therapy of Autoimmune Skin Diseases. *Front Med* (2023) 10:1143454. doi:10.3389/fmed.2023.1143454
70. Sunderkötter C, Becker K, Kutzner H, Meyer T, Blödorn-Schlicht N, Reischl U, et al. Molecular Diagnosis of Skin Infections Using Paraffin-embedded Tissue – Review and Interdisciplinary Consensus. *J Deutsche Derma Gesell* (2018) 16(2):139–47. doi:10.1111/ddg.13438
71. Kempf W, Flaig MJ, Kutzner H. Molecular Diagnostics in Infectious Skin Diseases. *J Deutsche Derma Gesell* (2013) 11(s4):50–8. doi:10.1111/ddg.12069_supp
72. Parkhi M, Kumar SM, De D, Yadav R, Sethi S, Radotra BD, et al. Diagnostic Utility of Biplex/Multiplex Polymerase Chain Reaction in Infectious Granulomatous Dermatitis in North Indian Population. *Am J Dermatopathology* (2020) 43(8):567–73. doi:10.1097/DAD.0000000000001878
73. Chen X, Xing Y, He J, Tan F, You Y, Wen Y. Develop and Field Evolution of Single Tube Nested PCR, SYBRGreen PCR Methods, for the Diagnosis of Leprosy in Paraffin-Embedded Formalin Fixed Tissues in Yunnan Province, a Hyper Endemic Area of Leprosy in China. *Plos Negl Trop Dis* (2019) 13(10):e0007731. doi:10.1371/journal.pntd.0007731
74. Podbićanin-Ziburt A, Falk TM, Metze D, Böer-Auer A. Diagnosis of Lyme Borreliosis With a Novel, Seminested Real-Time Polymerase Chain Reaction Targeting the 5S-23S Intergenic Spacer Region: Clinical Features, Histopathology, and Immunophenotype in 44 Patients. *The Am J Dermatopathology* (2021) 44:338–47. doi:10.1097/DAD.0000000000002119

75. Laga AC. Update in Infectious Disease Diagnosis in Anatomic Pathology. *Clin Lab Med* (2020) 40(4):565–85. doi:10.1016/j.cll.2020.08.012
76. Marrero RM. Histopathology of Infectious Diseases: A Practical Approach to Slide Examination and Interpretation: Part I or II. *Clin Microbiol Newsl* (2023) 45(20):167–76. doi:10.1016/j.clinmicnews.2024.01.001
77. Hosler GA, Murphy KM. *Molecular Diagnostics for Dermatology*. Springer eBooks. Springer Nature (2014).
78. Frickmann H, Künne C, Hagen RM, Podbielski A, Normann J, Poppert S, et al. Next-generation Sequencing for Hypothesis-Free Genomic Detection of Invasive Tropical Infections in Poly-Microbially Contaminated, Formalin-Fixed, Paraffin-Embedded Tissue Samples – A Proof-Of-Principle Assessment. *BMC Microbiol* (2019) 19(1):75. doi:10.1186/s12866-019-1448-0
79. Nienhold R, Mensah N, Frank A, Graber A, Koike J, Schwab N, et al. Unbiased Screen for Pathogens in Human Paraffin-Embedded Tissue Samples by Whole Genome Sequencing and Metagenomics. *Front Cell Infect Microbiol* (2022) 12: 968135. doi:10.3389/fcimb.2022.968135
80. Thakur S, Joshi J, Kaur S. Leishmaniasis Diagnosis: An Update on the Use of Parasitological, Immunological and Molecular Methods. *J Parasitic Dis* (2020) 44(2):253–72. doi:10.1007/s12639-020-01212-w
81. Howell SA. Dermatopathology and the Diagnosis of Fungal Infections. *Br J Biomed Sci* (2023) 80:11314. doi:10.3389/bjbs.2023.11314
82. Rosa MFde AP, Quintella LP, Ferreira LC, Cuzzi T. Immunohistochemical Detection of Treponema pallidum in Skin Samples with Clinical and Histopathological Correlations and Warthin-Starry Staining Critical Analysis. *Anais Brasileiros de Dermatologia* (2023) 98(4):480–6. doi:10.1016/j.abd.2022.02.008
83. Jensen E. Technical Review: *In situ* Hybridization. *Anat Rec (Hoboken)* (2014) 297(8):1349–53. doi:10.1002/ar.22944
84. Nouri-Aria KT. *In situ* Hybridization. *Methods Mol Med* (2008) 138:331–47. doi:10.1007/978-1-59745-366-0_27
85. Liu HY, Hopping GC, Vaidyanathan U, Ronquillo YC, Hoopes PC, Moshirfar M. Polymerase Chain Reaction and its Application in the Diagnosis of Infectious Keratitis. *Med Hypothesis Discov Innov Ophthalmol* (2019) 8(3):152–5.
86. Garibyan L, Avashia N. Polymerase Chain Reaction. *J Invest Dermatol* (2013) 133(3):1–4. doi:10.1038/jid.2013.1
87. Hashim HO, Al-Shuhaib MB. Exploring the Potential and Limitations of PCRRFLP and PCR-SSCP for SNP Detection: A Review. *J Appl Biotechnol Rep* (2019) 6(4):137–44. doi:10.29252/JABR.06.04.02
88. Gebhardt C, Eyerich K, Garzorz-Stark N. Status Quo And Future Perspectives of Molecular Diagnostics in Dermatology. *J der.Deutschen Dermatologischen Gesellschaft* (2023) 21(4):415–8. doi:10.1111/ddg.15010
89. Lyubchenko T, Collins Hk., Goleva E, Donald Y, Leung M. Skin Tape Sampling Technique Identifies Proinflammatory Cytokines in Atopic Dermatitis Skin. *Ann Allergy Asthma Immunol* (2021) 126(1):46–53.e2. doi:10.1016/j.anai,2020.08.397
90. Kup T-C, Wang P-H, Wang Y-ke, Chang C-I, Chang C-Y, Tseng YJ. RSDB: A Rare Skin Disease Database to Link Drugs With Potential Drug Targets for Rare Skin Diseases. *Sci Data* (2022) 9:521–7. doi:10.1038/s41597-022-01654-2
91. McGenity C, Clarke EL, Jennings C, Matthews G, Cartlidge C, FreduahAgyemang H, et al. Artificial Intelligence in Digital Pathology: A Systematic Review and Meta-Analysis of Diagnostic Test Accuracy. *NPJ Digit Med* (2024) 7(1):114. doi:10.1038/s41746-024-01106-8
92. Abdelsamea MM, Zidan U, Senousy Z, Gaber MM, Rakha E, Ilyas M. A Survey on Artificial Intelligence in Histopathology Image Analysis. *WIREs Data Min Knowl* (2022) 12. doi:10.1002/widm.1474
93. Williams CG, Lee HJ, Asatsuma T, Vento-Tormo R, Haque A. An Introduction to Spatial Transcriptomics for Biomedical Research. *Genome Med* (2022) 14(1):68. doi:10.1186/s13073-022-01075-1
94. Ganier C. Unlocking Skin's Symphony: Single-Cell and Spatial Transcriptomics Reveal the Harmonious Interplay Among Diverse Cell Populations. *J Invest Dermatol* (2024) 144(9):1917–20. doi:10.1016/j.jid.2024.01.039
95. Francis L, McCluskey D, Ganier C, Jiang T, Du-Harpur X, Gabriel J, et al. Single-Cell Analysis of Psoriasis Resolution Demonstrates an Inflammatory Fibroblast State Targeted by IL-23 Blockade. *Nat Commun* (2024) 15(1):913. doi:10.1038/s41467-024-44994-w
96. Ganier C, Mazin P, Herrera-Oropeza G, Du-Harpur X, Blakeley M, Gabriel J, et al. Multiscale Spatial Mapping of Cell Populations across Anatomical Sites in Healthy Human Skin and Basal Cell Carcinoma. *Proc Natl Acad Sci U S A* (2024) 121(2):e2313326120. doi:10.1073/pnas.2313326120
97. Tizek L, Schuster B, Gebhardt C, Reich K, von Kiedrowski R, Biedermann T, et al. Molecular Diagnostics in Dermatology: An Online Survey to Study Usage, Obstacles and Requirements in Germany. *J Dtsch Dermatol Ges* (2022) 20(3):287–95. doi:10.1111/ddg.14659

IBMS Institute of Biomedical Science | BJBS

ORIGINAL RESEARCH
published: 19 March 2024
doi: 10.3389/bjbs.2024.12319

# Double Immunohistochemical Labelling of PRAME and Melan A in Slow Mohs Biopsy Margin Assessment of Lentigo Maligna and Lentigo Maligna Melanoma

*R. Salih*[*†], *F. Ismail* and *G. E. Orchard*[†]

*St. John's Histopathology Department, Synnovis Analytics, St. Thomas' Hospital, London, United Kingdom*

**Introduction:** Lentigo maligna (LM) and lentigo maligna melanoma (LMM) predominantly affect the head and neck areas in elderly patients, presenting as challenging ill-defined pigmented lesions with indistinct borders. Surgical margin determination for complete removal remains intricate due to these characteristics. Morphological examination of surgical margins is the key form of determining successful treatment in LM/LMM and underpin the greater margin control provided through the Slow Mohs micrographic surgery (SMMS) approach. Recent assessments have explored the use of immunohistochemistry (IHC) markers, such as Preferentially Expressed Antigen in Melanoma (PRAME), to aid in LM/LMM and margin evaluation, leveraging the selectivity of PRAME labelling in malignant melanocytic neoplasms.

**Methods:** A Novel double-labelling (DL) method incorporating both PRAME and MelanA IHC was employed to further maximise the clinical applicability of PRAME in the assessment of LM/LMM in SMMS biopsies. The evaluation involved 51 samples, comparing the results of the novel DL with respective single-labelling (SL) IHC slides.

**Results:** The findings demonstrated a significant agreement of 96.1% between the DL method and SL slides across the tested samples. The benchmark PRAME SL exhibited a sensitivity of 91.3% in the SMMS specimens and 67.9% in histologically confirmed positive margins.

**Discussion:** This study highlights the utility of PRAME IHC and by extension PRAME DL as an adjunctive tool in the assessment of melanocytic tumours within staged excision margins in SMMS samples.

**Keywords: immunohistochemistry, slow Mohs micrographic surgery (SMMS), PRAME, Melan A, lentigo maligna (LM) lentigo maligna melanoma (LMM)**



***Correspondence**
*R. Salih,*
*rasiyan.salih@gstt.nhs.uk*

**†ORCID:**
*R. Salih*
*orcid.org/0009-0000-6253-5113*
*G. E. Orchard*
*orcid.org/0000-0002-4757-022*

***Received:*** *27 October 2023*
***Accepted:*** *05 March 2024*
***Published:*** *19 March 2024*

***Citation:***
*Salih R, Ismail F and Orchard GE (2024) Double Immunohistochemical Labelling of PRAME and Melan A in Slow Mohs Biopsy Margin Assessment of Lentigo Maligna and Lentigo Maligna Melanoma. Br J Biomed Sci 81:12319. doi: 10.3389/bjbs.2024.12319*

## INTRODUCTION

Lentigo maligna (LM) is a unique subtype of melanoma *in situ* (MIS), distinguished by its lentiginous growth pattern observed in chronically sun-damaged skin. If an LM lesion becomes invasive, it is no longer confined to the epidermis and can no longer be considered MIS. This invasive form of LM is subsequently referred to as Lentigo Maligna Melanoma (LMM), which acquires a comparable prognosis to other forms of invasive melanomas when comparing Breslow thickness [1].

The histologically assessed surgical removal of the lesion is the primary form of treatment with both wide local excision (WLE), and more specialised staged excision (SE) approaches such as the Mohs Micrographic Surgery (MMS) technique, having been described [2]. However, prior studies have shown that the superior margin control expressed through specialised SE approaches such as MMS, proves to be superior to traditional WLE methods, when treating LM/LMM lesions of patients that present on the head and neck [3, 4]. This is evident in the lower local recurrence rates of 0.61% by MMS when compared to 7.8% by WLE when used to treat cutaneous head and neck melanomas [4]. Furthermore, only 1% of total margins are evaluated through WLE with subsequent vertical sectioning, which is in comparison to the 100% complete demonstration of both deep and peripheral margins offered by MMS [5]. The superior margin control offered by MMS, coupled with the tailored-to-tumour surgical removal of tissue allowing for greater cosmetic consideration, makes the MMS approach particularly suited for treating LM and LMM patients presenting on the head and neck regions [5]. This has led to MMS becoming the standard of care for LM patients, in particular when manifesting in the most common cosmetically-sensitive regions such as the head and neck [2].

In the case of in-situ melanomas such as LM, a variant of the MMS technique known as the "slow" Mohs procedure is typically employed [5, 6]. This alternate method utilises the same lesional mapping and staged surgical approach to traditional frozen sectioning MMS, but with the addition of permanent formalin-fixed paraffin-embedded (FFPE) processing for each Mohs layer, forgoing the use of frozen sections entirely. This longer FFPE excursion is essential for providing the gold standard morphological visualisation of melanocytic lesions that is free from the interpretational and artefactual challenges that is often associated with frozen sections [5]. In addition, routine immunohistochemistry (IHC) adjunct labelling can also be used with FFPE samples in order to aid in LM/LMM margin assessment by reporting pathologists.

A number of IHC "melanocytic markers," such as SOX10 and Melanoma antigen recognised by T cells (MART-1 or Melan A), have been delineated to directly detect and visualise melanocytes in the skin through differing labelling patterns, both nuclear and cytoplasmic respectively. These markers can potentially facilitate the diagnosis of LM or the assessment of residual LM in surgical margins within the sun-damaged skin setting. Both SOX10 and Melan A can be used to determine a prime parameter; the cellularity or density of melanocytes within slow Mohs sections, which can help facilitate residual LM/LMM identification and by extension, margin clearance [7].

It is important to note however that markers such as SOX-10 and Melan A, whilst they have their usage in LM studies, they both lack the ability to differentiate malignant from benign melanocytes. This labelling of "all" melanocytes, significantly limits their use in differentiating LM from its mimics [8]. However, Preferentially expressed Antigen in MElanoma (PRAME), has been the subject of intense study within the last 5 years, having shown promise in this regard [7–17]. Studies have showed differential PRAME expression within benign and malignant melanocytes, showing high expression in a variety of malignant melanocyte populations—in particular, melanoma and in-situ melanomas such as LM/LMM, with contrasting little to no expression in benign entities such as melanocytic nevi [8–11]. This denotes a differential PRAME expression and specificity towards malignant melanocytes, as opposed to traditional melanocyte markers such as Melan A and SOX-10, that do not discriminate and label all melanocyte populations, both benign and malignant, in varying labelling profiles.

A Key study by Lezcano et al. (2018) sought to evaluate the utility of PRAME IHC as a potentially useful adjunct tool for the assessment of melanocytic tumours, showing early yet promising evidence for PRAME IHC as a useful adjunctive tool within both melanoma and margin assessment studies [9]. Since then, many others have sought to evaluate PRAME using a variety of approaches and subject matter, seeking to further elucidate the strengths, limitations and pitfalls of PRAME IHC focusing on the differentiation of benign and malignant melanocytic entities [7–18].

Most congruously, some recent studies have explored the potential for PRAME nuclear labelling, to be used in various double-labelling methods, combined with cytoplasmic HMB-45 or Melan A, in order to further enhance the utility of PRAME within melanocytic investigations [7, 8, 11–13].

This study will seek to determine the utility of PRAME IHC by establishing the sensitivity of PRAME SL within the novel application of LM/LMM SMMS biopsies. The study will also seek to demonstrate and directly compare a novel PRAME/Melan A DL protocol to the aforementioned PRAME SL benchmark for agreement. This is to determine whether PRAME/Melan A DL IHC can be used as a useful alternative to PRAME SL IHC, providing additional information through cytoplasmic Melan A labelling, within the same section. Once established, the novel DL could therefore be used as an adjunct to H&E routine morphology within SMMS LM/LMM margin assessment.

# MATERIALS AND METHODS

## Case Selection and Histological Characteristics

Records from the dermatopathology Laboratory at St. John's Institute of Dermatology were searched for Slow Mohs excision biopsies from 2020 to 2022 for cases diagnosed with LM/LMM. A total of 23 anonymised LM/LMM slow Mohs cases were selected. Of all 23 cases, the histological characteristics of 15/23 de-bulk sections and 22/28 positive margin sections were available within the pathology reports examined. Within each of the applicable reports examined, the use of several histological features supporting LM/LMM were tabulated and are summarised in **Table 1**. The 3 highest histological features in support of LM found within the reports to describe both de-bulk and positive margins respectively were pleomorphism/atypia (100%/100%), increased number of melanocytes (86.7%/91%) and confluency (60%/77.3%). Other features such as adnexal involvement (33%/31.8%) and nest formation (20%/22.27%) were less frequent. From these cases, a total of 51 formalin-fixed paraffin-embedded (FFPE) blocks, comprised of 23 de-bulk

**TABLE 1 |** Summary of the histological characteristics of LM/LMM cases examined.

| H&E morphological criteria used for LM/LMM diagnosis | De-bulk *N* = 15 | Positive margins *N* = 22 |
|---|---|---|
| Aytpia/pleiomorphism | 15 (100%) | 22 (100%) |
| Increased number of melanocytes | 13 (86.7% | 20 (91%) |
| Irregular pigment deposition | 1 (6.7% | 0 |
| Pagetiod spread | 1 (6.7%) | 2 (9.1%) |
| Epidermal atrophy/effacement | 2 (13.3%) | 2 (9.1%) |
| confluency | 9 (60%) | 17 (77.3%) |
| Nest formation | 3 (20% | 5 (22.7%) |
| Adnexal involvement | 5 (33.3%) | 7 (31.8%) |

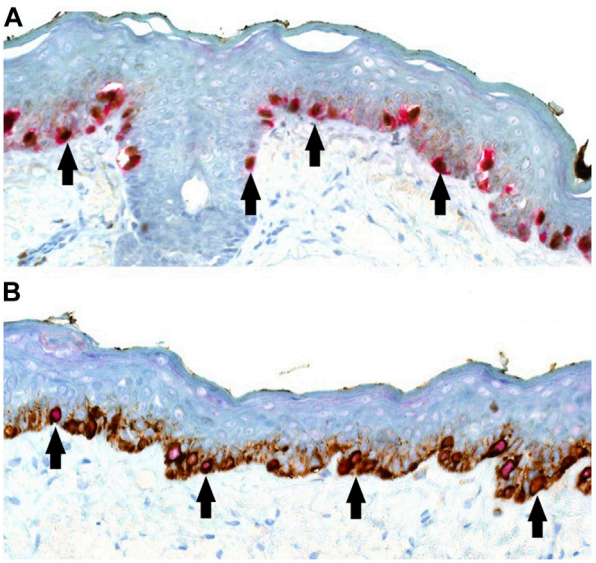


**FIGURE 1 | (A,B)** PRAME/Melan A double labelling within LM control sections (×20 magnification) demonstrating possible visual outcomes depending on chromogen selection. **(A)** Alternative PRAME nuclear labelling in brown, combined with Melan A cytoplasmic labelling in red. **(B)** Showing the selected method of PRAME with red nuclear labelling, combined with brown Melan A cytoplasmic labelling of respective LM melanocytes. For both chromogen arrangements, double-labelled melanocytes are shown with arrows.

and 28 histologically confirmed positive margins were incorporated within the study. For larger cases, more than one histologically positive margin FFPE block was used. All Blocks were labelled with letters corresponding to the respective sections of each histology report for histological correlation. Given the retrospective nature of the study, each of these blocks were stained with an initial H&E to ensure block viability and relevance to the anonymised histology reports provided, which were checked by Consultant BMS GEO. All further IHC tests, Melan A SL IHC, PRAME SL IHC, and PRAME/Melan A IHC DL were performed on serially sectioned slides for direct comparison.

## Test Selection and Technical Considerations

PRAME/Melan A DL IHC combines Melan A cytoplasmic labelling to highlight all melanocyte populations within a section, with the added nuclear labelling of PRAME to label "malignant" melanocytes. This allows for the visualisation of dual-labelled malignant melanocytes alongside benign melanocytes labelled with Melan A in the same section.

At present, there is no existing literature regarding the utilisation of PRAME/Melan A DL IHC in the context of margin assessment for SMMS biopsies within LM/LMM. As a result, the current study has utilised the established PRAME SL IHC as the benchmark for clinical correlation, alongside the novel DL method in parallel for establishing agreement between both methods. Melan A SL IHC were run in parallel in order to validate the Melan A component of the DL.

In addition to IHC stains, H&E staining was also used for demonstrating the morphology and histological criteria of LM/LMM.

All slides and tests were generated in a serial manner for accurate interpretation and juxtaposition of photography. An

**TABLE 2 |** PRAME SL IHC labelling results obtained from the analysis of 23 LM/LMM slow mohs cases. Cases were broken down into 23 de-bulk sections (one for each case) and a collection of 28 histologically positive margins across the 23 cases incorporated. PRAME was only concluded as positive or "diffuse" if +4 (>75% of lesional cells) threshold was met.

| LM positive sections *n* = 51 | PRAME IHC labelling criteria denoted as a percentage of labelled lesional tumour nuclei | | | | |
|---|---|---|---|---|---|
| | Negative 0 (0%) | +1 (1%–25%) | +2 (25%–50%) | +3 (51%–75%) | Positive (>75%) "diffuse" |
| De-bulk sections (*n* = 23) | 1[a] | 0 | 0 | 1 | 21 |
| Positive margin sections (*n* = 28) | 2[a] | 3 | 2 | 2 | 19 |

[a]*One case examined was reported as LM histologically but was negative for PRAME IHC in both the de-bulk and two margin sections.*

**TABLE 3 |** Comparison of PRAME/Melan A DL to PRAME SL IHC and Melan A SL IHC. Each slide is compared and categorised according to labelling outcomes between the SL and DL.

| SL IHC results | PRAME | | | | | Melan A |
|---|---|---|---|---|---|---|
| | Immunoreactivity absent - 0 | +1 | +2 | +3 | +4 | Positive |
| | *N* = 3 | *N* = 3 | *N* = 2 | *N* = 3 | *N* = 40 | *N* = 51 |
| DL IHC results | 3 | 2 | 1 | 3 | 40 | 51 |
| DL IHC concordance to SL IHC (%) *N* = 51 | | 96.1% (49/51) | | | | 100% (51/51) |

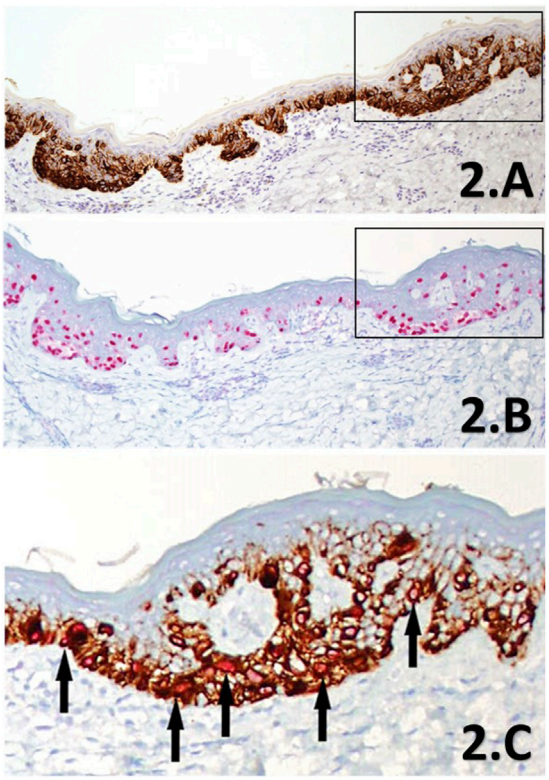


**FIGURE 2 | (A–C)** IHC sections of a SMMS LM de-bulk specimen derived from the left forehead. Melan A IHC SL **(A)** showing intense cytoplasmic labelling of melanocytes within the junctional component in brown chromogen, highlighting the increased proliferation of intraepidermal melanocytes in a lentiginous pattern, with accompanying nest formation (×10 magnification). PRAME IHC SL **(B)** shows diffuse nuclear labelling with almost all lesional melanocytes (>75%) within the junctional component are labelled with the red chromogen (×10 magnification). The black rectangles highlight the direct region of the corresponding magnified area within the PRAME/Melan A DL IHC **(C)** section for comparison to the SL counterparts. The DL (×20 magnification) shows clear double-labelling (black arrows) of almost all junctional melanocytes with bothPRAME red nuclear labelling, and brown cytoplasmic labelling of the cytoplasmic Melan A. Almost all melanocytes can be seen to be labelled with PRAME (both the DL and SL) in this select region showing strong concordance between the three IHC methods, providing further support in favour of LM.

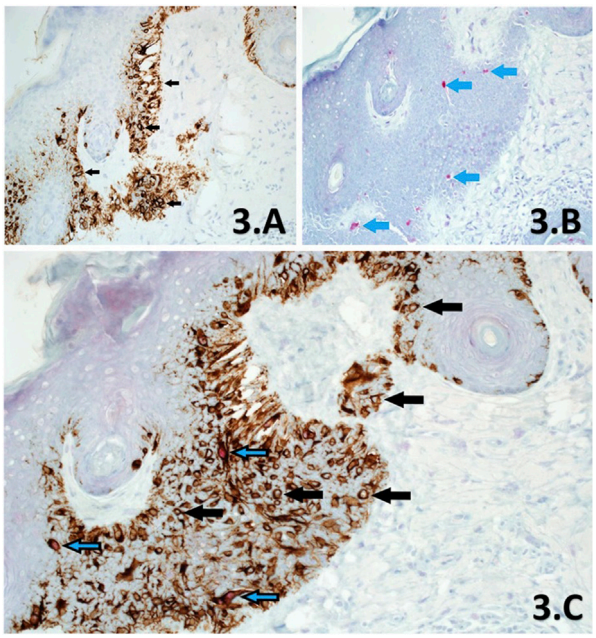


**FIGURE 3 | (A–C)**. Sections of skin derived from a previously reported residual LM, from a slow Mohs excision margin taken from the left side of nose. Melan A SL IHC **(A)** shows significant proliferation of melanocytes at the basal layer through cytoplasmic labelling of all melanocytes within the section, showing dendritic processes (×10 magnification). Examples of melanocytes are shown (black arrows) with clear nuclei. PRAME SL IHC **(B)** shows +1 red nuclear labelling of a few (<10%) melanocytes (blue arrows) within the same area of the lesion (×10 magnification). This section is interpreted as PRAME negative. PRAME/Melan A DL IHC **(C)** at ×20 magnification, shows both populations of melanocytes within the same area of the lesion, exhibiting labelling that is in agreement to both respective SL counterparts **(A,B)**. Note that PRAME negative melanocytes (black arrows) make up >90% of the lesion and lack any nuclear labelling or artefactual distortions as a result of double-labelling, which is comparable to the Melan A SL **(A)**. Similarly, PRAME positive melanocytes are demonstrated through DL with a red nuclear component (blue/black arrows). DL melanocytes comprised <10% of the lesional population within the same area, which is in direct accordance to the PRAME SL IHC control **(B)**. The DL is also interpreted as PRAME negative.

initial set of positive control material was used to select the combination of chromogen for IHC DL based on visual performance and contrast, with the latter combination of red nuclear PRAME labelling with brown cytoplasmic Melan A labelling, being taken forward for the study (**Figure 1B**). Both the SL Melan A (brown) and PRAME (red) used the same respective chromogen for direct comparisons to be made.

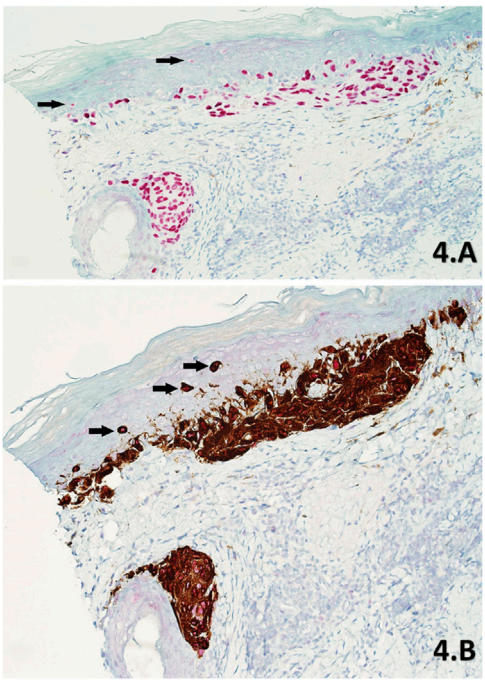


**FIGURE 4 | (A,B)** Skin sections of a part of residual LM from a slow Mohs de-bulk biopsy labelled with PRAME SL IHC **(A)** and PRAME/Melan A DL IHC **(B)** respectively (×20 magnification). Both sections show diffuse +4 positive red nuclear labelling of atypical melanocytes within the lesion. The lesion is comprised of atypical melanocytes that have formed densely packed nests at the base of the epidermis and nearby hair follicle. The DL **(B)** also shows intense cytoplasmic Melan A labelling of dendritic processes within these nests, with subsequent PRAME red nuclear labelling being detectable at higher magnifications. Upward pagetoid migration of atypical melanocytes (Black arrows) is seen more clearly in the DL **(B)** than the SL **(A)**.

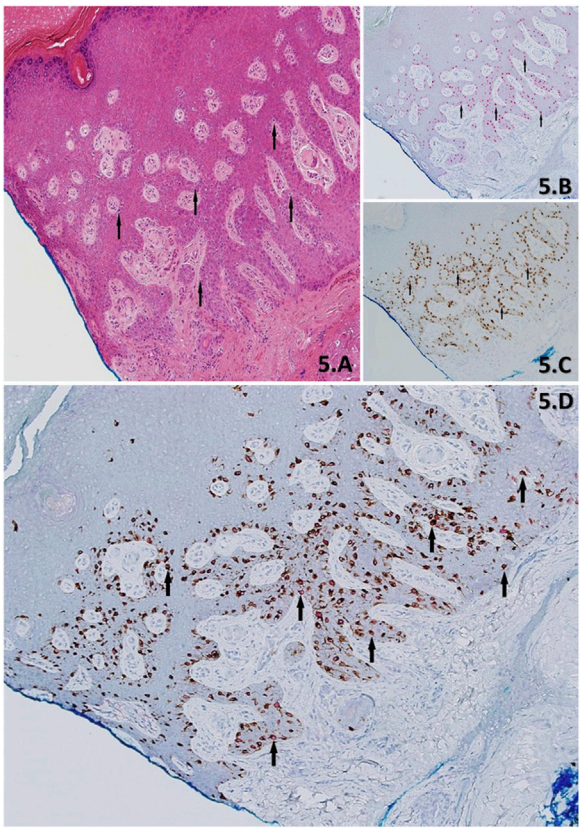


**FIGURE 5 | (A–D)** Demonstration of skin with residual LM from a stage-II slow Mohs biopsy, using H&E **(A)**, PRAME IHC SL **(B)**) Melan A IHC SL **(C)** and PRAME/Melan A DL IHC **(D)**. H&E Section shows acral skin with cross-cutting, with an eccentrically located lesion that extends into the blue inked peripheral margin. The lesion is comprised of lentiginous melanocytes (black arrows) exhibiting severe cytological atypia. IHC show in support of residual LM and is denoted by; >75% (+4) red nuclear labelling of "atypical" melanocytes (black arrows) within the lesion by the PRAME SL **(B)**, concordant >75% (+4) of dual-labelled "atypical" melanocytes (black arrow) of PRAME with red nuclear labelling and Melan A brown cytoplasmic labelling DL **(D)**, and Melan A SL **(C)** brown cytoplasmic labelling of melanocytes (black arrow) showing the entire melanocyte population. All images taken at ×10 magnification.

## Histological Material Preparation

All anonymised FFPE blocks used within the study were sectioned by author RS over the course of 4 batches which were carried out on 4 consecutive days with key factors controlled for, such as, water bath set to 37°C, same equipment used each day, and same batch numbers for reagents used. This was to reduce batch-to-batch variability.

All slides were sectioned at 3 μm and picked up on either TOMO® IHC adhesive slides (Solmedia Ltd., Shrewsbury, United Kingdom) for IHC labelling with positive control material or on SuperFrost®Plus Adhesion Slides (VWR®, Leicestershire, United Kingdom) for H&E sections which will have been consistent to the original H&E slides for reporting.

H&E staining was performed using the automated Leica Autostainer XL [Leica Microsystems (UK) Ltd. Milton Keynes, United Kingdom], using a commercially available Harris' haematoxylin and a 1% aqueous Eosin [Leica Microsystems (UK) Ltd. Milton Keynes, United Kingdom]. H&E staining was carried out using the same routine protocol that is used within the laboratory.

Cut slides for IHC were left to dry in a 37°C oven for 10 min before being transferred to a 60°C oven to bake for 1 h. Slides were then labelled according to the anonymised format given and loaded onto the IHC labelling platform on the same day that each batch was produced.

## IHC

A total of 153 IHC slides were performed, 51 slides per each IHC test. All slides were generated using the Roche Ventana Benchmark ULTRA IHC automated immunostaining platform (Roche Diagnostics Limited, West Sussex, United Kingdom). The same IHC machine was used throughout the study in order to prevent any potential variability that may occur during the IHC procedure.

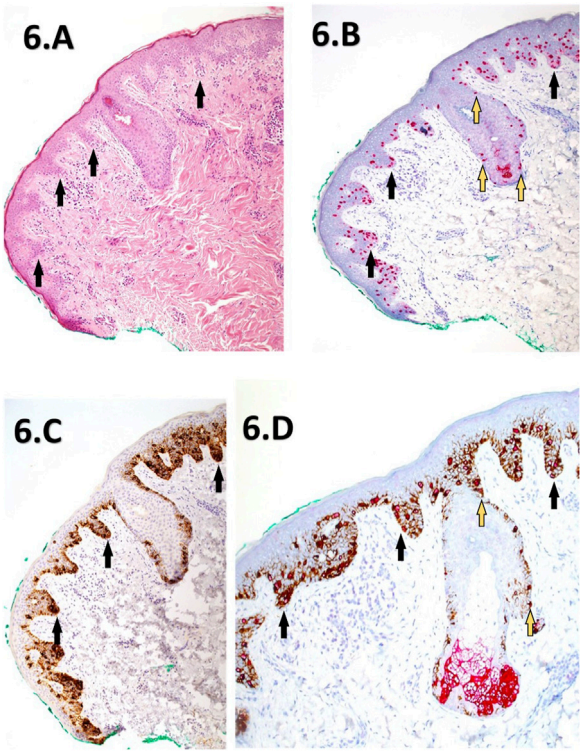


**FIGURE 6 | (A–D)** Corresponding images depicting a slow Mohs excision margin of a previously reported residual LM from the right cheek. The images include H&E staining **(A)** at (×10 magnification), PRAME SL IHC **(B)** at ×10 magnification, Melan A SL IHC **(C)** at ×10 magnification, dual labelling (DL) at ×20 magnification **(D)**. The H&E section **(A)** reveals mild hyperkeratosis and elongation of rete ridges, with atypical melanocytes exhibiting lentiginous and focal nested proliferations (black arrows) at the dermal-epidermal junction. Descent down the adnexal hair follicle epithelium is also noted. PRAME SL IHC **(B)** displays strong +4 diffuse positivity of melanocytes within the lesion, extending into nearby adnexal structures (yellow-blue arrows). Melan A SL IHC **(C)** shows cytoplasmic labelling of a lentiginous proliferation of melanocytes within the junctional component, featuring focal nests (black arrows). The DL image **(D)** demonstrates similar +4 PRAME nuclear labelling, with most melanocytes dual-labelled with the Melan A cytoplasmic component. The IHC sections collectively support the presence of residual LM extending to the green peripheral margin.

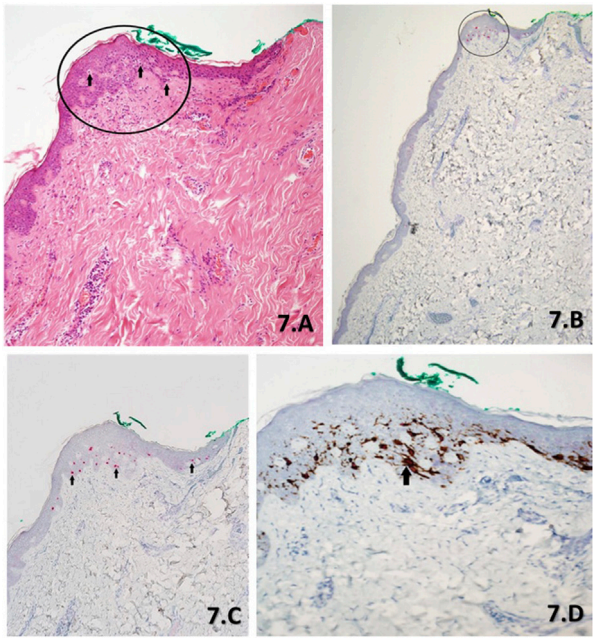


**FIGURE 7 | (A–D)**. Serial sections of a slow Mohs margin biopsy stained with H&E **(A)** at ×10 magnification, PRAME SL IHC **(B)** at ×4 magnification, PRAME SL IHC **(C)** at ×10 magnification and DL **(D)** at ×20 magnification. The H&E **(A)** morphology as per the report showed lentiginous hyperplasia of non-contiguous melanocytes with focal cytological atypia throughout the epidermis. However, there is a focal proliferation of melanocytes with severe cytological atypia (black arrows), 0.5 mm from the green peripheral margin (black circle). These atypical melanocytes appear contiguous and are suspicious for a small focus of residual LM. PRAME SL IHC ×4 magnification **(B)** and PRAME SL IHC ×10 magnification **(C)** draw attention to the focally located atypical melanocytes with positive +4 PRAME nuclear labelling (red) when accounting for the small focal area. The DL **(D)** shows almost all melanocytes as depicted with brown cytoplasmic labelling of Melan A within the focal area, to have corresponding PRAME nuclear labelling to the SL **(B,C)**. Additionally, a group of contiguous atypical melanocytes can be seen (black arrow).

Melan A IHC was carried out using the Roche ready-to-use (RTU) anti-MART-1/Melan A (A103 clone, from Roche Diagnostics Limited, West Sussex, United Kingdom) mouse monoclonal primary antibody. PRAME IHC was carried out using anti-PRAME (QR005 clone) RTU rabbit monoclonal primary antibody which was obtained from AnatoPath limited (, Saxmundham, England). Both primary antibodies and their subsequent IHC protocols were validated well in advance by GEO and FI. The DL protocol was developed and optimised in-house prior to use in this study. All three IHC protocols, Melan A SL, PRAME SL and PRAME/MelanA DL followed manufacturer recommendations where possible. This involved the same antigen retrieval step using commercially available Roche (Roche Diagnostics Limited, West Sussex, United Kingdom) ULTRA Cell Conditioning Solution 1 (ULTRA CC1) for heat-mediated antigen retrieval, coupled with polymer based detection kits also supplied by Roche (Roche Diagnostics Limited, West Sussex, United Kingdom) for both brown (OptiView DAB IHC Detection Kit, Ref: 760-700) and red chromogen (ultraView Universal Alkaline Phosphatase Red Detection Kit, Ref: 760-501) respectively. Counterstain of IHC slides were all carried out using Roche (Roche Diagnostics Limited, West Sussex, United Kingdom) Hematoxylin II which is designed for FFPE tissues on the BenchMark IHC automated platform.

A known positive control was also added to each IHC slide as an extra layer of validation.

## Evaluation of DL and Scoring Criteria for PRAME and Melan A

The technical evaluation of the DL was done through direct qualitative comparison to each respective single IHC slide,

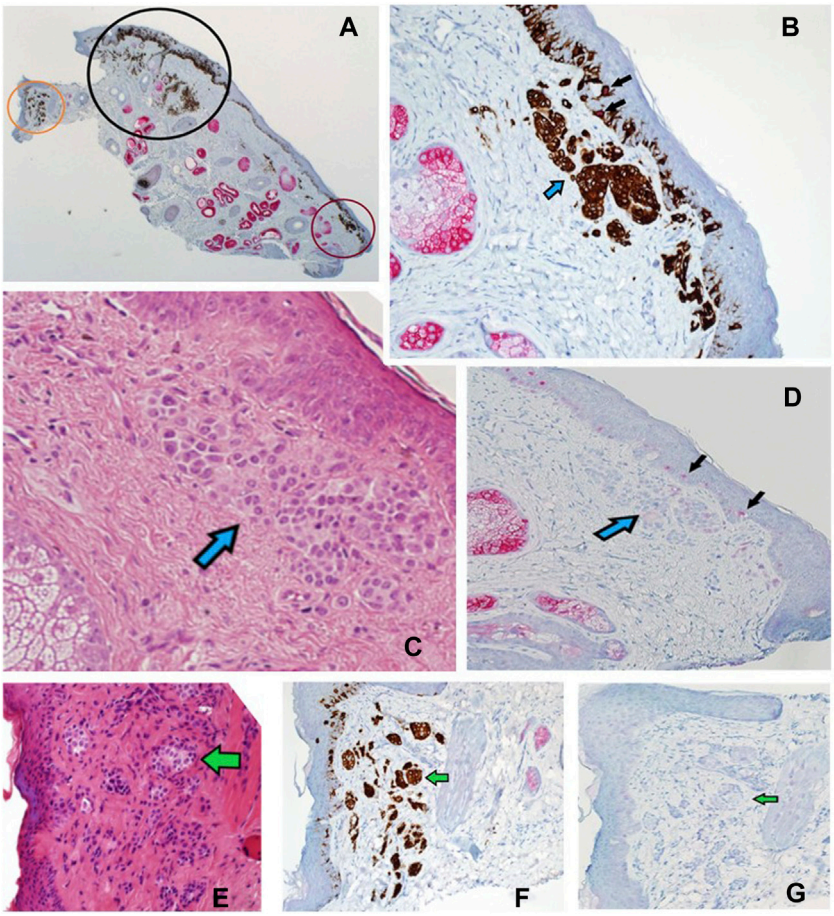


**FIGURE 8 | (A–G)** Sections of a Mohs de-bulk specimen reported as a LM with underlying naevus. PRAME/Melan A DL **(A)** at ×2 magnification showing the overall localisation of melanocytic proliferations (brown chromogen) into three distinct areas, a left non-involved region (orange circle), a middle region with LM component (black circle), and a right non-involved region (red circle). Sections B-D show the red circled region at higher power. **(B)** Shows DL labelling (×20 magnification) that highlights both junctional and dermal (blue arrow) melanocytic components with a lack of PRAME labelling in most cells. Only two melanocytes are seen with dual-labelling (black arrows), overall suggestive of a benign process. **(C)** Shows H&E (20x magnification) staining depicting a large dermal melanocytic proliferation (blue arrow) that amounts to a benign dermal nevus that is found within the red circled region. **(D)** Shows PRAME SL IHC (×10 magnification) that is negative for PRAME within the dermal nevus (blue arrow) but some weak positivity (+1) within the epidermis (black arrows). **(E)** Shows H&E (×20 magnification) staining of the orange circled region depicting another dermal naevus proliferation (green arrow). This is highlighted by the DL (×20 magnification) within the same orange region **(F)** showing only Melan A cytoplasmic labelling without any PRAME (green arrow). **(G)** PRAME SL IHC (×20 magnification) showing lack of labelling (green arrow) in the orange region, suggestive of a benign dermal naevus.

PRAME SL and Melan A SL, to ensure that there was no artefactual, or potential pitfalls in the appearance of the DL—namely focusing on false loss or gain or obscurity in PRAME or Melan A components when juxtaposed. Comparison of IHC stains as well as the scoring of PRAME, were done through visual assessment under a light microscope by a Consultant BMS G.E.O.

Scoring criteria of the PRAME SL IHC benchmark within the study was based on the percentage of PRAME positive tumour cells that were present within the lesion examined. Thus 0—negative, +1 (1%–25%), +2 (26%–50%), +3 (51%–75%), +4 (>75% diffuse/positive) [9]. Only lesions that exhibited more than 75% (+4 labelling) of PRAME positive lesional cells were scored as positive. 0% indicates a complete absence of any PRAME labelling and was therefore negative. Intermediate labelling, +1, +2, +3, was also interpreted as negative within the study, which was in line with prior investigations [7–11, 13–15]. In summary PRAME IHC slides were scored as either positive (+4 diffuse) or negative (0, +1, +2, +3) within the study when assessing the sensitivity of PRAME within SMMS biopsies. However, when assessing the novel DL technique to the PRAME SL, each slide was assessed for agreement based on the specific labelling of PRAME that was seen, 0, +1, +2. +3 and +4 respectively.

Melan A SL IHC was used as the comparative benchmark for the Melan A component of the novel DL. Melan A IHC interpretation was based on the positive or negative presence (+ve) or absence (−ve) of cytoplasmic melanocyte labelling within SMMS biopsies respectively.

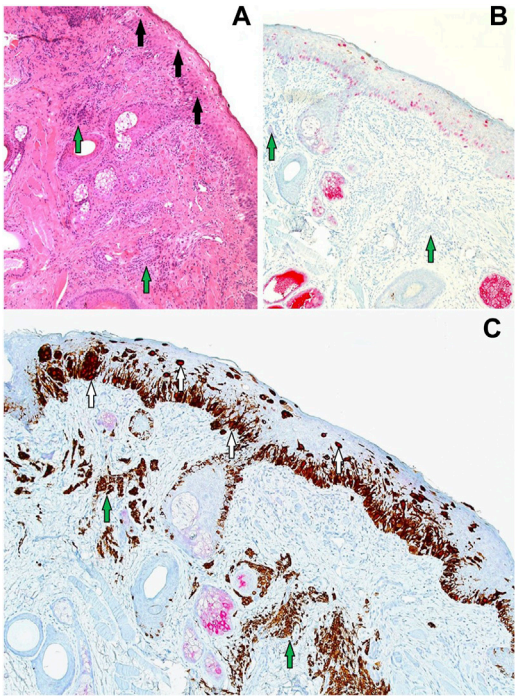


**FIGURE 9 | (A–C)** Sections (all at ×20 magnification) corresponding to the black circled region from **Figure 8**. **(A)** H&E showing a proliferation of contiguous atypical melanocytes along the junctional component, arranged in a lentiginous pattern with marked upward pagetiod spread (black arrows). The features of the overlying junctional component are in keeping with LM. There is also an underlying melanocytic proliferation with suggestive features of a dermal naevus (green arrows). **(B)** PRAME SL IHC showing +4 PRAME positivity (red nuclear labelling) of atypical melanocytes that are confined to the epidermis with upward pagetoid spread. No PRAME labelling is seen in the underlying dermal naevus (green arrows) which is in favour of an underlying naevus. **(C)** PRAME/Melan A DL IHC illustrates two melanocyte populations: the LM junctional component featuring double-labelled atypical melanocytes (white arrows) and the underlying dermal nevus exhibiting solely Melan A brown cytoplasmic labelling (green arrows).

## Statistical Analysis

Statistical analysis and measurement of agreement between the novel DL and SL was performed using SPSS software (IBM Corp. Released 2021. IBM SPSS Statistics for Windows, Version 29.0. Armonk, NY: IBM Corp), utilising the Kappa statistic.

# RESULTS

## Evaluation of PRAME SL IHC in Slow Mohs Sections

Results of the PRAME SL IHC can be found in **Table 2**. 21/23 LM de-bulk sections that were used for PRAME SL IHC were found to be diffusely positive (>75% threshold). Of the remaining 2/23 de-bulk sections one exhibited an intermediate +3 PRAME labelling, with the other section showing absent 0 PRAME immunoreactivity. The same PRAME negative (0) de-bulk section had PRAME negativity (0) at both histologically positive margins. All sections that showed 0 immunoreactivity for PRAME (0) were all derived from the same case. By using +4 as the positivity threshold for PRAME, a PRAME IHC sensitivity of 91.3% was obtained with respect to de-bulk sections examined ($n$ = 23). A lower PRAME sensitivity of 67.9% (19/28) was observed with respect to PRAME SL IHC labelling at the margins ($n$ = 28) using the same +4 positivity criteria. Of the 9/28 histologically confirmed positive slides that failed to meet the +4 threshold for positivity, 2/28 were the aforementioned slides with 0 labelling, 3/28 exhibited +1 labelling, 2/28 showed +2 labelling and finally, 2/28 demonstrated +3 labelling. The combined sensitivity for PRAME including both de-bulk and positive margins, 40/51, was 78.4%.

## Evaluation of PRAME/Melan A IHC DL

There was an overall substantial agreement between the novel DL and the PRAME SL of 96.1% (Kappa = 0.895 with $p$-value = <0.001). All Melan A ($n$ = 51) IHC seen between the novel DL method and the control Melan A SL were 100% concordant with all slides showing positive cytoplasmic labelling of melanocytes where present. The 2/48 non-concordant DL slides were derived from histologically positive margins that showed weak +1 and +2 PRAME immunoreactivity on the respective PRAME SL slides. Both respective DL slides showed no PRAME nuclear immunoreactivity when compared to the PRAME SL control. Comparison of the novel DL is summarised in **Table 3**.

## Qualitative Comparisons of Novel DL to SL and Morphological H&E

Following qualitative assessment by G.E.O, several superimposed and annotated, concordant photographs were taken to provide direct qualitative comparison between the novel DL and the PRAME SL IHC and Melan A SL IHC controls **Figures 2–4**. These images were selected for performance and technical aspects relating to the DL method.

Several images **Figures 5–9** were selected from the study to highlight superimposed DL and SL with various morphological H&E appearances in order to assess the potential utility and application of the novel DL as a potentially useful adjunct within margin assessment investigations.

# DISCUSSION

Several instances of PRAME DL IHC have been described in the literature, combining PRAME with cytoplasmic Melan A or HMB45 [11–15]. Three of these studies ran parallel PRAME SL IHC as the control for the novel DL, correlating results through semi-quantitative scoring [11, 13, 14]. Therefore, the current study design and methodology align with previous research, allowing for comparisons to laboratory aspects of PRAME DL and obtained results to established methods (PRAME SL IHC).

Interpretation and scoring of PRAME IHC results with respect to both distribution and intensity is currently lacking in

standardisation. As a result, greater consideration within the study has been made towards the PRAME IHC scoring criteria in which to assess both PRAME SL within SMMS and by extension, assessment of the Novel DL. Many studies, including those which have explored PRAME DL techniques have utilized the >75% threshold for positivity, irrespective of intensity, established by Lezcano et al [7–15]. This scoring method is used in the current study for its high correlation to LM, whilst providing a simpler and direct comparison of results to prior studies [11–15].

While an additional scoring criterion incorporating PRAME labelling intensity has been described in the literature, it was not included in this study due to anticipated technical challenges which could not be controlled for given the retrospective nature of the study [16]. In particular, PRAME intensity scoring has only been described for SL IHC methods, not factoring in the potential for chromogen overlap within a DL protocol, making the interpretation of weaker intensity scoring potentially difficult, further complicating analysis [16, 18]. This is further confounded by the often observed and seemingly inherent variability of intensity for PRAME, within practice - constituting a known pitfall of PRAME IHC [18].

To our knowledge, the literature lacks instances of using a red chromogen for PRAME and a brown chromogen for Melan A in demonstrating DL for PRAME/Melan A [11, 13–15]. Previous studies opted for the reverse chromogen set-up (**Figure 1A**), citing potential interpretation difficulties with native melanin pigment as a result [13, 14]. In contrast, this study employed and explored the use of red chromogen for PRAME in conjunction with brown chromogen for Melan A, in order avoid challenges due to melanin pigment. However, it is evident that there are accompanying interpretation concerns in relation to the current chromogen arrangement used in the study as shown in **Figures 4**, **9**. These examples, while nuclear PRAME labelling can still be seen, the intense darker background produced by the brown chromogen kit and the cytoplasmic labelling of dense melanocytic nests by Melan A, produce a challenging image for interpretation. In these instances, the reverse chromogen arrangement could be beneficial for pathologists as an alternative (**Figure 1A**).

Further protocol optimisation could also be explored towards the reduction of the IHC Melan A cytoplasmic component, through the dilution of primary antibodies used, which may also help facilitate sensitivity to PRAME scoring based on intensity, making it easier to discern lower intensity PRAME labelling within the DL method. However, given the use of a closed IHC system and RTU antibodies, this constitutes as a limitation to current study design—setting the basis for future technical exploration through other IHC systems.

The agreement between DL and SL slides was 96.1% (49/51) for PRAME and 100% for Melan A (51/51). The loss of signal focused on PRAME within the DL, with one +1 slide (1/5) and another +2 slide (1/2) being discordant within positive margin specimens only. Reasons for the loss of PRAME in the two discordant positive margin DL slides could be due to a number factors, from the pre-analytical processing of tissues, to the aforementioned technical considerations and the DL protocol itself. Furthermore, the weaker +1 and +2 PRAME labelling in the SL benchmark, indicates the presence of a smaller number of LM cells, which could be harder to detect through the novel DL protocol given that the proportionality of malignant (LM) to benign (background melanocytic hyperplasia) melanocytes will shift further towards the latter. Nevertheless, most examples of weaker (**Figure 3**) +1 (4/5) PRAME labelling within positive margins was detected successfully in the DL demonstrating high analytical sensitivity.

The total PRAME sensitivity in this study was 78.4% (40/51) utilising a >75% threshold, with a further breakdown showing 91.3% sensitivity in de-bulk specimens and 67.9% at morphologically positive margins. A comparable study by De Wet, Du Plessis, and Schneider (2022) reported a similar PRAME IHC sensitivity profile of 63% within SE LM margin biopsies, using the same criteria of >75% positivity threshold for tumor nuclei [7]. In addition, they emphasized the need for further investigation into the significance of lesser PRAME labelling (+1, +2, +3), raising questions in regards to the suitability of the >75% threshold for PRAME "diffuse" positivity, specifically within SE LM margins. These sentiments are echoed in the current study findings whereby a significant number of PRAME SL slides (7/28) showed intermediate or non-diffuse (classified as negative) PRAME positivity within the margins. The heterogeneous nature of LM, combined with a background of benign atypical melanocytic hyperplasia in sun-damaged skin, may necessitate alternative scoring methods for PRAME positivity within SMMS biopsies. Ultimately however, interpretation of PRAME IHC results, irrespective of scoring methods, should be done so within the context of morphological and clinical correlation—allowing for PRAME IHC to be interpreted as "positive/supportive" of LM without the need for the widely adopted "diffuse +4" scoring criteria set out by Lezcano et al [18].

Not all melanomas show diffuse positivity for PRAME and this pitfall extends to rare LM populations in which further PRAME IHC investigations would be invalid and therefore exclusion is advised [7, 8, 18]. Nonetheless, an alternative approach could be to use PRAME/Melan A DL as a "first-line" test in the rare cases whereby the PRAME status is unknown. In this way, adjunct IHC can still be captured through the highly sensitive cytoplasmic component of the Melan A, to help aid in margin assessment. De Wet, Du Plessis, and Schneider (2022) emphasize the importance of IHC as sole reliance on the gold standard H&E and histological criteria may lead to poorer patient management and morbidity [7]. This underscores the need for adjunct IHC as an integral part of LM/LMM margin assessment, advocating for tests like PRAME SL IHC and by extension PRAME/Melan A DL IHC. This is particularly relevant as IHC stains are not routinely used in the slow Mohs procedure at St. John's Dermatopathology Department in which this study has been conducted.

The successful outcomes of this pilot study, providing context and performance for both PRAME SL and PRAME DL within SMMS margin assessment, could pave the way for future investigations. In particular, the prospective use of such stains at the time of initial work-up, with direct pathologist involvement, may become the standard for the diagnosis of SMMS cases.

## SUMMARY TABLE

### What Is Known About This Subject

- Staged excision techniques such as (slow) Mohs Micrographic Surgery, offer greater margin control over traditional methods.
- Adjunct PRAME Immunohistochemistry (IHC) can help in margin assessment of LM/LMM excision biopsies.
- PRAME can be combined with other markers in novel double-labelling (DL) techniques to further maximise utility.

### What This Paper Adds

- Novel PRAME/Melan A DL IHC is a promising alternative to single labelling counterparts, showing high concordance (96.1%).
- Adjunct PRAME/Melan A DL IHC may aid in the assessment of challenging melanocytic lesions and residual LM within margins.
- Further research on interpreting PRAME in LM/LMM lesions with weak to intermediate labelling at margins would be valuable.

This work represents an advance in biomedical science because it demonstrates successfully, a novel PRAME/Melan A IHC DL technique within LM/LMM SMMS biopsies for aiding in margin assessment.

## DATA AVAILABILITY STATEMENT

The raw data supporting the conclusion of this article will be made available by the authors, without undue reservation.

## ETHICS STATEMENT

The requirement of ethical approval was waived by the Chief Scientific Officer of Synnovis at Guy's and St. Thomas trust, for the studies involving humans because it is a retrospective study. The studies were conducted in accordance with the local legislation and institutional requirements. The requirement of written informed consent for participation from the participants or the participants' legal guardians/ next of kin was waived because no additional material was collected from any subjects during this work. All material used within this article have been approved using formal organizational procedures.

## AUTHOR CONTRIBUTIONS

Authors RS and GO participated in the design and nature of the study. Interpretation of test material was carried out by GO and subsequent analysis of the data carried out by RS with following review by GO. RS conducted the experiments, with FI and GO involved in the development and optimisation of key labelling protocols. RS wrote the manuscript with further input and review by GO. All authors contributed to the article and approved the submitted version.

## CONFLICT OF INTEREST

The authors declare that the research was conducted in the absence of any commercial or financial relationships that could be construed as a potential conflict of interest.

## ACKNOWLEDGMENTS

This paper expands and extends the authors work reported in a poster presented at the IBMS Congress, held in September 2023, which appeared as a short article in the December 2023 issue of Pathology in Practice (PIP).

## REFERENCES

1. Koh HK, Michalik EE, Sober AJ, Lew RA, Day CL, Clark WH, et al. Lentigo Maligna Melanoma Has No Better Prognosis Than Other Types of Melanoma. *J Clin Oncol* (1984) 2(9):994–1001. doi:10.1200/JCO.1984.2.9.994
2. Iznardo H, Garcia-Melendo C, Yélamos O. Lentigo Maligna: Clinical Presentation and Appropriate Management. *Clin Cosmet Investig Dermatol* (2020) 13:837–55. doi:10.2147/CCID.S224738
3. Bosbous MW, Dzwierzynski WW, Neuburg M. Staged Excision of Lentigo Maligna and Lentigo Maligna Melanoma: A 10-Year Experience. *Plast Reconstr Surg* (2009) 124(6):1947–55. doi:10.1097/PRS.0b013e3181bcf002
4. Bittar PG, Bittar JM, Etzkorn JR, Brewer JD, Aizman L, Shin TM, et al. Systematic Review and Meta-Analysis of Local Recurrence Rates of Head and Neck Cutaneous Melanomas After Wide Local Excision, Mohs Micrographic Surgery, or Staged Excision. *J Am Acad Dermatol* (2021) 85(3):681–92. doi:10.1016/j.jaad.2021.04.090
5. Beaulieu D, Fathi R, Srivastava D, Nijhawan R. Current Perspectives on Mohs Micrographic Surgery for Melanoma. *Clin Cosmet Investig Dermatol* (2018) 11: 309–20. doi:10.2147/CCID.S137513
6. Cohen LM, McCall MW, Zax RH. Mohs Micrographic Surgery for Lentigo Maligna and Lentigo Maligna Melanoma. A Follow-Up Study. *Dermatol Surg* (1998) 24(6):673–7. doi:10.1111/j.1524-4725.1998.tb04226.x
7. de Wet J, du PPJ, Schneider JW. Staged Excision of Lentigo Maligna of the Head and Neck: Assessing Surgical Excision Margins With Melan A, SOX10, and PRAME Immunohistochemistry. *The Am J Dermatopathology* (2023) 45(2):107–12. doi:10.1097/DAD.0000000000002354
8. Gradecki SE, Valdes-Rodriguez R, Wick MR, Gru AA. PRAME Immunohistochemistry as an Adjunct for Diagnosis and Histological Margin Assessment in Lentigo Maligna. *Histopathology* (2020) 78(7): 1000–8. doi:10.1111/his.14312
9. Lezcano C, Jungbluth AA, Nehal KS, Hollmann TJ, Busam KJ. PRAME Expression in Melanocytic Tumors. *Am J Surg Pathol* (2018) 42(11): 1456–65. doi:10.1097/PAS.0000000000001134
10. Lohman ME, Steen AJ, Grekin RC, North JP. The Utility of PRAME Staining in Identifying Malignant Transformation of Melanocytic Nevi. *J Cutan Pathol* (2021) 48(7):856–62. doi:10.1111/cup.13958
11. Lezcano C, Jungbluth AA, Busam KJ. PRAME Immunohistochemistry as an Ancillary Test for the Assessment of Melanocytic Lesions. *Surg Pathol Clin* (2021) 14(2):165–75. doi:10.1016/j.path.2021.01.001
12. Ricci C, Dika E, Ambrosi F, Lambertini M, Veronesi G, Barbara C. Cutaneous Melanomas: A Single Center Experience on the Usage of Immunohistochemistry Applied for the Diagnosis. *Int J Mol Sci* (2022) 23(11):5911. doi:10.3390/ijms23115911
13. Lezcano C, Pulitzer M, Moy AP, Hollmann TJ, Jungbluth AA, Busam KJ. Immunohistochemistry for PRAME in the Distinction of Nodal Nevi From

Metastatic Melanoma. *Am J Surg Pathol* (2020) 44(4):503–8. doi:10.1097/PAS.0000000000001393

14. Grillini M, Ricci C, Pino V, Pedrini S, Fiorentino M, Corti B. HMB45/PRAME, a Novel Double Staining for the Diagnosis of Melanocytic Neoplasms: Technical Aspects, Results, and Comparison With Other Commercially Available Staining (PRAME and Melan A/PRAME). *Appl Immunohistochem Mol Morphol* (2021) 30(1):14–8. doi:10.1097/PAI.0000000000000972
15. Carvajal P, Zoroquiain P. PRAME/MELAN-A Double Immunostaining as a Diagnostic Tool for Conjunctival Melanocytic Lesions: A South American Experience. *Pathol - Res Pract* (2023) 250:154776. doi:10.1016/j.prp.2023.154776
16. Santandrea G, Valli R, Zanetti E, Ragazzi M, Pampena R, Longo C, et al. Comparative Analysis of PRAME Expression in 127 Acral and Nail Melanocytic Lesions. *Am J Surg Pathol* (2022) 46(5):579–90. doi:10.1097/PAS.0000000000001878
17. Raghavan SS, Wang JY, Kwok S, Rieger KE, Novoa RA, Brown RA. PRAME Expression in Melanocytic Proliferations With Intermediate Histopathologic or Spitzoid Features. *J Cutan Pathol* (2020) 47(12):1123–31. doi:10.1111/cup.13818
18. Lezcano C, Jungbluth AA, Busam KJ. Immunohistochemistry for PRAME in Dermatopathology. *Am J Dermatopathology* (2023) 45(11):733–47. doi:10.1097/DAD.0000000000002440

IBMS Institute of Biomedical Science | BJBS

REVIEW
published: 24 November 2023
doi: 10.3389/bjbs.2023.11809

# Diagnostic Techniques in Autoimmune Blistering Diseases

*John B. Mee**

*Immunodermatology Laboratory, St John's Institute of Dermatology, Synnovis Analytics, St Thomas' Hospital, London, United Kingdom*

Autoimmune blistering diseases (AIBD) comprise a heterogeneous group of uncommon disorders of the skin and mucous membranes, characterised by antibodies targeting structural proteins within epithelial tissue and the underlying basement membrane. There can be significant overlap in clinical presentation of these diseases and accurate diagnosis relies on the detection and characterisation of relevant autoantibodies. Immunofluorescence provides the gold-standard diagnostic tool for these diseases, identifying both tissue-bound autoantibodies in biopsy material using direct immunofluorescence and circulating antibodies in serum through indirect immunofluorescence. Following advances in the identification and subsequent characterisation of numerous antigenic targets in these diseases, the development of antigen-specific tests, in particular, enzyme-linked immunosorbent assays on serum specimens, has provided a third key tool to not only identify, but also quantify AIBD autoantibodies. This quantification has proven particularly useful in monitoring disease activity and informing clinical management decisions. Accurate diagnosis of these diseases is important since optimal treatment strategies differ between them and, prognostically, some diagnoses are associated with an increased risk of malignancy. This review outlines the molecular pathology underlying the major AIBD and describes how the three principal techniques can be used in combination, to provide best practice for diagnosis and treatment monitoring.

**Keywords: immunobullous disorders, immunofluorescence, autoantibody, desmosome, hemidesmosome, pemphigus, pemphigoid**

OPEN ACCESS

***Correspondence:**
*John B. Mee*
*john.mee@synnovis.co.uk,*
*orcid.org/0009-0007-0993-8467*

***Received:** 17 July 2023*
***Accepted:** 23 October 2023*
***Published:** 24 November 2023*

***Citation:***
*Mee JB (2023) Diagnostic Techniques in Autoimmune Blistering Diseases. Br J Biomed Sci 80:11809. doi: 10.3389/bjbs.2023.11809*

## INTRODUCTION

Autoimmune blistering diseases (AIBD) encompass a group of serious disorders of the skin and mucous membranes which are characterised by the production of autoantibodies which typically target structural proteins within epithelial tissue and in the underlying basement membrane zone, connecting epithelium with either dermis in skin or the lamina propria in mucosal tissue. This results in loss of structural integrity of these tissues and consequent blistering [1]. Prior to the development of modern immunosuppressive therapies, these diseases were commonly life-threatening, due to the loss of barrier function [2]. Accurate diagnosis of these diseases is important, both therapeutically, since diseases within this group respond differently to the range of treatment management options available and prognostically, due to increased risk of malignancy with certain diagnoses. Immunofluorescence techniques have provided the gold standard diagnostic tool for AIBD for over 50 years [3, 4] and facilitate visualisation of both tissue-binding autoantibodies by direct immunofluorescence (DIF) and circulating autoantibodies in serum by indirect immunofluorescence

(IIF), using a variety of substrate tissues. With the subsequent identification and characterisation of specific antigens targeted by the autoantibodies in these diseases, development of a series of enzyme-linked immunosorbent assays (ELISA) has provided a third principal technique for not only identifying, but also quantifying specific circulating autoantibodies in patient serum samples [5, 6]. This has relevance both for monitoring disease activity and informing therapeutic management. In this review, the molecular pathology underlying the major AIBD will be outlined, the three principal diagnostic techniques will be described and typical results for the most common AIBD will be discussed, to illustrate how best practice diagnostics can be achieved using a combination of these methodologies.

## MOLECULAR PATHOLOGY OF IMMUNOBULLOUS DISEASES

AIBD can be divided into two categories; those producing autoantibodies targeting antigens within the epithelium, termed the intra-epithelial autoimmune bullous diseases and those which generate autoantibodies that bind to a distinct group of structural proteins found in the region beneath the epithelium, comprising the sub-epithelial autoimmune bullous diseases [7]. More specifically, the structures targeted in these diseases are termed desmosomes and hemidesmosomes, respectively and their roles are outlined below.

### Desmosomes and the Basement Membrane Zone

To maintain structural integrity, keratinocytes, the predominant epithelial cell type within human skin and mucosae, anchor themselves to adjacent keratinocytes via desmosomes, a type of cell junction. Desmosomes facilitate the direct connection of cytoskeletal keratin filaments between cells and are randomly located at the plasma membrane [8]. They are comprised of three protein superfamilies. Those of the plakin family (principally desmoplakin) and armadillo proteins, including plakoglobin and plakophilin, form a plaque structure on the intracellular side of the plasma membrane and attach directly to keratin intermediate filaments [9]. Cell adhesion molecules of the cadherin superfamily (principally desmogleins and desmocollins) are transmembrane proteins which are anchored to the plakin proteins within a keratinocyte [10]. They bridge the space between adjacent cells by binding in a heterophilic manner with other cadherins expressed by the adjacent cell. Hence, desmoglein molecules expressed by one keratinocyte bind desmocollin molecules on the adjacent cell and *vice versa* [11]. In humans, four desmoglein and three desmocollin genes have been identified [12]. All may be expressed in epithelial tissue, however, desmoglein 1 (DSG1) and desmoglein 3 (DSG3) are specifically targeted in AIBD.

The interface where epithelial cells attach to the underlying connective tissue is termed the basement membrane zone (BMZ) and is sometimes used synonymously with the dermo-epidermal junction in skin. It is a distinct structure, comprising four major ultrastructural regions and describes the area where focal attachment structures within basal keratinocytes interact with a series of molecules in the acellular space directly beneath the epithelium, to form a tight connection between the two layers, which also creates a selective barrier [13].

Within basal keratinocyte plasma membranes, structures called hemidesmosomes serve to bundle keratin intermediate filaments of the cytoskeleton together and attach them to other members of the plakin superfamily, in particular, plectin and dystonin (commonly referred to as BP230 or bullous pemphigoid antigen 1/BPAG1) [14]. These proteins associate, in turn, with a group of transmembrane proteins, notably β4 integrin and collagen XVII (synonymous with BP180 or bullous pemphigoid antigen 2/BPAG2). The extracellular domains of these proteins interact with anchoring filaments composed of laminin proteins, principally laminin 332 and laminin 311 in the electron-lucent zone known as the lamina lucida [15]. Beneath this layer is an electron-dense region known as the lamina densa, which is principally composed of type IV collagen, but also contains further laminin chains, nidogen-1 and proteoglycans.

The sublamina densa region (sometimes termed the fibrillar zone), directly beneath the lamina densa, comprises collagen VII anchoring fibrils, anchoring plaques composed of collagen IV and laminin, and collagen and elastic fibres. The anchoring fibrils not only link the lamina densa with the anchoring plaques of the underlying papillary dermis (or lamina propria in mucosal tissues) but also interact with laminin 332 in the lamina lucida, thus providing a direct link between hemidesmosomes in basal keratinocytes and papillary dermis/lamina propria, which is pivotal in maintaining a strong attachment between the epithelium and underlying connective tissue [16].

### Intra-Epithelial Blistering Diseases

Autoantibodies directed against epitopes on the transmembrane adhesion molecules of desmosomes have been shown to be pathogenic in the intra-epithelial blistering diseases which comprise the pemphigus family [17, 18], all of which present with flaccid blisters or erosions, as a result of the loss of epidermal integrity elicited by targeting the inter-keratinocyte "glue." The most common of these diseases, pemphigus vulgaris (PV), is primarily a disease of oral mucosal blistering and DSG3 is the principal target antigen [19]. A subset of PV patients develops cutaneous blisters, in addition to mucosal ones and these patients typically produce antibodies against DSG1, in addition to DSG3. Pemphigus foliaceus (PF) describes patients whose blistering is limited to cutaneous sites, who generate antibodies against DSG1 alone, in all but a handful of cases [20]. Paraneoplastic pemphigus (PNP) is an uncommon disease which occurs in the context of an underlying (typically lymphoproliferative) malignancy, resulting in autoantibodies against plakin proteins (principally envoplakin and periplakin), in addition to DSG3, being produced [21]. PNP is now recognised as the epithelial manifestation of a broader paraneoplastic autoimmune multiorgan syndrome [22].

Antibodies of the IgG isotype predominate in most cases of pemphigus. However, a small proportion of pemphigus patients

produce IgA autoantibodies exclusively, which are most commonly directed against the desmoglein homolog, desmocollin-1 [23].

Prior to the advent of corticosteroids (e.g., prednisolone) in the 1950s, approximately 75% of pemphigus cases were fatal [2]. However, the subsequent development of potent immunosuppressive therapies, such as cyclophosphamide, azathioprine and mycophenolate mofetil, along with new 'biologic' therapies, such as the chimeric, anti-CD20 monoclonal antibody, rituximab, have reduced the mortality rate (excluding PNP) to approximately 5% [24], although 5 years mortality has been reported as 23% in a recent French study [25], predominantly due to co-morbidities in a relatively elderly population.

## Sub-Epithelial Blistering Diseases

In contrast to the pemphigus family, individuals with diseases in the sub-epithelial blistering disease group produce autoantibodies which target proteins associated with the basement membrane zone, producing tense, pruritic blisters, clinically, which are sub-epithelial on histological examination [26]. The most common of these is bullous pemphigoid (BP), a disease usually seen in patients over the age of 70, unlike the (less common) pemphigus, which typically presents initially one to two decades earlier [27]. The most common autoantigen in BP is BP180/collagen XVII [28], specifically the non-collagen (NC)16A domain, found proximal to the plasma membrane, on the extracellular side. BP230/dystonin, an intracellular binding partner of BP180, is the second most commonly targeted autoantigen in BP [29] and >90% of BP sera are positive for circulating IgG antibodies directed against one (or both) of these molecules [30].

Mucous membrane pemphigoid (MMP) is distinguished from BP, clinically, by predominant mucosal involvement with oral and ocular sites being the two most commonly affected areas [31]. In addition to BP180, the α3 chain of laminin 332 is a target for autoantibodies in approximately 10%–20% of MMP cases [32]. MMP patients may also produce antibodies of the IgA isotype, in addition to IgG, which predominates in BP and such patients typically exhibit more severe and persistent disease [33].

Linear IgA disease (LAD) is characterised, immunopathologically, by production of BMZ-localising IgA antibodies, in which the soluble, ectodomain of BP180, rather than the (uncleaved) NC16A region, is the principal autoantigen [34]. Conversely, pemphigoid gestationis is an immunobullous disorder of pregnancy, in which low levels of IgG antibodies against BP180 NC16A are produced [35].

The most recently identified pemphigoid variant is characterised by the presence of antibodies against the laminin-γ1 chain, which was shown to be the target antigen in what had previously been termed anti-p200 pemphigoid [36], although, by comparison with BP or MMP, anti laminin γ1 pemphigoid is an uncommon variant.

Epidermolysis bullosa acquisita (EBA) is a sub-epithelial blistering disease that can be difficult to distinguish from BP, clinically, but can be diagnosed by detection of autoantibodies binding to type VII collagen [37].

Dermatitis herpetiformis (DH) is typically seen as the cutaneous manifestation of coeliac disease and most commonly presents as pruritic, symmetrically distributed papules and blisters at the extensor surfaces of upper and lower limbs [38]. DH is an IgA-mediated disease, however, unlike the previously discussed sub-epithelial blistering diseases, the autoantigen is not a hemidesmosomal component but epidermal transglutaminase [39], an enzyme expressed in the spinous layer of the epidermis. The major autoantigens identified in each AIBD are summarised in **Table 1**.

# IMMUNOPATHOLOGICAL DIAGNOSTIC TECHNIQUES

There are currently three widely used techniques to assist clinicians in the diagnosis and monitoring of AIBD: direct immunofluorescence microscopy of biopsy material, for detection of *in situ* tissue autoantibodies, indirect immunofluorescence microscopy, using patient sera and a range of tissue substrates to detect and titrate circulating autoantibodies and, less commonly, ELISA of serum specimens, to detect and quantitatively determine levels of autoantibodies to defined autoantigens in these diseases.

## Direct Immunofluorescence (DIF)

DIF is a single-step procedure used to identify antibodies bound to cutaneous or mucosal antigens *in situ* and other proteins of relevance to AIBD. A primary antibody directed against the protein of interest and conjugated with a fluorescent dye (typically fluorescein isothiocyanate) is added to tissue sections derived from a patient biopsy. Any specific immune complexes formed during incubation of the tissue sections with these antibodies are then visualised using fluorescence microscopy with appropriate filters. The most commonly used panel of fluorescently conjugated antibodies detects tissue-bound IgA, IgG, and IgM immunoglobulins, in addition to the C3c subunit of complement and fibrinogen [40]. The sensitivity of DIF is superior to that of indirect immunofluorescence, since AIBD antibody concentrations are much higher in tissue than serum, hence it is the preferred method for establishing a diagnosis [41]. However, DIF provides limited information on quantities of antibodies present and no information on the antigenic targets of the immunoglobulins detected.

Biopsy material for direct immunofluorescence cannot be fixed in formalin, prior to analysis, since the resultant cross-linking of proteins inhibits antibody binding and even short exposure of a few minutes can render specimens unsuitable for DIF analysis [42]. The transport medium of choice is the immunofluorescence-specific solution, Michel's medium [43], which is widely available commercially and preserves immune complexes for up to 6 months at room temperature [44]. Following receipt in the laboratory, specimens are typically rinsed in phosphate buffered saline, to remove ammonium salts present in Michel's medium and then snap-frozen in an embedding compound such as OCT, following careful orientation of the specimen [45]. A series of frozen tissue

**TABLE 1 |** Principal auto-antibody specificities in immunobullous disorders.

| Disease | Major Auto-antigen(s) | Other auto-antigens |
|---|---|---|
| | Intra-epithelial | |
| Pemphigus vulgaris | Desmoglein 3, desmoglein 1 | Desmocollin 3 |
| Pemphigus foliaceus | Desmoglein 1 | |
| Paraneoplastic pemphigus | Desmoglein 3, envoplakin, periplakin | Desmoglein 1, desmoplakin I, desmoplakin II, BP230, plectin, desmoglein 1, desmocollin II |
| IgA pemphigus | Desmocollin 1, desmoglein 1, desmoglein 3 | Desmocollin 2, Desmocollin 3 |
| | Sub-epithelial | |
| Bullous pemphigoid | BP180, BP230 | |
| Pemphigoid gestationis | BP180 | BP230 |
| Linear IgA disease | BP180 | BP230 |
| Mucous membrane pemphigoid | BP180, BP230 | Laminin 332, α6β4 integrin |
| Anti laminin γ1/p200 pemphigoid | Laminin γ1 | |
| Epidermolysis bullosa acquisita | Type VII collagen | |
| Dermatitis herpetiformis | Epidermal transglutaminase | |

sections, ideally of 4–5 μm thickness, are cut using a cryostat and placed on microscope slides, prior to addition of fluorescent conjugates and incubation, to facilitate immune complex formation. Following incubation, slides are washed, to remove unbound antibodies, then dried, mounted in buffered glycerol and examined by fluorescence microscopy. Inclusion of both positive and negative control material representing all conjugates under investigation and processed contemporaneously with test material, is essential for the accurate interpretation of direct immunofluorescence microscopy.

## Indirect Immunofluorescence (IIF)

IIF is a two-step procedure used to identify circulating autoantibodies to cutaneous or mucosal antigens in patient serum. These antibodies are most commonly of IgG and IgA isotypes. Although serological antibody concentrations are typically much lower than those found in tissues of patients with AIBD and DIF has a higher sensitivity for detection of these diseases [46], IIF is a useful tool, both for confirming diagnoses made using DIF and for facilitating titration of antibody levels, which can be useful in treatment monitoring if ELISA is unavailable or less common antigens are targeted. This technique can also be used to establish a primary diagnosis in patients where a tissue biopsy is not possible or considered inappropriate. In recent years, IIF techniques have been performed alongside ELISA methodologies, to improve detection sensitivity and provide data on autoantibody specificity [47].

Following blood sample collection, serum is separated by centrifugation and can be stored at 4°C for up to 1 month, prior to analysis. To detect circulating autoantibodies, tissues containing corresponding antigens must be used as a substrate. Two principal tissue types are commonly employed. Monkey oesophagus provides a rich source of desmoglein proteins, particularly desmoglein-3 and is therefore the substrate of choice for the detection of pemphigus vulgaris antibodies [48]. Commercial slides are widely used and can be stored at 4°C for several months, prior to use. Normal human skin, usually derived from discarded surgical material, is the second most commonly used tissue substrate for IIF studies. Whilst both tissues can be used to screen for, and titrate out, circulating antibodies in most AIBD, normal human skin offers several advantages, including greater sensitivity (with the exception of antibodies associated with pemphigus vulgaris) [49] and antigenic localisation options unavailable when using monkey oesophagus. In addition, there are two key limitations to the use of monkey oesophagus substrate for IIF. Firstly, this tissue is known to exhibit non-specific intercellular fluorescence of epithelium in sera from a sub-population of individuals with no underlying immunobullous disease, potentially resulting in false positive diagnoses of pemphigus. Pre-adsorption of test sera with soluble A/B blood group antigens, as a blocking step, may reduce this non-specificity [50]. Secondly, monkey oesophagus expresses very low levels of BP180 protein, the most common antigen targeted in bullous pemphigoid and, therefore, false negative diagnosis of this disease is possible if monkey oesophagus is the sole substrate used in IIF analysis [51].

In addition to normal human skin substrate, use of human salt-split skin provides a valuable third substrate for IIF. The split-skin method is a relatively straightforward and reliable technique for distinguishing between epidermal and dermal-binding autoantibodies in sub-epithelial AIBD [52]. It relies on splitting human skin through a defined cleavage plane in the lamina lucida, such that BP antigens typically localise to the epidermal side (often referred to as the "roof" of the split) whereas components of the lamina densa, including laminin proteins and the EBA antigen, type VII collagen, are found on the dermal side (i.e., the "base" or "floor" of the split). Various methods exist to split skin through the lamina lucida, the most commonly used being incubation of skin in 1M sodium chloride for 24–72 h at 4°C [53]. Following incubation, the epidermis can be gently teased apart from the underlying dermis using a fine pair of forceps. In addition to providing a substrate for IIF screening, this technique can also be used to split biopsies in DIF studies, to localise BMZ antibody distribution (**Figure 1**).

A fourth, less frequently used IIF substrate is rat (or monkey) urinary bladder, or similar tissues, that contain transitional epithelium. Unlike stratified squamous epithelium found in skin, transitional epithelium does not produce DSG1 or DSG3, but expresses significant levels of desmosomal plakin family

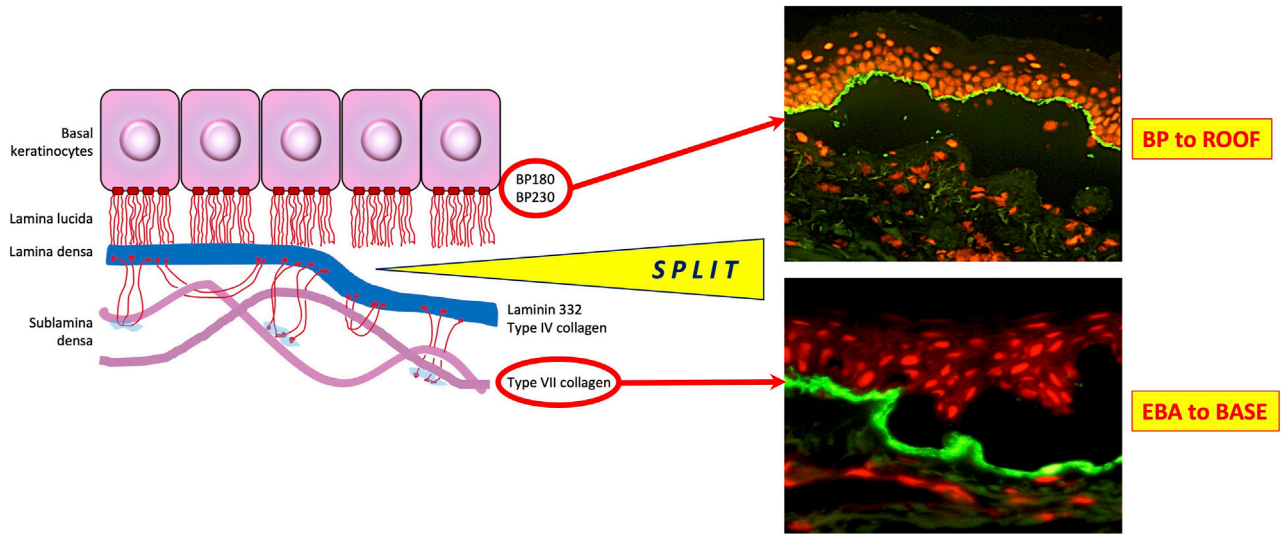


**FIGURE 1 |** Utility of salt-split skin in differentiating autoimmune bullous dermatoses. BP, bullous pemphigoid; EBA, epidermolysis bullosa acquisita. Modified from [54].

proteins, especially envoplakin, periplakin and desmoplakin [55]. Antibodies against these proteins are found in the serum of patients with PNP and intercellular IgG fluorescence on this substrate may provide a diagnostic indicator of this disease [56], although it is not seen in all patients.

To detect circulating autoantibodies in a patient with a suspected AIBD, slides prepared with 4–5 μm frozen sections of appropriate tissue substrates are incubated with diluted patient serum. After incubation, slides are washed to remove unbound antibodies and incubated again with fluorescently labelled anti-human IgG or IgA conjugates. They are then washed again and dried, prior to mounting and subsequent fluorescence microscopy. Results are typically reported either qualitatively (positive or negative for intercellular or basement membrane zone fluorescence) or semi-quantitatively (by end-point titre of serial serum dilutions) for both IgG and IgA conjugates [57]. As with direct immunofluorescence, inclusion of appropriate positive and negative control sera for all substrates and conjugates used with test specimens is essential for valid interpretation of results.

## Enzyme-Linked Immunosorbent Assay (ELISA)

In addition to IIF techniques, circulating antibodies in serum from patients with AIBD can be detected using ELISA. Unlike IIF, ELISA techniques are specific for known autoantigens and offer higher sensitivity and a greater degree of quantitation [58], which can be particularly useful for treatment monitoring of patients. They are routinely performed using 96 well microtitre plates that have been pre-coated with recombinant antigenic peptides. Diluted serum is added and any specific antibodies in the serum will bind to the immobilised antigen. Following washing to remove unbound antibodies, a secondary antibody raised against human IgG and conjugated with an enzyme that catalyses a colorimetric reaction is added. After further incubation and washing steps, a substrate for the enzyme conjugated to the secondary antibody is added and a colour change occurs which is directly proportional to the quantity of specific antibody present in the patient serum sample. This colour change is quantified using spectrophotometry and compared with that produced from known standards in other wells on the plate to generate quantitative data.

ELISAs are typically performed using commercial kits to assess the most commonly occurring autoantibodies seen in AIBD, i.e., DSG1 & DSG3 antibodies in pemphigus [59], BP180 & BP230 antibodies in pemphigoid diseases [60, 61] and collagen VII antibodies in EBA [62]. A limitation of these assays is that ELISA systems only detect antibodies against specific, known antigens and are, therefore, of limited value in assessing patient sera that predominantly contain antibodies to other, less common antigens seen in AIBD. This technique is, therefore, most useful when used in combination with IIF methodologies or for monitoring levels of antibodies in patients with previously characterised, specific antigen positivity, undergoing continued treatment [63].

# DIAGNOSTIC FINDINGS

Application of DIF methodologies to tissue biopsies and IIF protocols to serum specimens from patients with suspected AIBD produces two principal types of fluorescence pattern. Those patients with intra-epithelial AIBD display an intercellular pattern, as a result of antibody binding to disrupted desmosomes located on epithelial cell membranes, whereas patients with sub-epithelial AIBD exhibit sharp, linear fluorescence at the basement membrane zone, due to antibody binding to hemidesmosomal targets in these tissues. Further diagnostic clues in DIF are provided by spatial localisation of fluorescence and the combination and relative fluorescence

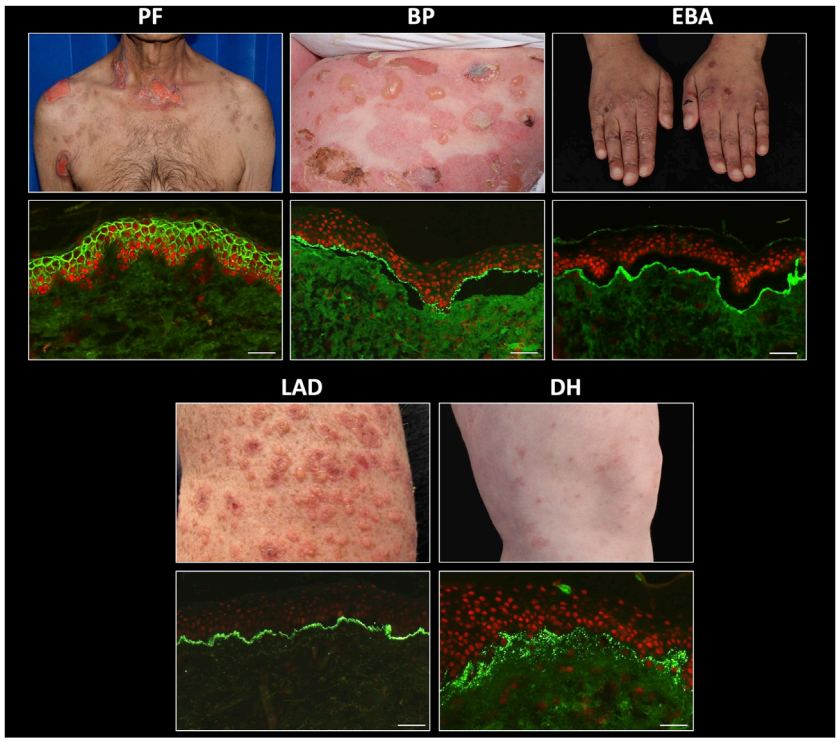


**FIGURE 2 |** Direct immunofluorescence findings in autoimmune bullous dermatoses. PF, pemphigus foliaceus; BP, bullous pemphigoid; EBA, epidermolysis bullosa acquisita; LAD, linear IgA disease; DH, dermatitis herpetiformis. Scale bar = 100 μm.

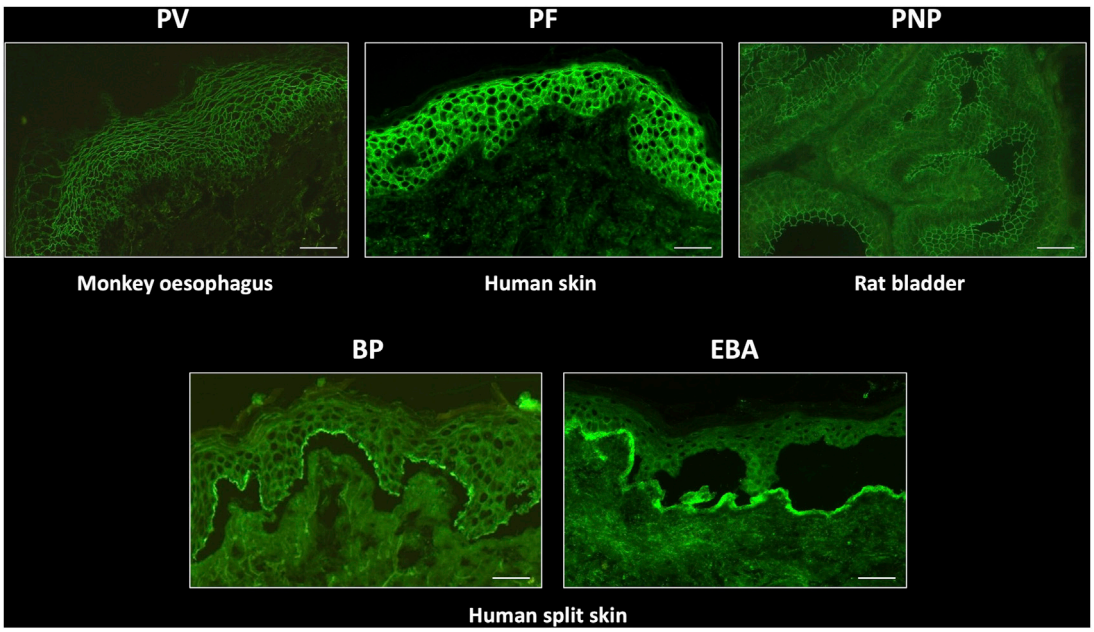


**FIGURE 3 |** Typical indirect immunofluorescence findings in autoimmune bullous dermatoses. PV, pemphigus vulgaris; PF, pemphigus foliaceus; PNP, paraneoplastic pemphigus; BP, bullous pemphigoid; EBA, epidermolysis bullosa acquisita. Scale bar = 100 μm.

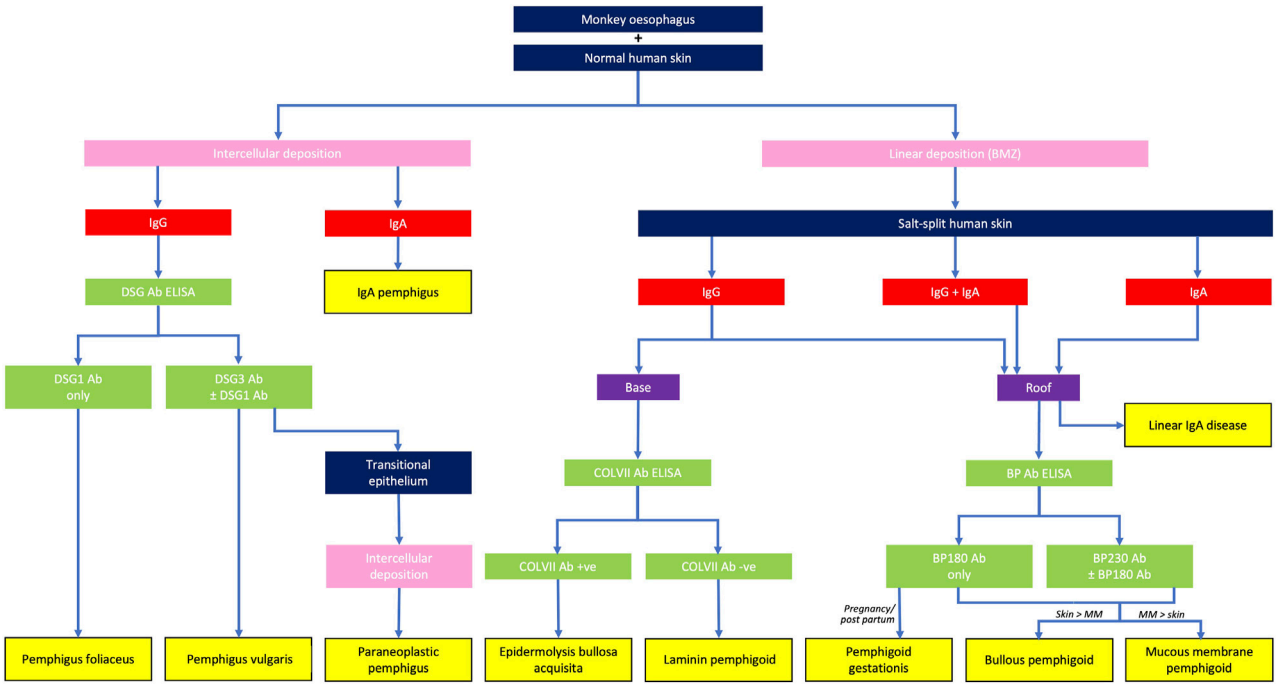


**FIGURE 4 |** Differential diagnoses of autoimmune blistering diseases, based on the serological detection of autoantibodies. BMZ, basement membrane zone; MM, mucous membranes.

intensity of positive conjugates observed. A combination of substrate positivity, fluorescence pattern seen (intercellular vs. linear), conjugate positivity (IgG vs. IgA), split skin analysis and relevant ELISA positivity can be used to provide a diagnosis from a serum sample (**Figure 2**). Specific findings for the most commonly seen AIBD are described below.

## Pemphigus

Direct immunofluorescence in patients with all types of pemphigus produces a characteristic, sharp, "chicken-wire" pattern with IgG and/or C3 conjugates, localising to epithelial cell membranes (**Figure 3**). IgA may also be seen in a similar pattern in a small number of cases. This finding is diagnostic for pemphigus [46]. Despite differences in the expression patterns of DSG1 and DSG3 between cutaneous and mucosal epithelial tissues, it can be challenging to reliably differentiate between PV and PF in DIF studies. In addition, quantitation of antibody levels is not possible by DIF. In a very small number of cases, the presence of linear IgG and/or C3 deposition at the BMZ, in addition to epithelial intercellular IgG, raises the possibility of PNP, which also requires serological investigations for accurate diagnosis. Therefore, serum should be requested from all patients with positive DIF for pemphigus, for further characterisation.

Monkey oesophagus is most commonly used as a substrate to titrate IgG antibodies from the serum of patients with PV, whereas patients with PF exhibit IgG antibodies which bind preferentially to human skin substrate. This substrate distinction is not absolute, since serum from patients with the mucocutaneous variant of PV, who produce autoantibodies against both DSG1 and DSG3, display immunofluorescence on both substrates and monkey oesophagus typically also fluoresces in PF. Quantitation of specific anti-DSG1 and DSG3 antibodies can be achieved with DSG ELISA and facilitates pemphigus sub-typing. Patients with DSG1 antibodies alone are defined as having PF, whereas those with anti DSG3 (with or without additional anti DSG1 antibodies) are predominantly patients with PV [19]. DSG antibody ELISA values generally correlate well with IIF titres and disease severity [64], although the greater sensitivity and specificity of ELISA makes it the preferred technique for monitoring disease activity and treatment response [63].

IIF using rat transitional epithelium substrate can be performed on sera from patients with suspected PNP, who typically also express DSG3 ± DSG1 antibodies. PNP can be differentiated from PV by the additional finding of intercellular IgG deposition on transitional epithelium (**Figure 4**), due to the presence of plakin family antibodies in this disease, most commonly envoplakin and periplakin [65]. Specific envoplakin antibody ELISA can also be used to indicate a PNP diagnosis.

## Pemphigoid

Diseases of the pemphigoid sub-family show a linear deposition pattern of IgG and/or C3 at the BMZ of epithelial tissue by DIF, due to the hemidesmosomal location of antigens targeted in these diseases (**Figure 3**). IgA linear BMZ fluorescence is also seen in some pemphigoid patients, particularly those with MMP. Salt-splitting of biopsies from most pemphigoid patients and subsequent repeated processing for DIF reveals localisation of linear fluorescence to the epidermal side (roof) of the split, typically representative of antibodies to epitopes within BP180 and/or BP230 proteins (**Figure 2**). Localisation of linear fluorescence to

the dermal side (base) of salt-split skin is indicative either of EBA or a dermal-binding pemphigoid, including those that target chains of laminin proteins (e.g., laminin-332 and γ1 laminin), which have a higher association with malignancy [66] and are difficult to treat [67].

Indirect immunofluorescence on sera from BP patients, using split normal human skin as a substrate, typically produces circulating autoantibody titres that are higher than those seen in pemphigus. In addition, IIF permits differentiation of this disease from EBA, in cases where biopsy material is not available for DIF analysis, in addition to identification of patients with a heterogeneous autoantibody response, which may be observed as immunolocalisation to both the roof and base on the split skin substrate. A specific ELISA for anti BP180 and/or BP230 antibodies provides confirmation of a BP diagnosis with approximately 90% sensitivity [68]. BP180 ELISA values correlate with disease activity [69], although there is no strong correlation between BP230 ELISA levels and disease activity [61] and a number of pemphigoid patients have no detectable circulating antibodies against either of these proteins. This is most often observed in patients with MMP, in whom up to 50% of cases are undetectable by either IIF [70] or anti BP180/BP230 antibody ELISA [71]. Anti-BP180 ELISA is a particularly useful tool for diagnosing patients with pregnancy-associated pemphigoid gestationis, who exhibit low levels of IgG binding to BP180 antigens which is often detectable only with the C3 conjugate in DIF. However, strong anti-BP180 ELISA positivity from serum can be diagnostic for PG, in the appropriate clinical context [72].

### Linear IgA Disease

Patients with linear IgA disease show a bright, linear deposition of IgA at the BMZ on DIF. In addition, there may be a weak linear IgG and/or C3 band present in some patients. The relative intensities of the IgA and IgG deposits can be useful in differentiating linear IgA disease from MMP, if this is unclear from the clinical or histological presentations. Since BP180 is the predominant target antigen in linear IgA disease, split-skin IIF in these patients typically shows localisation of IgA to the roof of the split, although titres are lower, compared with IgG levels seen in pemphigoid patients. A small proportion of linear IgA cases show base-binding localisation, which may be attributable to collagen VII reactivity, since this is the predominant antigen in cases of drug-induced linear IgA disease precipitated by the antibiotic, vancomycin [73]. Commercial anti BP180 antibody ELISA is uninformative for this disease since kits use an anti-IgG conjugate for detection of signal.

### Epidermolysis Bullosa Acquisita

DIF on biopsies from EBA patients shows linear deposition of IgG, with or without C3, at the basement membrane zone, in a similar pattern to that seen in BP patients. However, careful microscopic examination may indicate a slightly thicker band than that seen in BP, with a u-serrated pattern seen at higher magnifications [74]. Salt-splitting of the biopsy and repeated DIF analysis results in localisation of the linear deposition to the base of the split. This facilitates differentiation from most cases of pemphigoid, except those targeting chains of laminin proteins. IIF for EBA using human split skin shows the same basal localisation of linear BMZ fluorescence and anti collagen VII antibody ELISA is useful to confirm EBA, differentiate it from dermal-binding (laminin) pemphigoid cases and to help guide treatment decisions, since circulating anti COLVII antibody levels correlate with disease activity [75].

### Dermatitis Herpetiformis

Biopsies from patients with DH exhibit a characteristic pattern of granular (sometimes fibrillar) deposition of IgA at or just below the dermo-epidermal junction (**Figure 2**). Deposits may be subtle and IIF using standard substrates is usually negative, possibly due to an absence of tissue-fixed epidermal transglutaminase [76], although the precise mechanism by which IgA immune deposits localize at the dermo-epidermal junction in this disease remains incompletely understood [77].

## CONCLUSION

Direct immunofluorescence remains the gold standard for the diagnosis of AIBD from cutaneous and mucosal biopsies. Advances in the characterisation of the autoantibodies produced in these diseases and their antigenic targets has facilitated the development of additional serological assays which can be used both to confirm and refine the diagnosis indicated by DIF. In particular, the availability of autoantibody-specific ELISA has increased serological sensitivity of AIBD detection over the last 25 years and provided quantitation of antibody production that has become a valuable tool in the therapeutic management of patients. Combined use of DIF, multi-substrate IIF and ELISA methodologies currently provides the optimal strategy for diagnosis and immunological monitoring in these diseases. Future developments will likely focus on the continued development of multiplex assays that facilitate simultaneous measurement of multiple antibodies in a single serum sample, including multi-substrate BIOCHIP mosaics for IIF [78], multiparameter ELISA kits [79, 80] and multiplex bead-based immunoassays [81]. Correlation of the resulting antibody profiles from such assays with prognostic outcomes raises the possibility of individualised treatment options.

## AUTHOR CONTRIBUTIONS

The author confirms being the sole contributor of this work and has approved it for publication.

## CONFLICT OF INTEREST

The author declares that the research was conducted in the absence of any commercial or financial relationships that could be construed as a potential conflict of interest.

## ACKNOWLEDGMENTS

The author is grateful to Dr. Thomas Tull for provision of clinical images and to the patients for consenting to publication of these images.

## REFERENCES


1. Egami S, Yamagami J, Amagai M. Autoimmune Bullous Skin Diseases, Pemphigus and Pemphigoid. *J Allergy Clin Immunol* (2020) 145:1031–47. doi:10.1016/j.jaci.2020.02.013
2. Bystryn JC, Steinman NM. The Adjuvant Therapy of Pemphigus. An Update. *Arch Dermatol* (1996) 132:203–12. doi:10.1001/archderm.132.2.203
3. Beutner EH, Re J. Demonstration of Skin Antibodies in Sera of Pemphigus Vulgaris Patients by Indirect Immunofluorescent Staining. *Proc Soc Exp Biol Med* (1964) 117:505–10. doi:10.3181/00379727-117-29622
4. Jordon RE, Beutner EH, Witebsky E, Blumental G, Hale WL, Lever WF. Basement Zone Antibodies in Bullous Pemphigoid. *JAMA* (1967) 200:751–6. doi:10.1001/jama.200.9.751
5. Zillikens D, Mascaro JM, Rose PA, Liu Z, Ewing SM, Caux F, et al. A Highly Sensitive Enzyme-Linked Immunosorbent Assay for the Detection of Circulating Anti-BP180 Autoantibodies in Patients With Bullous Pemphigoid. *J Invest Dermatol* (1997) 109:679–83. doi:10.1111/1523-1747.ep12338088
6. Ishii K, Amagai M, Hall RP, Hashimoto T, Takayanagi A, Gamou S, et al. Characterization of Autoantibodies in Pemphigus Using Antigen-Specific Enzyme-Linked Immunosorbent Assays With Baculovirus-Expressed Recombinant Desmogleins. *J Immunol* (1997) 159:2010–7. doi:10.4049/jimmunol.159.4.2010
7. Baum S, Sakka N, Artsi O, Trau H, Barzilai A. Diagnosis and Classification of Autoimmune Blistering Diseases. *Autoimmun Rev* (2014) 13:482–9. doi:10.1016/j.autrev.2014.01.047
8. Müller L, Hatzfeld M, Keil R. Desmosomes as Signaling Hubs in the Regulation of Cell Behavior. *Front Cel Dev Biol* (2021) 9:745670. doi:10.3389/fcell.2021.745670
9. Green KJ, Gaudry CA. Are Desmosomes More Than Tethers for Intermediate Filaments. *Nat Rev Mol Cel Biol* (2000) 1:208–16. doi:10.1038/35043032
10. Hegazy M, Perl AL, Svoboda SA, Green KJ. Desmosomal Cadherins in Health and Disease. *Annu Rev Pathol Mech Dis* (2022) 17:47–72. doi:10.1146/annurev-pathol-042320-092912
11. Harrison OJ, Brasch J, Lasso G, Katsamba PS, Ahlsen G, Honig B, et al. Structural Basis of Adhesive Binding by Desmocollins and Desmogleins. *Proc Natl Acad Sci U S A* (2016) 113:7160–5. doi:10.1073/pnas.1606272113
12. Dusek RL, Godsel LM, Green KJ. Discriminating Roles of Desmosomal Cadherins: Beyond Desmosomal Adhesion. *J Dermatol Sci* (2007) 45:7–21. doi:10.1016/j.jdermsci.2006.10.006
13. Chan LS. Human Skin Basement Membrane in Health and in Autoimmune Diseases. *Front Biosci* (1997) 2:d343–52. doi:10.2741/a196
14. Roig-Rosello E, Rousselle P. The Human Epidermal Basement Membrane: A Shaped and Cell Instructive Platform That Aging Slowly Alters. *Biomolecules* (2020) 10:1607. doi:10.3390/biom10121607
15. Walko G, Castañón MJ, Wiche G. Molecular Architecture and Function of the Hemidesmosome. *Cell Tissue Res* (2015) 360:529–44. doi:10.1007/s00441-015-2216-6
16. Ko MS, Marinkovich MP. Role of Dermal-Epidermal Basement Membrane Zone in Skin, Cancer, and Developmental Disorders. *Dermatol Clin* (2010) 28:1–16. doi:10.1016/j.det.2009.10.001
17. Stanley JR, Koulu L, Klaus-Kovtun V, Steinberg MS. A Monoclonal Antibody to the Desmosomal Glycoprotein Desmoglein I Binds the Same Polypeptide as Human Autoantibodies in Pemphigus Foliaceus. *J Immunol* (1986) 136:1227–30. doi:10.4049/jimmunol.136.4.1227
18. Amagai M, Klaus-Kovtun V, Stanley JR. Autoantibodies Against a Novel Epithelial Cadherin in Pemphigus Vulgaris, a Disease of Cell Adhesion. *Cell* (1991) 67:869–77. doi:10.1016/0092-8674(91)90360-b
19. Amagai M, Tsunoda K, Zillikens D, Nagai T, Nishikawa T. The Clinical Phenotype of Pemphigus Is Defined by the Anti-Desmoglein Autoantibody Profile. *J Am Acad Dermatol* (1999) 40:167–70. doi:10.1016/s0190-9622(99)70183-0
20. Schmidt E, Kasperkiewicz M, Joly P. Pemphigus. *Lancet* (2019) 394:882–94. doi:10.1016/S0140-6736(19)31778-7
21. Anhalt GJ, Kim SC, Stanley JR, Korman NJ, Jabs DA, Kory M, et al. Paraneoplastic Pemphigus. An Autoimmune Mucocutaneous Disease Associated With Neoplasia. *N Engl J Med* (1990) 323:1729–35. doi:10.1056/NEJM199012203232503
22. Amber KT, Valdebran M, Grando SA. Paraneoplastic Autoimmune Multiorgan Syndrome (PAMS): Beyond the Single Phenotype of Paraneoplastic Pemphigus. *Autoimmun Rev* (2018) 17:1002–10. doi:10.1016/j.autrev.2018.04.008
23. Hashimoto T, Kiyokawa C, Mori O, Miyasato M, Chidgey MA, Garrod DR, et al. Human Desmocollin 1 (Dsc1) Is an Autoantigen for the Subcorneal Pustular Dermatosis Type of IgA Pemphigus. *J Invest Dermatol* (1997) 109:127–31. doi:10.1111/1523-1747.ep12319025
24. Chams-Davatchi C, Valikhani M, Daneshpazhooh M, Esmaili N, Balighi K, Hallaji Z, et al. Pemphigus: Analysis of 1209 Cases. *Int J Dermatol* (2005) 44:470–6. doi:10.1111/j.1365-4632.2004.02501.x
25. Jelti L, Cordel N, Gillibert A, Lacour JP, Uthurriague C, Doutre MS, et al. Incidence and Mortality of Pemphigus in France. *J Invest Dermatol* (2019) 139(2):469–73. doi:10.1016/j.jid.2018.07.042
26. Schmidt E, Zillikens D. Pemphigoid Diseases. *Lancet* (2013) 381:320–32. doi:10.1016/S0140-6736(12)61140-4
27. Langan SM, Smeeth L, Hubbard R, Fleming KM, Smith CJ, West J. Bullous Pemphigoid and Pemphigus Vulgaris--Incidence and Mortality in the UK: Population Based Cohort Study. *BMJ* (2008) 337:a180. doi:10.1136/bmj.a180
28. Diaz LA, Ratrie H, Saunders WS, Futamura S, Squiquera HL, Anhalt GJ, et al. Isolation of a Human Epidermal cDNA Corresponding to the 180-kD Autoantigen Recognized by Bullous Pemphigoid and Herpes Gestationis Sera. Immunolocalization of This Protein to the Hemidesmosome. *J Clin Invest* (1990) 86:1088–94. doi:10.1172/JCI114812
29. Stanley JR, Tanaka T, Mueller S, Klaus-Kovtun V, Roop D. Isolation of Complementary DNA for Bullous Pemphigoid Antigen by Use of Patients' Autoantibodies. *J Clin Invest* (1988) 82:1864–70. doi:10.1172/JCI113803
30. Charneux J, Lorin J, Vitry F, Antonicelli F, Reguiai Z, Barbe C, et al. Usefulness of BP230 and BP180-NC16a Enzyme-Linked Immunosorbent Assays in the Initial Diagnosis of Bullous Pemphigoid: A Retrospective Study of 138 Patients. *Arch Dermatol* (2011) 147:286–91. doi:10.1001/archdermatol.2011.23
31. Chan LS, Ahmed AR, Anhalt GJ, Bernauer W, Cooper KD, Elder MJ, et al. The First International Consensus on Mucous Membrane Pemphigoid: Definition, Diagnostic Criteria, Pathogenic Factors, Medical Treatment, and Prognostic Indicators. *Arch Dermatol* (2002) 138:370–9. doi:10.1001/archderm.138.3.370
32. Patzelt S, Schmidt E. Autoimmunity against Laminin 332. *Front Immunol* (2023) 14:1250115. doi:10.3389/fimmu.2023.1250115
33. Setterfield J, Shirlaw PJ, Kerr-Muir M, Neill S, Bhogal BS, Morgan P, et al. Mucous Membrane Pemphigoid: A Dual Circulating Antibody Response With IgG and IgA Signifies a More Severe and Persistent Disease. *Br J Dermatol* (1998) 138:602–10. doi:10.1046/j.1365-2133.1998.02168.x
34. Fortuna G, Marinkovich MP. Linear Immunoglobulin A Bullous Dermatosis. *Clin Dermatol* (2012) 30:38–50. doi:10.1016/j.clindermatol.2011.03.008
35. Giudice GJ, Emery DJ, Zelickson BD, Anhalt GJ, Liu Z, Diaz LA. Bullous Pemphigoid and Herpes Gestationis Autoantibodies Recognize a Common Non-Collagenous Site on the BP180 Ectodomain. *J Immunol* (1993) 151:5742–50. doi:10.4049/jimmunol.151.10.5742
36. Dainichi T, Kurono S, Ohyama B, Ishii N, Sanzen N, Hayashi M, et al. Anti-Laminin Gamma-1 Pemphigoid. *Proc Natl Acad Sci U S A* (2009) 106:2800–5. doi:10.1073/pnas.0809230106
37. Koga H, Prost-Squarcioni C, Iwata H, Jonkman MF, Ludwig RJ, Bieber K. Epidermolysis Bullosa Acquisita: The 2019 Update. *Front Med (Lausanne)* (2018) 5:362. doi:10.3389/fmed.2018.00362
38. Collin P, Salmi TT, Hervonen K, Kaukinen K, Reunala T. Dermatitis Herpetiformis: A Cutaneous Manifestation of Coeliac Disease. *Ann Med* (2017) 49:23–31. doi:10.1080/07853890.2016.1222450
39. Sárdy M, Kárpáti S, Merkl B, Paulsson M, Smyth N. Epidermal Transglutaminase (TGase 3) Is the Autoantigen of Dermatitis Herpetiformis. *J Exp Med* (2002) 195:747–57. doi:10.1084/jem.20011299
40. Mutasim DF, Adams BB. Immunofluorescence in Dermatology. *J Am Acad Dermatol* (2001) 45:803–22. doi:10.1067/mjd.2001.117518
41. Sárdy M, Kostaki D, Varga R, Peris K, Ruzicka T. Comparative Study of Direct and Indirect Immunofluorescence and of Bullous Pemphigoid 180 and 230 Enzyme-Linked Immunosorbent Assays for Diagnosis of Bullous

Pemphigoid. *J Am Acad Dermatol* (2013) 69:748–53. doi:10.1016/j.jaad.2013.07.009
42. Arbesman J, Grover R, Helm TN, Beutner EH. Can Direct Immunofluorescence Testing Still Be Accurate if Performed on Biopsy Specimens After Brief Inadvertent Immersion in Formalin. *J Am Acad Dermatol* (2011) 65:106–11. doi:10.1016/j.jaad.2010.06.019
43. Michel B, Milner Y, David K. Preservation of Tissue-Fixed Immunoglobulins in Skin Biopsies of Patients With Lupus Erythematosus and Bullous Diseases--Preliminary Report. *J Invest Dermatol* (1972) 59:449–52. doi:10.1111/1523-1747.ep12627611
44. Vaughan Jones SA, Salas J, McGrath JA, Palmer I, Bhogal GS, Black MM. A Retrospective Analysis of Tissue-Fixed Immunoreactants From Skin Biopsies Maintained in Michel's Medium. *Dermatology* (1994) 189(1):131–2. doi:10.1159/000246955
45. Shetty VM, Subramaniam K, Rao R. Utility of Immunofluorescence in Dermatology. *Indian Dermatol Online J* (2017) 8:1–8. doi:10.4103/2229-5178.198774
46. Giurdanella F, Diercks GF, Jonkman MF, Pas HH. Laboratory Diagnosis of Pemphigus: Direct Immunofluorescence Remains the Gold Standard. *Br J Dermatol* (2016) 175(1):185–6. doi:10.1111/bjd.14408
47. Saschenbrecker S, Karl I, Komorowski L, Probst C, Dähnrich C, Fechner K, et al. Serological Diagnosis of Autoimmune Bullous Skin Diseases. *Front Immunol* (2019) 10:1974. doi:10.3389/fimmu.2019.01974
48. Harman KE, Gratian MJ, Bhogal BS, Challacombe SJ, Black MM. The Use of Two Substrates to Improve the Sensitivity of Indirect Immunofluorescence in the Diagnosis of Pemphigus. *Br J Dermatol* (2000) 142:1135–9. doi:10.1046/j.1365-2133.2000.03538.x
49. Goldberg DJ, Sabolinski M, Bystryn JC. Bullous Pemphigoid Antibodies. Human Skin as a Substrate for Indirect Immunofluorescence Assay. *Arch Dermatol* (1985) 121:1137–40. doi:10.1001/archderm.121.9.1137
50. Lee FJ, Silvestrini R, Fulcher DA. False-Positive Intercellular Cement Substance Antibodies Due to Group A/B Red Cell Antibodies: Frequency and Approach. *Pathology* (2010) 42:574–7. doi:10.3109/00313025.2010.508792
51. Emtenani S, Yuan H, Lin C, Pan M, Hundt JE, Schmidt E, et al. Normal Human Skin Is superior to Monkey Oesophagus Substrate for Detection of Circulating BP180-NC16A-Specific IgG Antibodies in Bullous Pemphigoid. *Br J Dermatol* (2019) 180:1099–106. doi:10.1111/bjd.17313
52. Gammon WR, Fine J-D, Forbes M, Briggaman RA. Immunofluorescence on Split Skin for the Detection and Differentiation of Basement Membrane Zone Autoantibodies. *J Am Acad Dermatol* (1992) 27:79–87. doi:10.1016/0190-9622(92)70161-8
53. Gammon WR, Briggaman RA, Inman AO, Queen LL, Wheeler CE. Differentiating Anti-Lamina Lucida and Anti-Sublamina Densa Anti-BMZ Antibodies by Indirect Immunofluorescence on 1.0 M Sodium Chloride-Separated Skin. *J Invest Dermatol* (1984) 82:139–44. doi:10.1111/1523-1747.ep12259692
54. Bolognia JL, Schaffer JV, Cerroni L. *Dermatology: 2-Volume Set*. London: Elsevier Health Sciences (2017). Figure 28.8. Used with permission, conveyed through Copyright Clearance Center Inc.
55. Poot AM, Diercks GF, Kramer D, Schepens I, Klunder G, Hashimoto T, et al. Laboratory Diagnosis of Paraneoplastic Pemphigus. *Br J Dermatol* (2013) 169:1016–24. doi:10.1111/bjd.12479
56. Liu AY, Valenzuela R, Helm TN, Camisa C, Melton AL, Bergfeld WF. Indirect Immunofluorescence on Rat Bladder Transitional Epithelium: A Test With High Specificity for Paraneoplastic Pemphigus. *J Am Acad Dermatol* (1993) 28:696–9. doi:10.1016/0190-9622(93)70095-b
57. Jindal A, Rao R, Bhogal BS. Advanced Diagnostic Techniques in Autoimmune Bullous Diseases. *Indian J Dermatol* (2017) 62:268–78. doi:10.4103/ijd.IJD_196_17
58. Tampoia M, Giavarina D, Di Giorgio C, Bizzaro N. Diagnostic Accuracy of Enzyme-Linked Immunosorbent Assays (ELISA) to Detect Anti-Skin Autoantibodies in Autoimmune Blistering Skin Diseases: A Systematic Review and Meta-Analysis. *Autoimmun Rev* (2012) 12:121–6. doi:10.1016/j.autrev.2012.07.006
59. Harman KE, Gratian MJ, Seed PT, Bhogal BS, Challacombe SJ, Black MM. Diagnosis of Pemphigus by ELISA: A Critical Evaluation of Two ELISAs for the Detection of Antibodies to the Major Pemphigus Antigens, Desmoglein 1 and 3. *Clin Exp Dermatol* (2000) 25:236–40. doi:10.1046/j.1365-2230.2000.00624.x
60. Kobayashi M, Amagai M, Kuroda-Kinoshita K, Hashimoto T, Shirakata Y, Hashimoto K, et al. BP180 ELISA Using Bacterial Recombinant NC16a Protein as a Diagnostic and Monitoring Tool for Bullous Pemphigoid. *J Dermatol Sci* (2002) 30:224–32. doi:10.1016/s0923-1811(02)00109-3
61. Yoshida M, Hamada T, Amagai M, Hashimoto K, Uehara R, Yamaguchi K, et al. Enzyme-Linked Immunosorbent Assay Using Bacterial Recombinant Proteins of Human BP230 as a Diagnostic Tool for Bullous Pemphigoid. *J Dermatol Sci* (2006) 41:21–30. doi:10.1016/j.jdermsci.2005.11.002
62. Komorowski L, Müller R, Vorobyev A, Probst C, Recke A, Jonkman MF, et al. Sensitive and Specific Assays for Routine Serological Diagnosis of Epidermolysis Bullosa Acquisita. *J Am Acad Dermatol* (2013) 68:e89–e95. doi:10.1016/j.jaad.2011.12.032
63. Schmidt E, Zillikens D. Modern Diagnosis of Autoimmune Blistering Skin Diseases. *Autoimmun Rev* (2010) 10:84–9. doi:10.1016/j.autrev.2010.08.007
64. Schmidt E, Dähnrich C, Rosemann A, Probst C, Komorowski L, Saschenbrecker S, et al. Novel ELISA Systems for Antibodies to Desmoglein 1 and 3: Correlation of Disease Activity With Serum Autoantibody Levels in Individual Pemphigus Patients. *Exp Dermatol* (2010) 19:458–63. doi:10.1111/j.1600-0625.2010.01069.x
65. Nagata Y, Karashima T, Watt FM, Salmhofer W, Kanzaki T, Hashimoto T. Paraneoplastic Pemphigus Sera React Strongly With Multiple Epitopes on the Various Regions of Envoplakin and Periplakin, Except for the C-Terminal Homologous Domain of Periplakin. *J Invest Dermatol* (2001) 116:556–63. doi:10.1046/j.1523-1747.2001.01263.x
66. Egan CA, Lazarova Z, Darling TN, Yee C, Coté T, Yancey KB. Anti-Epiligrin Cicatricial Pemphigoid and Relative Risk for Cancer. *Lancet* (2001) 357(9271):1850–1. doi:10.1016/S0140-6736(00)04971-0
67. Shi L, Li X, Qian H. Anti-Laminin 332-Type Mucous Membrane Pemphigoid. *Biomolecules* (2022) 12:1461. doi:10.3390/biom12101461
68. Roussel A, Benichou J, Randriamanantany ZA, Gilbert D, Drenovska K, Houivet E, et al. Enzyme-Linked Immunosorbent Assay for the Combination of Bullous Pemphigoid Antigens 1 and 2 in the Diagnosis of Bullous Pemphigoid. *Arch Dermatol* (2011) 147:293–8. doi:10.1001/archdermatol.2011.21
69. Tsuji-Abe Y, Akiyama M, Yamanaka Y, Kikuchi T, Sato-Matsumura KC, Shimizu H. Correlation of Clinical Severity and ELISA Indices for the NC16A Domain of BP180 Measured Using BP180 ELISA Kit in Bullous Pemphigoid. *J Dermatol Sci* (2005) 37:145–9. doi:10.1016/j.jdermsci.2004.10.007
70. Witte M, Zillikens D, Schmidt E. Diagnosis of Autoimmune Blistering Diseases. *Front Med (Lausanne)* (2018) 5:296. doi:10.3389/fmed.2018.00296
71. Rashid H, Meijer JM, Diercks GFH, Sieben NE, Bolling MC, Pas HH, et al. Assessment of Diagnostic Strategy for Mucous Membrane Pemphigoid. *JAMA Dermatol* (2021) 157:780–7. doi:10.1001/jamadermatol.2021.1036
72. Al Saif F, Jouen F, Hebert V, Chiavelli H, Darwish B, Duvert-Lehembre S, et al. Sensitivity and Specificity of BP180 NC16A Enzyme-Linked Immunosorbent Assay for the Diagnosis of Pemphigoid Gestationis. *J Am Acad Dermatol* (2017) 76:560–2. doi:10.1016/j.jaad.2016.09.030
73. Yamagami J, Nakamura Y, Nagao K, Funakoshi T, Takahashi H, Tanikawa A, et al. Vancomycin Mediates IgA Autoreactivity in Drug-Induced Linear IgA Bullous Dermatosis. *J Invest Dermatol* (2018) 138:1473–80. doi:10.1016/j.jid.2017.12.035
74. Terra JB, Meijer JM, Jonkman MF, Diercks GF. The N-vs. U-Serration Is a Learnable Criterion to Differentiate Pemphigoid From Epidermolysis Bullosa Acquisita in Direct Immunofluorescence Serration Pattern Analysis. *Br J Dermatol* (2013) 169:100–5. doi:10.1111/bjd.12308
75. Kim JH, Kim YH, Kim S, Noh EB, Vorobyev A Serum Levels of Anti-Type VII Collagen Antibodies Detected by Enzyme-Linked Immunosorbent Assay in Patients With Epidermolysis Bullosa Acquisita Are Correlated With the Severity of Skin Lesions. *J Eur Acad Dermatol Venereol* (2013) 27:e224–30. doi:10.1111/j.1468-3083.2012.04617.x
76. Zone JJ, Schmidt LA, Taylor TB, Hull CM, Sotiriou MC, Jaskowski TD, et al. Dermatitis Herpetiformis Sera or Goat Anti-Transglutaminase-3 Transferred to Human Skin-Grafted Mice Mimics Dermatitis Herpetiformis Immunopathology. *J Immunol* (2011) 186:4474–80. doi:10.4049/jimmunol.1003273

77. Antiga E, Maglie R, Quintarelli L, Verdelli A, Bonciani D, Bonciolini V, et al. Dermatitis Herpetiformis: Novel Perspectives. *Front Immunol* (2019) 10:1290. doi:10.3389/fimmu.2019.01290
78. van Beek N, Rentzsch K, Probst C, Komorowski L, Kasperkiewicz M, Fechner K, et al. Serological Diagnosis of Autoimmune Bullous Skin Diseases: Prospective Comparison of the BIOCHIP Mosaic-Based Indirect Immunofluorescence Technique With the Conventional Multi-Step Single Test Strategy. *Orphanet J Rare Dis* (2012) 7:49. doi:10.1186/1750-1172-7-49
79. Horváth ON, Varga R, Kaneda M, Schmidt E, Ruzicka T, Sárdy M. Diagnostic Performance of the "MESACUP Anti-Skin Profile TEST". *Eur J Dermatol* (2016) 26:56–63. doi:10.1684/ejd.2015.2692
80. van Beek N, Dähnrich C, Johannsen N, Lemcke S, Goletz S, Hübner F, et al. Prospective Studies on the Routine Use of a Novel Multivariant Enzyme-Linked Immunosorbent Assay for the Diagnosis of Autoimmune Bullous Diseases. *J Am Acad Dermatol* (2017) 76:889–94. doi:10.1016/j.jaad.2016.11.002
81. Huber J, Schönthaler S, Hofner M, Gillitschka Y, Soldo R, Milchram L, et al. Accessing Antibody Reactivities in Serum or Plasma to (Auto-)antigens Using Multiplexed Bead-Based Protein Immunoassays. *Methods Mol Biol Serum/Plasma Proteomics* (2023) 2628:413–38. doi:10.1007/978-1-0716-2978-9_26

IBMS Institute of Biomedical Science | BJBS

ORIGINAL RESEARCH
published: 25 September 2023
doi: 10.3389/bjbs.2023.11591

# Evaluation of a New Mordant Based Haematoxylin Dye (Haematoxylin X) for Use in Clinical Pathology

*J. A. Gabriel[1]*†, C. D'Amico[1], U. Kosgodage[1], J. Satoc[1], N. Haine[2], S. Willis[2] and G. E. Orchard[1†]*

[1]St. John's Dermatopathology, Tissue Sciences, Synnovis Analytics, St. Thomas' Hospital, London, United Kingdom, [2]CellPath Ltd, Powys, United Kingdom

Recently, St John's Dermatopathology Laboratory and CellPath Ltd have developed a new patented haematoxylin dye (Haematoxylin X) that utilises a chromium-based mordant (Chromium Sulphate). In this study, the performance of this new haematoxylin (Haematoxylin X) was compared against some commonly utilised alum-based haematoxylins (Carazzi's, Harris' and Mayer's) when used as a part of formalin-fixed paraffin embedded (FFPE) tissue, special stains, immunohistochemical counterstaining and frozen section (Mohs procedure) staining procedures. FFPE sections of different tissue types and frozen skin tissues were sectioned and stained with each haematoxylin subtype to allow for a direct comparison of staining quality. The slides were independently evaluated microscopically by two assessors. A combined score was generated to determine the sensitivity (defined as the intensity of haematoxylin staining being too weak or too strong and the colour of the haematoxylin staining not being blue/black) and specificity (defined as the presence of haematoxylin background staining, uneven staining, and staining deposits) for each of the four haematoxylin subtypes. The scoring criteria were based on the UKNEQAS Cellular pathology techniques assessment criteria. In FFPE tissue, the results for specificity identified Harris haematoxylin scoring the highest (91.2%) followed by Haematoxylin X (88.0%) and Mayer's (87.0%). The sensitivity scores again identified Harris haematoxylin as scoring the highest (95.1%) followed by Haematoxylin X (90.0%) and Mayer's (88.0%). In frozen tissue, the results for specificity identified Haematoxylin X as scoring the highest (85.5%) followed by Carazzi's (80.7%) and Harris' (77.4%). The sensitivity scores again identified Haematoxylin X as scoring the highest (86.8%) followed by Carazzi's (82.0%) and Harris' (81.0%). The results achieved with all four haematoxylins showed a high degree of comparability, with Harris' haematoxylin scoring high scores overall compared to the other four when assessing FFPE sections. This may have been due to familiarity with the use of Harris' haematoxylin in-house. There was also evidence of more pronounced staining of extracellular mucin proteins with Haematoxylin X compared to the other alum haematoxylins that were assessed. Haematoxylin X scored highest when used in frozen section staining. In addition, Haematoxylin X has a potential applications for use in IHC and special stains procedures as a counterstain.

**Keywords: Haematoxylin X, Mohs micrographic surgery, routine staining, haematoxylin, paraffin processed and frozen tissue**



***Correspondence:**
*J. A. Gabriel*
*jeyrroy.gabriel@synnovis.co.uk*

**†ORCID:**
*J. A. Gabriel*
*orcid.org/0000-0003-4492-5200*
*G. E. Orchard*
*orcid.org/0000-0002-4757-0022*

***Received:** 18 May 2023*
***Accepted:** 11 September 2023*
***Published:** 25 September 2023*

***Citation:***
*Gabriel JA, D'Amico C, Kosgodage U, Satoc J, Haine N, Willis S and Orchard GE (2023) Evaluation of a New Mordant Based Haematoxylin Dye (Haematoxylin X) for Use in Clinical Pathology. Br J Biomed Sci 80:11591. doi: 10.3389/bjbs.2023.11591*

## INTRODUCTION

The haematoxylin dye remains the gold standard for microscopic nuclear visualisation of cellular and tissue components in Histopathology [1]. When used in combination with eosin dye, it remains the staple in the interpretation of pathological changes of tissue sections under microscopic evaluation. However, whilst most diagnostic tools have advanced in the last decades, the haematoxylin dyes have remained relatively unchanged since the 1980s. Recently, St John's Dermatopathology Laboratory and CellPath Ltd developed a new patented haematoxylin dye (Haematoxylin X) that utilises a chromium-based mordant (Chromium Sulphate) [2]. In this study, the performance of this new haematoxylin (Haematoxylin X) was compared against some commonly utilised alum-based haematoxylins (Carazzi's, Harris' and Mayer's) when used as a part of formalin-fixed paraffin embedded (FFPE) tissue, special stains, immunohistochemical counterstaining and frozen section (Mohs procedure) staining procedures.

The haematoxylin dye is extracted from the bark of the logwood tree *Haematoxylum campechianum* [2]. The logwood tree genus *Haematoxylum* is derived from the Greek word haima: blood and xylon: wood, which is in reference to the dark-red colour of the logwood [3]. The species name *campechianum* is in reference to its city of origin, which is Campeche, located on the Yucatan peninsula of Mexico [3].

The haematoxylin dye, which is weakly anionic in nature, once bound to a mordant becomes basic and positively charged [4]. This results in the dye binding to substances which are acidic in nature resulting in its ability to bind to DNA/RNA, which are basophilic and negatively charged due to the phosphate backbone in their structure [4]. The negatively charged backbone binds with the basic dye resulting in the formation of salts [4]. However, the haematoxylin dye itself does not stain the cellular components, but the oxidised form haematin, which achieves the distinct blue/black colour [5]. The conversion of haematoxylin to haematin is achieved by one of two methods;

1) Natural oxidation (ripening), which achieves oxidation with exposure to air and light. This is the slower of the two options and can take up to 4–10 weeks [3].
2) Chemical oxidations achieve conversion by using a chemical agent (e.g., Sodium Iodate or Mercuric Oxide). It is the faster of the two methods and can achieve results with immediate effect [3].

Haematin is anionic in nature, resulting in a reduced ability to bind to tissue, with nuclear staining only achieved with the use of a mordant [4]. The mordants utilised are usually metal cations such as Chromium, Iron, Aluminium, Molybdenum, Lead and Tungsten [4]. These heavy metal salts or hydroxides provide a valency of two or three, resulting in a net positive charge to the complex formed by replacing a hydrogen atom from the haematoxylin dye, allowing the anionic dye to bind to cellular components [4]. There are a broad range of mordants utilised, which can impact the tissue components stained and the colour of staining.

**TABLE 1 |** Factors that were used to assess the sensitivity and specificity of all haematoxylin subtypes.

| Sensitivity factors | Specificity factors |
|---|---|
| -Haematoxylin intensity too strong | -Haematoxylin background staining |
| -Haematoxylin Intensity too weak | -Uneven staining |
| -Haematoxylin colour not purple/blue | -Stain deposit present |
| -Clarity of chromatin detail | -Non-specific staining of cells/tissue |
| -Crisp and clear demonstration of nucleoli | -Poor haematoxylin to eosin balance |

There has been little advancement in the haematoxylin dye chemistry since the 1980s. The lack of research into new methods or formulations (e.g., new mordants) can hinder any improvements in quality of performance and efficiency. The development of Haematoxylin X, which utilises a novel Chromium Sulphate mordant, is the first major change in haematoxylin composition in decades. In this study, we assessed the performance of this new haematoxylin (Haematoxylin X) against some commonly utilised alum-based haematoxylins (Carazzi's, Mayers and Harris) when used as a part of formalin-fixed paraffin-embedded (FFPE) tissue sections, special stains, immunohistochemistry (IHC) counterstaining and frozen section (Mohs procedure) staining process. The selection of the three alum haematoxylins was based on the author's previous publication, which assessed the staining quality of nine different haematoxylin subtypes [6]. The final three selected represented dyes that scored across the spectrum of well, moderately, and poorly as determined by the criteria set out in **Table 1**.

## MATERIALS AND METHODS

As part of the FFPE tissue staining analysis, ten tissue types were selected, comprising of normal skin, fibrofatty tissue (lipoma), small bowel, liver, breast, prostate, uterus, keloid and lymph node material. For each tissue type, ten different tissue blocks were generated, with one section being cut on each to produce 100 slides. The samples were first fixed in 10% neutral buffered formalin (Genta Medical Ltd, York, United Kingdom, see **Table 2**) for 24 h before undergoing paraffin wax processing on a routine overnight protocol (shown in **Table 3**) set up on a Sakura VIP 6AI tissue processor (Sakura Finetek, Thatcham, United Kingdom). Following the embedding of each of the ten tissues into histological cassettes, the samples were sectioned at 4um and mounted on uncharged glass microscope slides (CellPath Ltd, Powys, United Kingdom, see **Table 2**). To ensure adequate adherence of the sections to the glass slides, the tissue sections were baked in a 68°C oven for 20 min before the staining process was initiated.

To ensure standardisation of the staining process, the staining was performed on an automated Leica XL autostainer (Leica Biosystems, Milton Keynes, United Kingdom). The staining protocol for each of the four haematoxylin dyes (Haematoxylin X, Harris', Mayer's and Carazzi's) was individually optimised by increasing or decreasing the immersion times in haematoxylin and/or acid alcohol. The

**TABLE 2 |** Reagent and consumable list.

| Product name | Volume | Supplier/ Manufacturer | Product code | Dilution (if applicable) |
|---|---|---|---|---|
| Carazzi's | 1 L | CellPath Ltd | HST001 | N/a |
| Harris Haematoxylin | 5 L | Leica Microsystem Ltd | 3801560BBE | N/a |
| Haematoxylin X | 1 L | CellPath Ltd | TBC | N/a |
| Mayer's | 1 L | Solmedia Ltd | HST011 | N/a |
| Eosin | 5 L | Leica Microsystem Ltd | 3801590BBE | For Frozen protocol: 0.125% (Mix 625 mL of eosin with 4375 mL of distilled water |
| Scott's Tap Water | 5 L | Leica Microsystem Ltd | 3802901E | N/a |
| Hydrochloric acid (for acid alcohol) | 2 L | VWR International Ltd | 20255.29 | For frozen protocol: 0.225% (Mix 12.50 mL of HCL with 5 L of IDA) For paraffin protocol: 1% (Mix 50 mL of HCL with 5 L of IDA99%) |
| 32% Ammonia (for ammonia alcohol) | 2 L | VWR International Ltd | 21192.298 | For paraffin protocol: 0.13% (Mix 6.5 mL of Ammonia with 4,993.5 mL of IDA99%) |
| Industrial Denatured Alcohol 99% (IDA 99%) | 5 L | Genta Medical Ltd | I99050 | N/a |
| 10% neutral buffered formalin | 5 L | Genta Medical Ltd | BFN050 | N/a |
| Xylene | 5 L | Genta Medical Ltd | XYL050 | N/a |
| CV mount | 250 mL | Leica Biosystem Ltd | 14046430011 | N/a |
| Super frost slide | N/a | VWR International Ltd | 631-0108 | N/a |
| CLARITEX SLIDE, PINKCOAT, 1.0–1.2 mm, 90°, GROUND | N/a | CellPath Ltd | MAF-0108-03A | N/a |
| Coverglass | N/a | Leica Biosystem Ltd | 3800146G | N/a |
| Glacial Acetic Acid | 1 L | VWR International Ltd | 84528.29 | N/a |
| Periodic Acid 50% | 100 mL | VWR International Ltd | 294604D | N/a |
| Schiff's | 500 mL | Merck Life science UK | 1090330500 | N/a |
| Alcian Blue | 100 g | Merck Life Science UK | A5268-100G | N/a |
| Ponceau Xylidine | 50 g | Merck Life Science UK | P2395-50G | N/a |
| Acid Fuchsin | 100 g | Merck Life Science UK | A-3908-25G | N/a |
| Aniline Blue diammonium salt | 50 g | Merck Life Science UK | 415049-50G | N/a |
| BenchMark Ultra LCS | N/a | Roche Diagnostics Ltd | 5424534001 | N/a |
| EZ PREP SOLUTION 10X | N/a | Roche Diagnostics Ltd | 5279771001 | N/a |

concentration and timing of the remaining reagent constituents of the H&E staining process (i.e., eosin, ammoniated alcohol, industrial denatured alcohol 99%, and xylene) remained unchanged for all four haematoxylin dyes. Before the staining process, each haematoxylin dye was filtered before use to remove any precipitate that may have formed. The optimal staining protocol for each of the four dyes was determined by the microscopic evaluation of the stained slides by two of the authors, who are approved UKNEQAS CPT scheme assessors (GEO and CD) to determine which variable (haematoxylin and/or acid alcohol immersion times) needed to be amended to produce the optimum quality of staining. The assessment was performed by comparing the staining against the assessment criteria set out in **Table 1**. The optimised protocol-stained slides were then independently reviewed by the UKNEQAS

**TABLE 3 |** Tissue processor protocol for routine overnight processing.

| Reagent | Duration (Hr) | P/V | Temperature°C | Mix |
|---|---|---|---|---|
| 100% Alcohol | 3 | P/V | 37 | Continued |
| 100% Alcohol | 0.5 | P/V | 37 | Continued |
| 100% Alcohol | 0.5 | P/V | 37 | Continued |
| 100% Alcohol | 0.5 | P/V | 37 | Continued |
| 100% Alcohol | 0.5 | P/V | 37 | Continued |
| 100% Alcohol | 0.5 | P/V | 37 | Continued |
| 100% Alcohol | 0.5 | P/V | 37 | Continued |
| Xylene | 1 | P/V | 37 | Continued |
| Xylene | 1 | P/V | 37 | Continued |
| Xylene | 1.5 | P/V | 37 | Continued |
| Paraffin Wax | 1 | P/V | 65 | Continued |
| Paraffin Wax | 1 | P/V | 65 | Continued |
| Paraffin Wax | 1 | P/V | 65 | Continued |
| Paraffin Wax | 1 | P/V | 65 | Continued |

**TABLE 4** | H&E protocols times for the staining of FFPE tissue by each haematoxylin subtype.

| Haematoxylin subtype | Xylene X3 (mins) | Industrial denatured alcohol 99% X3 (mins) | Wash in running water (mins) | Time in haematoxylin (mins) | Wash in running water (mins) | Time in acid alcohol (seconds) | Wash in running water (mins) | Time in ammoniated alcohol (mins) | Wash in running water (mins) | Time in Eosin (mins) | Wash in running water (sec) | Industrial denatured alcohol 99% X3 (mins) | Xylene X3 (mins) |
|---|---|---|---|---|---|---|---|---|---|---|---|---|---|
| Carazzi's | 2 | 2 | 2 | 8 | 1 | 3 | 1 | 1 | 1 | 4 | 40 | 2 | 1 |
| Harris | 2 | 2 | 2 | 6 | 1 | 3 | 1 | 1 | 1 | 4 | 40 | 2 | 1 |
| Haematoxylin X | 2 | 2 | 2 | 8 | 1 | 3 | 1 | 1 | 1 | 4 | 40 | 2 | 1 |
| Mayer's | 2 | 2 | 2 | 8 | 1 | 3 | 1 | 1 | 1 | 4 | 40 | 2 | 1 |

CPT team, who provided feedback on the staining quality. The finalised protocols for each haematoxylin subtype are shown in **Table 4**. The last step involved the dehydration and clearing of the slides in industrial denatured alcohol 99% (Genta Medical Ltd, York, United Kingdom, see **Table 2**) and xylene (Genta Medical Ltd, York, United Kingdom, see **Table 2**) before the application of a mountant (Leica CV mount, Leica Biosystems, Milton Keynes, United Kingdom, see **Table 2**) and a glass coverslip (Leica Biosystems, Milton Keynes, United Kingdom, see **Table 2**).

As part of the fresh tissue staining analysis, 250 anonymised sample tissues were selected from patients who had undergone the Mohs procedure for the treatment of cutaneous malignancies. All the samples were sectioned at 15 μm thickness on a Leica CM 1950 cryostat (Leica Biosystems, Milton Keynes, United Kingdom) and picked up on a charged Super frost glass slides (VWR international, Leicestershire, England, see **Table 2**). Before the initiation of the staining process, all slides were baked on a hot plate set at 80°C for 2 min, followed by 2 min in industrial denatured alcohol 99% (Genta Medical Ltd, York, United Kingdom, see **Table 2**) and water for an additional 3 min. To allow for increased standardisation, all staining of the fresh samples was carried out on a Linistat Linistainer (Thermofisher Scientific, Paisley, United Kingdom). Each of the haematoxylins were individually optimised by staining debulk sections, by increasing or decreasing the immersion times in haematoxylin and/or acid alcohol. As with FFPE staining process, the concentration and timing of the remaining reagents constituents of the H&E staining process (i.e., eosin, Scott's tap water, industrial denatured alcohol 99%, and xylene) remained unchanged for all four haematoxylin dyes. The optimal staining protocols were determined by the author's GEO and JG (who are approved UKNEQAS CPT scheme assessors) by microscopic assessment of each stained slide to elucidate which variable was required to be amended (haematoxylin and/or acid alcohol immersion times) to improve the staining result. The slides were assessed against the criteria set out in **Table 1**. The optimised protocol-stained slides were then independently reviewed by the UKNEQAS CPT team, who provided feedback on the staining quality. The finalised staining protocol for fresh tissue samples for each of the haematoxylin dyes is shown in **Table 5**. Once the slides were stained, they were dehydrated and cleared. Finally, CV mountant (Leica Biosystems, Milton Keynes, United Kingdom, see **Table 2**) was applied and a glass coverslip (Leica Biosystems, Milton Keynes, United Kingdom, see **Table 2**) was placed on top.

Upon completion of staining of all FFPE and fresh tissue cases with each of the haematoxylin dyes, the slides were assessed independently by two of the authors in a blind trial approach. The scoring of the slides was based upon a modified version of the United Kingdom External Quality Assurance Cellular Pathology Techniques (UKNEQAS CPT) Tissue Diagnostics and Mohs procedure assessment criteria [7, 8]. Each assessor allocated a score between 1 and 5 based on the modified UKNEQAS scoring criteria, with the assessment focusing on the quality of haematoxylin staining. The criteria utilised in this assessment are highlighted in **Table 1**.

**TABLE 5 |** H&E protocols times for the staining of Fresh tissue by each haematoxylin subtype.

| Haematoxylin subtype | Time in haematoxylin (seconds) | Wash in running water (seconds) | Time in acid alcohol (seconds) | Wash in running water (seconds) | Time in Scott's tap water (seconds) | Wash in running water (seconds) | Time in Eosin (seconds) | Wash in water (seconds) | Industrial denatured alcohol 99% (seconds) |
|---|---|---|---|---|---|---|---|---|---|
| Carazzi's | 40 | 10 | 10 | 10 | 10 | 10 | 10 | 10 | 20 |
| Harris | 30 | 10 | 10 | 10 | 10 | 10 | 10 | 10 | 20 |
| Haematoxylin X | 50 | 10 | 10 | 10 | 10 | 10 | 10 | 10 | 20 |
| Mayer's | 50 | 10 | 10 | 10 | 10 | 10 | 10 | 10 | 20 |

The results assigned by each judge for the specificity and sensitivity of each slide were then combined to generate an overall score for each slide out of 10. These results were then added together and divided by 100 to calculate the mean. The mean was then divided by 10 and multiplied by 100 to generate sensitivity and specificity scores as a percentage for each haematoxylin dye. These sensitivity and specificity scores generated were critically evaluated to determine the staining quality of Haematoxylin X against the other commonly used haematoxylins.

To perform the special stains, initially, the FFPE blocks were sectioned at 4 μm thickness on a Leica Histocore biocut rotary microtome (Leica Biosystems, Milton Keynes, United Kingdom) and picked up on a charged Super frost glass slides (VWR international, Leicestershire, England, see **Table 2**). The slides were then baked on a hotplate set at 80°C for 15 min. The slides were then deparaffinised by running through three changes of xylene (Genta Medical Ltd, York, United Kingdom, see **Table 2**) and IDA99% (Genta Medical Ltd, York, United Kingdom, see **Table 2**), then into running tap water.

To perform the periodic acid Schiff stain the slides were treated with 1% periodic acid (VWR international, Leicestershire, England, see **Table 2**) for 10 min and then rinsed in running tap water. The slides were then treated in Schiff's reagent (Merck Life Science, Dorset, United Kingdom, see **Table 2**) for 20 min and then rinsed in running tap water for 10 min. Next, the sections were counterstained with Haematoxylin X for 2 min, rinsed and then differentiated in 1% acid alcohol for 5 s. The rinsed slides were then treated with ammoniated alcohol for 1 min and then rinsed in running tap water. Lastly, the slide was dehydrated rapidly in IDA 99% (Genta Medical Ltd, York, United Kingdom, see **Table 2**), cleared in xylene (Genta Medical Ltd, York, United Kingdom, see **Table 2**), and mounted with CV mount (Leica Biosystems, Milton Keynes, United Kingdom, see **Table 2**) and a cover glass (Leica Biosystems, Milton Keynes, United Kingdom, see **Table 2**).

To perform the Alcian blue stain, the sections were first stained with filtered Alcian blue solution (Merck Life Science, Dorset, United Kingdom, see **Table 2**) for 10 min. Next, the sections were rinsed with running tap water and then counterstained with Haematoxylin X for 5 min, rinsed and then differentiated in 1% acid alcohol for 5 s. The rinsed slides were then treated with ammoniated alcohol for 1 min and then rinsed in running tap water. Lastly, the slide was dehydrated rapidly in IDA 99% (Genta Medical Ltd, York, United Kingdom, see **Table 2**), cleared in xylene (Genta Medical Ltd, York, United Kingdom, see **Table 2**), and mounted with CV mount (Leica Biosystems, Milton Keynes, United Kingdom, see **Table 2**) and a cover glass (Leica Biosystems, Milton Keynes, United Kingdom, see **Table 2**).

To perform the Masson trichrome stain, the slide was stained with Haematoxylin X for 20 min and then washed in running tap water. The sections were then differentiated in 1% acid alcohol for 10 s and then blued in running tap water. Next, the sections were stained with the red cytoplasmic stain (two parts 1% Ponceau de Xylidine (Ponceau 2R) in 1% acetic acid and one part 1% acid fuchsin in 1% acetic acid) for 10 min and then washed in running tap water. The sections were differentiated in 1% phosphomolybdic acid until the collagen was decolourised and the muscle fibres, red blood cells and fibrin remained red. Once the slide was rinsed in distilled water, the section was stained with 0.5% aniline blue in 1% acetic acid for 1 min and then rinsed in 1% acetic acid (VWR international, Leicestershire, England, see **Table 2**). Lastly, the slide was blot dried, dehydrated rapidly in IDA 99% (Genta Medical Ltd, York, United Kingdom, see **Table 2**), cleared in xylene (Genta Medical Ltd, York, United Kingdom, see **Table 2**), and mounted with CV mount (Leica Biosystems, Milton Keynes, United Kingdom, see **Table 2**) and a cover glass (Leica Biosystems, Milton Keynes, United Kingdom, see **Table 2**).

To perform manual counterstaining in immunohistochemical staining, the slides were first allowed to stain in the Roche Ventana Benchmark Ultra (Roche Diagnostics Ltd, Burgess Hill, United Kingdom) without the selection of counterstaining. The slides were then removed before being washed with EZ prep solution (Roche Diagnostics Ltd, Burgess Hill, United Kingdom) and running water to remove any excess LCS solution (Roche Diagnostics Ltd, Burgess Hill, United Kingdom). The slides were then placed in filtered Haematoxylin X and allowed to stain for 3 min. The slides were then washed in running water and differentiated in acid alcohol for 3 s. Next, the slides were washed in running water and then blued in ammoniated alcohol for 30 s. Lastly, the slide was dehydrated rapidly in IDA 99% (Genta Medical Ltd, York, United Kingdom, see **Table 2**), cleared in xylene (Genta Medical Ltd, York, United Kingdom, see **Table 2**), and mounted with CV mount (Leica Biosystems, Milton Keynes, United Kingdom, see **Table 2**) and a cover glass (Leica Biosystems, Milton Keynes, United Kingdom, see **Table 2**).

## RESULTS

All the slides evaluated, which were stained with each of the four haematoxylin dyes, stained as expected with varying degrees of

**TABLE 6 |** Breakdown of specificity and sensitivity result for each haematoxylin subtype for frozen and paraffin sections.

| **Frozen** | | | |
|---|---|---|---|
| **Haematoxylin subtype** | **Mordant** | **Specificity (%)** | **Sensitivity (%)** |
| Carazzi's | Potassium Alum | 80.7 | 82.0% |
| Harris | Potassium Alum | 77.4 | 81.0% |
| X | Chromium Sulphate | 85.5 | 86.8% |
| Mayer's | Potassium Alum | 40.0 | 41.4% |
| **Paraffin** | | | |
| **Haematoxylin Subtype** | **Mordant** | **Specificity (%)** | **Sensitivity (%)** |
| Carazzi's | Potassium Alum | 78.1% | 85.2% |
| Harris | Potassium Alum | 91.2% | 95.1% |
| X | Chromium Sulphate | 88.0% | 90.0% |
| Mayer's | Potassium Alum | 87.0% | 88.0% |

nuclear staining intensity. The specificity and sensitivity results generated for each of the four haematoxylins as based on the UKNEQAS criteria set out in **Table 1** are shown in **Table 6**. **Figure 1** shows the specificity and sensitivity in a graphical format.

Carazzi's haematoxylin-stained fresh tissue sections produced good quality staining with clear visualisation of the nucleoli and chromatin details. There was an acceptable contrast between the eosin and haematoxylin staining, minimal background and uneven staining patterns (see **Figure 2A**). Carazzi's haematoxylin received the second highest score for specificity and sensitivity of 80.7% and 82.0%. In contrast, when used on FFPE tissue, Carazzi's haematoxylin produced a paler nuclear staining. However, the chromatin and nucleoli detail was still visible. There was a poorer haematoxylin-to-eosin balance due to the eosin overpowering the weaker haematoxylin staining (see **Figures 3A**, **4A**, **5A**, **6A**). Overall, Carazzi's haematoxylin scored 78.1% and 85.2% for specificity and sensitivity, respectively.

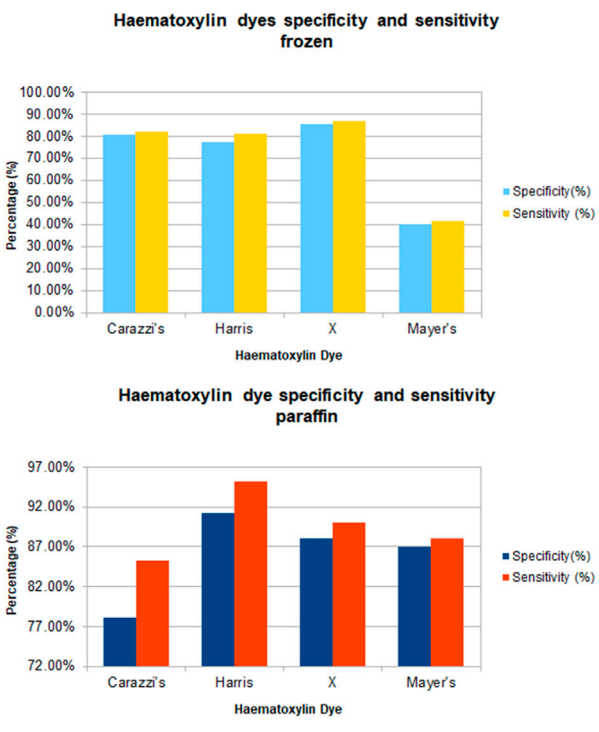


**FIGURE 1 |** Graph of sensitivity and specificity of all haematoxylin stain subtype for frozen and paraffin sections.

Harris haematoxylin-stained fresh tissue produced satisfactory nuclear staining with an adequate interpretation of the chromatin detail and nucleoli. The intensity of haematoxylin staining was variable amongst the cohort of slides stained. This may be due to variation in the fixation process of the tissue. Factors relating to the specificity that was observed included uneven staining patterns, and due to the weaker haematoxylin, there were areas of more pronounced eosin staining (see **Figure 2B**). Harris' haematoxylin scored 77.4% and 81.0% for specificity and sensitivity, respectively. Harris haematoxylin stained FFPE tissue produced a good level of nuclear staining with clear and crisp visualisation of the nucleoli and chromatin detail. There was also minimal background staining, uneven staining and staining deposits observed (see **Figures 3B**, **4B**, **5B**, **6B**). Overall, Harris haematoxylin ranked first for specificity and sensitivity, with scores of 91.2% and 95.1%.

Haematoxylin X-stained fresh tissue produced good quality nuclear staining with clear and crisp nucleoli and chromatin detail visualisation. The intensity of haematoxylin could be variable at times. The vast majority of factors relating to sensitivity were adhered to with only minimal areas of uneven staining due to slightly weaker haematoxylin nuclear staining in places (see **Figure 2C**). Overall, Haematoxylin X ranked first for sensitivity and specificity, with a score of 86.8% and 85.5%. Haematoxylin X-stained FFPE sections produced optimal nuclear staining allowing for good chromatin and nucleoli detail visualisation. Haematoxylin X-stained sections did not have the presence of factors related to specificity, with only a minimal level of uneven staining observed (see **Figures 3C**, **4C**, **5C**, **6C**). Haematoxylin X ranked second for specificity and sensitivity, with results of 88.0% and 90.0%.

Mayer's haematoxylin-stained fresh tissue produced suboptimal nuclear staining with pale haematoxylin staining.

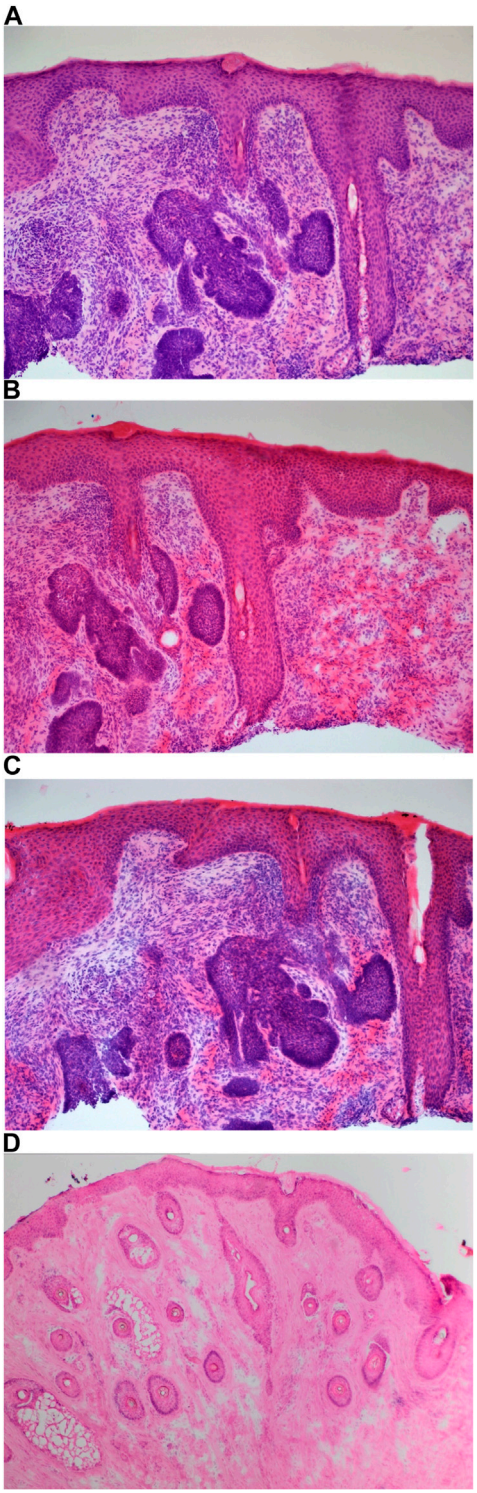


**FIGURE 2 |** Example of frozen section of skin stained with different haematoxylins. **(A)** (×20 magnification) shows a photomicrograph of an H&E section stained with Carazzi's haematoxylin. **(B)** (×20 magnification) shows a photomicrograph of an H&E section stained with Harris' haematoxylin. **(C)** (×20 magnification) shows a photomicrograph of an H&E section stained with Haematoyxlin X. **(D)** (×10 magnification) shows a photomicrograph of an H&E section stained with Mayer's haematoxylin.

As a result, the nucleoli and chromatin detail visualisation were not as easily achieved. Whilst Mayer's haematoxylin did not produce background staining, there was the presence of uneven staining and increased eosin staining in places due to weaker intensity of haematoxylin staining (see **Figure 2D**). Mayer's haematoxylin ranked last for specificity and sensitivity, with scores of 40.0% and 41.4%. Mayer's haematoxylin-stained FFPE tissue sections resulted in good nuclear staining, which allowed for the visualisation of the nucleoli and chromatin detail. Most of the factors relating to specificity were not present, but there were some uneven staining patterns observed (see **Figures 3D**, **4D**, **5D**, **6D**). Mayer's haematoxylin ranked third overall, with specificity and sensitivity scores of 87.0% and 88.0%.

Evaluation of slides stained with PAS (see **Figure 7**), Alcian blue, HVG (see **Figure 8**) special stains and counterstained with Haematoxylin X produced good quality staining with an optimal level of nuclear staining with good contrast.

However, when used in the Masson trichome staining, which encompasses acidic staining solutions, the Haematoxylin X nuclear staining was suboptimal and produced pale staining. When used as part of the immunohistochemistry staining process, Haematoxylin X produced clear and crisp nuclear staining. It produced good contrast, which allowed for a clear interpretation of the immunohistochemical staining (see **Figures 9A–C**).

## DISCUSSION

The haematoxylin dye remains the most critical dye for the microscopic interpretation of nuclear detail, which is crucial in the diagnosis of many pathological disorders in histopathology. There has been little advancement in the composition of the haematoxylin dye in several decades. This lack of research and innovation can hinder any progress and improvements in the dye that could aid with producing an improved quality of nuclear staining, efficiency and cost-effectiveness of the dye. The development of a chromium sulphate mordant-based haematoxylin dye is the first major change in the haematoxylin composition since the 1980s. In the future, with the implementation of digital pathology systems and with artificial intelligence becoming a potential tool for the reporting of histological sections, the staining quality of H&E-stained slides becomes of greater importance. Whilst a pathologist may be able to adapt to staining heterogeneity and variability, AI systems are not, and this is the main challenge faced when utilising these new technologies [9–11]. This study highlights that Haematoxylin X produced good nuclear staining in both FFPE and fresh tissue.

The analysis of the tissue sections stained with each of the four different haematoxylin subtypes (Carazzi's, Harris', Haematoxylin X and Mayer's) showed great comparability with the degree of nuclear staining. Haematoxylin X performed well in staining FFPE tissue and was only narrowly outperformed by Harris' haematoxylin. This could be due to the

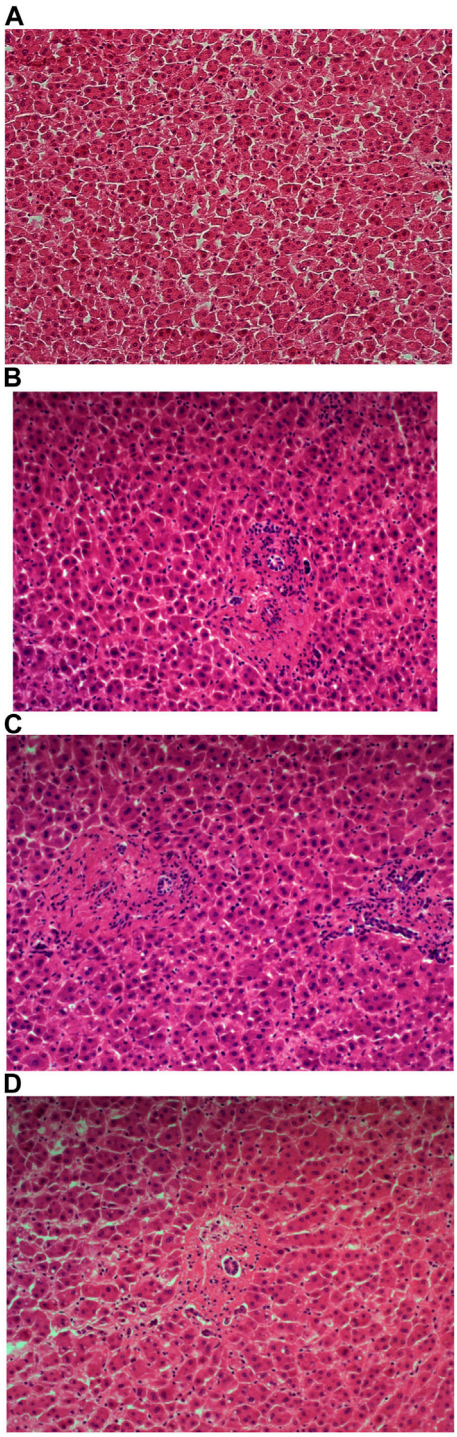


**FIGURE 3 |** Example of paraffin section of liver stained with different haematoxylins. **(A)** (×20 magnification) shows a photomicrograph of an H&E section stained with Carazzi's haematoxylin. **(B)** (×20 magnification) shows a photomicrograph of an H&E section stained with Harris' haematoxylin. **(C)** (×20 magnification) shows a photomicrograph of an H&E section stained with Haematoyxlin X. **(D)** (×20 magnification) shows a photomicrograph of an H&E section stained with Mayer's haematoxylin.

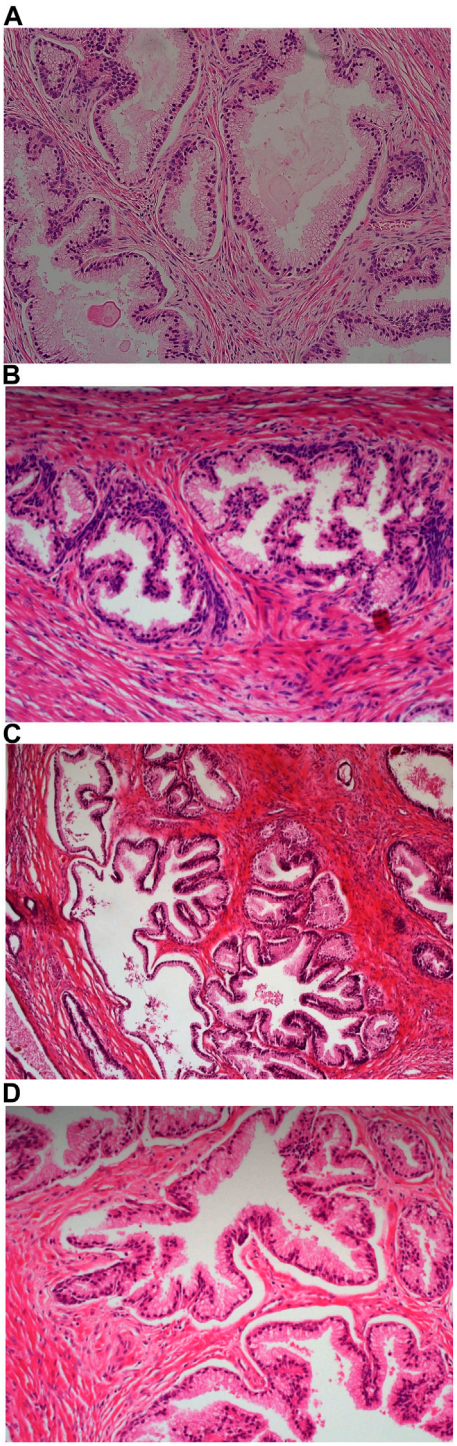


**FIGURE 4 |** Example of paraffin section of prostate stained with different haematoxylins. **(A)** (×20 magnification) shows a photomicrograph of an H&E section stained with Carazzi's haematoxylin. **(B)** (×20 magnification) shows a photomicrograph of an H&E section stained with Harris' haematoxylin. **(C)** (×20 magnification) shows a photomicrograph of an H&E section stained with Haematoyxlin X. **(D)** (×20 magnification) shows a photomicrograph of an H&E section stained with Mayer's haematoxylin.

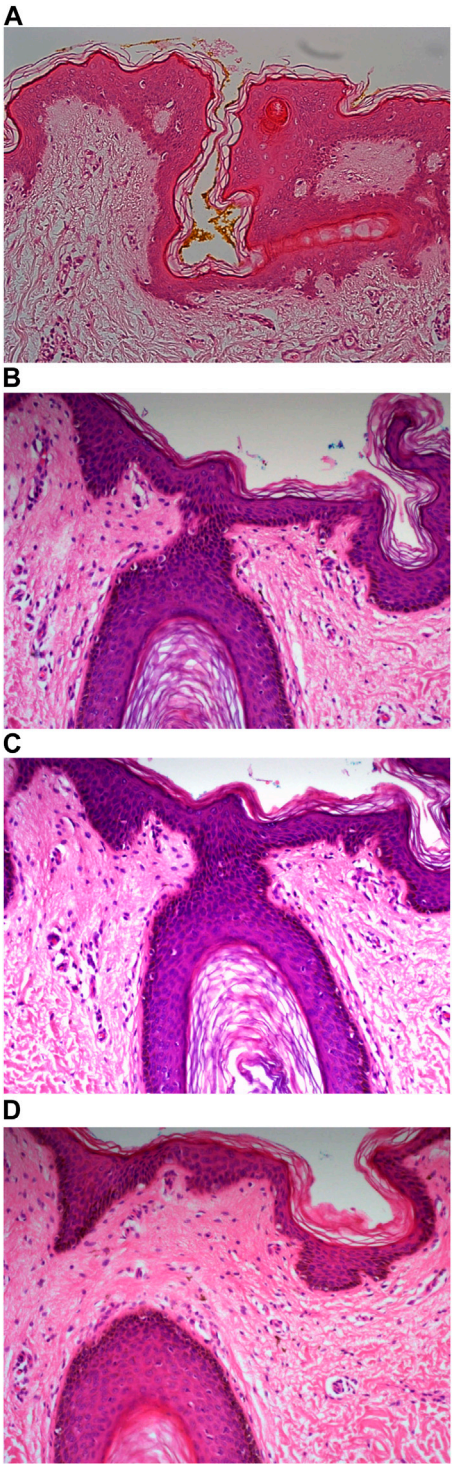


**FIGURE 5 |** Example of paraffin section of skin stained with different haematoxylins. **(A)** (×20 magnification) shows a photomicrograph of an H&E section stained with Carazzi's haematoxylin. **(B)** (×20 magnification) shows a photomicrograph of an H&E section stained with Harris' haematoxylin. **(C)** (×20 magnification) shows a photomicrograph of an H&E section stained with Haematoyxlin X. **(D)** (×20 magnification) shows a photomicrograph of an H&E section stained with Mayer's haematoxylin.

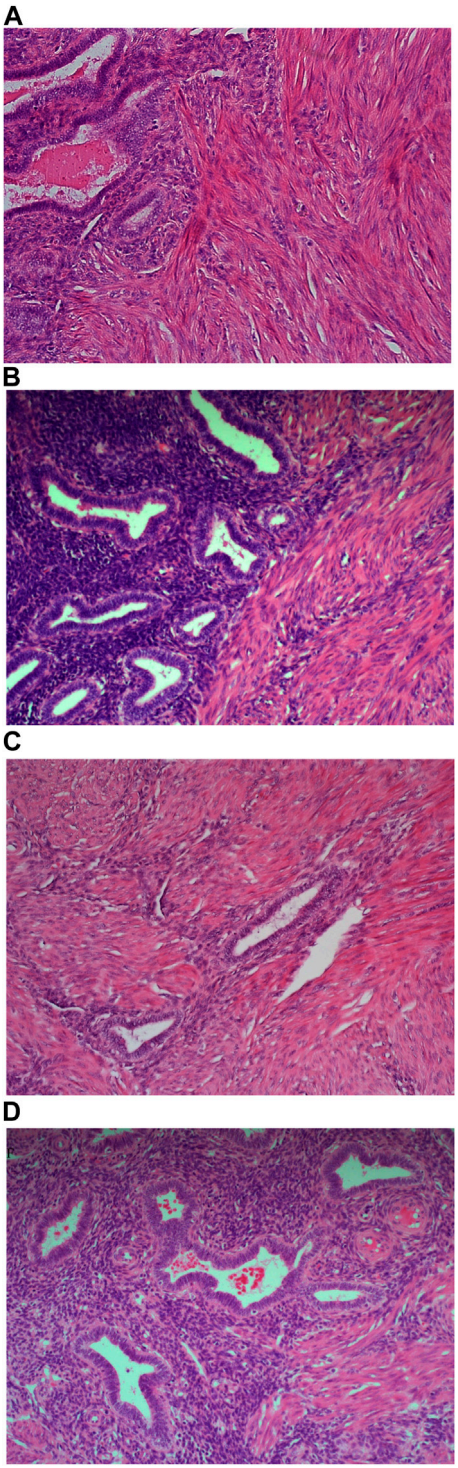


**FIGURE 6 |** Example of paraffin section of Uterus stained with different haematoxylins. **(A)** (×20 magnification) shows a photomicrograph of an H&E section stained with Carazzi's haematoxylin. **(B)** (×20 magnification) shows a photomicrograph of an H&E section stained with Harris' haematoxylin. **(C)** (×20 magnification) shows a photomicrograph of an H&E section stained with Haematoyxlin X. **(D)** (×20 magnification) shows a photomicrograph of an H&E section stained with Mayer's haematoxylin.

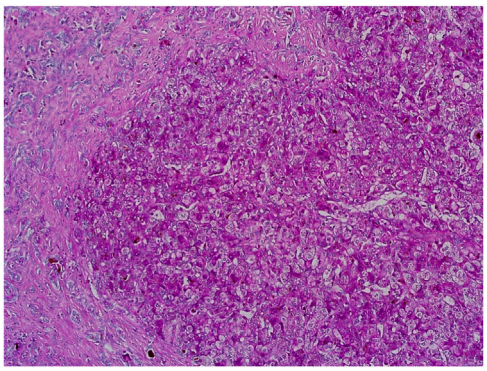

**FIGURE 7 |** Example of paraffin section of Liver stained with periodic acid Schiff's. (×20 magnification) shows a photomicrograph of a liver section stained with periodic acid Schiff's stain.

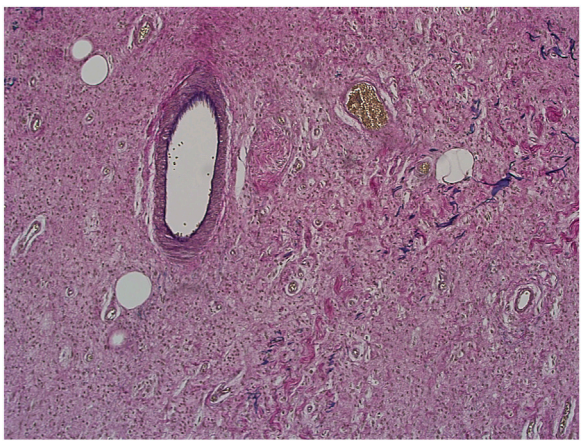

**FIGURE 8 |** Example of paraffin section of skin stained with haematoxylin and Van Gieson's stain. (×20 magnification) shows a photomicrograph of a skin section stained with haematoxylin and Van Gieson's stain.

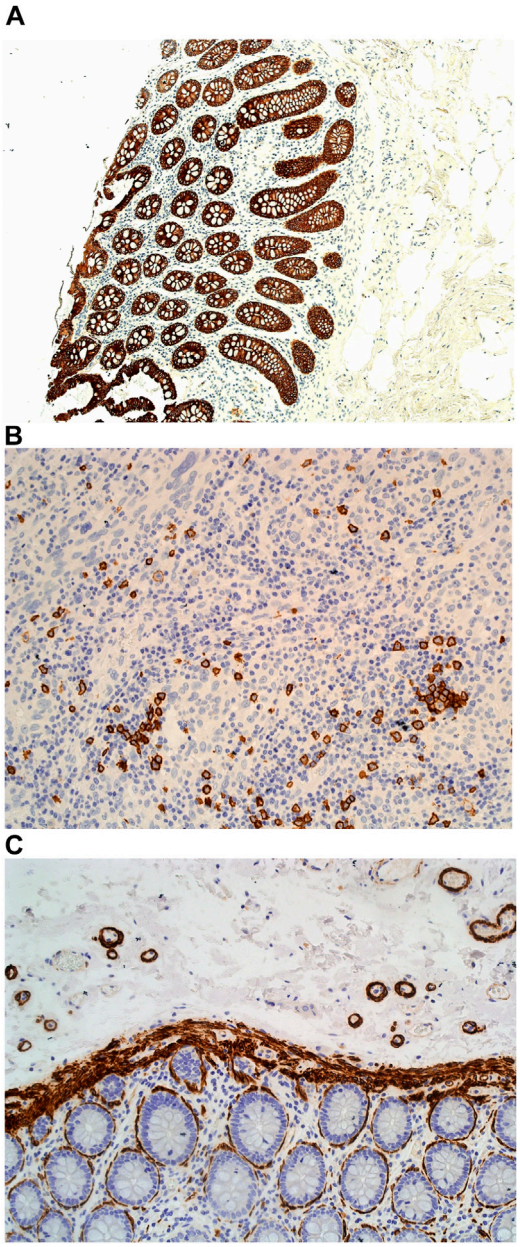


**FIGURE 9 |** Example of paraffin sections stained with CD20 and MNF116. **(A)** (×20 magnification) shows a photomicrograph of a colon section stained with MNF116. **(B)** (×20 magnification) shows a photomicrograph of a tonsil section stained with CD20. **(C)** (×20 magnification) shows a photomicrograph of a colon section stained with Caldesmon.

fact that Harris' haematoxylin is utilised as the routine dye, and as a result, the assessors are more familiar with this subtype. It was also noted that Haematoxylin X was efficacious in staining extracellular mucin, particularly in uterine tissue. While there was evidence of staining of mucins with Mayer's and, to a lesser extent Harris', Haematoxylin X produced the most prominent intensity of staining. This suggests that the new haematoxylin may have particular use in the morphological characterisation of mucin-producing tumours or associated pathologies, i.e., sebaceous carcinomas or adenocarcinomas.

Evaluation of fresh tissue sections stained with each of the haematoxylin subtypes again produced a comparable level of nuclear staining. Haematoxylin X produced the most optimal result when used as part of the frozen staining procedure when compared to the other alum-based haematoxylin dyes that were assessed. The clear and crisp nuclear staining allowed for ease of confirmation of basal cell carcinoma tumours from uninvolved epithelial cells. There was also clear visualisation of the chromatin and nucleoli detail which is essential in tumour characterisation. This supports the potential use of Haematoxylin X in rapid intraoperative procedures, which requires the performance of H&E staining on fresh tissue sections, i.e., Mohs micrographic surgery histological techniques. It was noted that Mayer's haematoxylin produced sub-optimal staining quality as part of the Mohs frozen section staining in this study. It could be argued that the staining could have been improved if the immersion time

was increased. However, the linistat linistainer is restricted to a maximum immersion time of 50 s. As a result, it was not feasible to increase the timing to improve the staining quality. Furthermore, intraoperative staining procedures such as Mohs require quick turn-around-times, as such, dyes which take longer would be less desirable than dyes which stain in a quicker time frame.

Haematoxylin X was observed to be suitable for use as part of both special staining (e.g., periodic acid Schiff's and Alcian blue) and immunohistochemistry counterstaining, with clear and crisp nuclear staining observed with good contrast. However, as with other non-iron mordant-based haematoxylins, it was found that the chromium-sulphate based haematoxylin was also not suitable for use with stains that incorporated acid solutions such as trichrome stains.

An observation that was also noted with Haematoxylin X was that it did not produce oxides and precipitates when left exposed to the air at ambient temperatures, which was prominent with commonly utilised alum haematoxylins such as Harris'. However, it was noted that there were some minor precipitates present in the tissue sections when viewed under higher magnification (×60 or higher). This is believed to be due to the formation of chromium salts. The formation of these salts is eradicated by performing a filtration procedure during the manufacturing of the dye. This study was conducted with an initial small batch of the Haematoxylin X formulation made by CellPath Ltd. The dye is currently being upscaled for mass production and is still undergoing testing at the time of this publication.

The diagnosis and classification of most pathological disorders rely on the information gathered from the evaluation of H&E-stained sections, with the interpretation of haematoxylin-stained nuclear detail playing an essential role in determining morphological characteristics. This study shows that the new chromium sulphate mordant-based Haematoxylin X performed well in both FFPE and fresh tissue staining, highlighting the dye as a good candidate for use as part of routine diagnostic H&E staining.

## SUMMARY TABLE

### What Is Known About This Subject?

- The haematoxylin dye remains the gold standard for microscopic nuclear visualisation of cellular and tissue components in Histopathology.
- However, whilst most diagnostic tools have advanced in the last decades, the haematoxylin dyes have remained relatively unchanged since the 1980s.

### What This Paper Adds

- The development of a chromium sulphate mordant-based haematoxylin dye (Haematoxylin X) constitutes a major change in the haematoxylin composition since the 1980s.
- Haematoxylin X produced good nuclear staining and may also have applications as a good counterstain for immunohistochemical staining and special stains.
- Haematoxylin X may also have a value in the morphological characterisation of mucin-producing tumours or associated pathologies.

## DATA AVAILABILITY STATEMENT

The original contributions presented in the study are included in the article/supplementary material, further inquiries can be directed to the corresponding author.

## ETHICS STATEMENT

"Evaluation of a new mordant based haematoxylin dye (Haematoxylin X) for use in Clinical Pathology", is an original service evaluation article that did not involve the use of additional material collected from any subjects and only residual and anonymized tissue was utilized. No clinical information was used and all material was disposed of using approved organizational procedures at the end of the evaluation.

## AUTHOR CONTRIBUTIONS

JG, CD'A, UK, JS, and GO where all involved in the technical assessments described in the submitted paper. NH and SW where involved in the manufacture of the newly developed haematoxylin dye (Haematoyxlin X). All authors contributed to the article and approved the submitted version.

## CONFLICT OF INTEREST

Authors NH and SW were employed by the company CellPath Ltd.

The remaining authors declare that the research was conducted in the absence of any commercial or financial relationships that could be construed as a potential conflict of interest.

## REFERENCES


1. Bancroft J. *Bancroft's Theory and Practice of Histological Techniques*. Elsevier (2015). p. 126–38.
2. Ortiz-Hidalgo C, Pina-Oviedo S. Hematoxylin: Mesoamerica's Gift to Histopathology. Palo de Campeche (Logwood Tree), Pirates' Most Desired Treasure, and Irreplaceable Tissue Stain. *Int J Surg Pathol* (2019) 27(1):4–14. doi:10.1177/1066896918787652
3. Titford M. The Long History of Hematoxylin. *Biotechnol Histochem* (2005) 80(2):73–8. doi:10.1080/10520290500138372
4. Orchard GE. Hematoxylin – The Story of the Blues. *Br J Biomed Sci* (2018) 75(3):149–52. doi:10.1080/09674845.2018.1439430
5. Ali FR, Orchard GE, Mallipeddi R. Hematoxylin in History—The Heritage of Histology. *JAMA Dermatol* (2017) 153(3):328. doi:10.1001/jamadermatol.2016.0506
6. Gabriel JA, Shams M, Orchard GE. Evaluation of Different Haematoxylin Stain Subtypes for the Optimal Microscopic Interpretation of Cutaneous Malignancy in Mohs Frozen Section Histological Procedure. *Br J Biomed*

*Sci* (2021) 78(2):78–86. Epub 2020 Dec 4. PMID: 33054567. doi:10.1080/09674845.2020.1838075
7. UKNEQAS. *Staining Criteria Handbook Mohs' Procedure*. edition 2. UKNEQAS CPT (2017).
8. UKNEQAS. *Staining Criteria Handbook Tissue Diagnostics' Procedure*. edition 2. UKNEQAS CPT (2017).
9. Boschman J, Farahani H. The Utility of Color Normalization for AI-Based Diagnosis of Haematoxylin and Eosin-Stained Pathology Images. *J Pathol* (2022) 256:15–4. doi:10.1002/path.5797
10. Marini N. Data-Driven Color Augmentation for H&E Stained Images in Computational Pathology. *J Pathol Inform* (2023) 14:2153–3539. doi:10.1016/j.jpi.2022.100183
11. Morales S, Engan K, Naranjo V. Artificial Intelligence in Computational Pathology – Challenges and Future Directions. *Digital Signal Process.* (2021) 119:1051–2004. doi:10.1016/j.dsp.2021.103196

IBMS Institute of Biomedical Science | BJBS

CASE REPORT
published: 13 June 2023
doi: 10.3389/bjbs.2023.11442

# Gout With Associated Cutaneous AA Amyloidosis: A Case Report and Review of the Literature

*G. E. Orchard* *

*Synnovis Analytics, St. John's Histopathology Department, St. Thomas' Hospital, London, United Kingdom*

Gout with associated AA amyloidosis is an unusual finding. This form of amyloid is associated with chronic inflammatory changes often associated with amyloid deposits in the urine, as well as tissue involvement, and organ enlargement in some cases. The large majority of cases in the literature to date refer to gout with AA amyloid within the kidney. However, this is not exclusive, with reports in the liver, gastrointestinal tract, adrenal glands rectum, skin, and subcutaneous fat. The pathophysiological association between these two disease processes is open to debate. The employment of specific anti-inflammatory treatments is believed to have an impact on reducing the incidence of AA amyloidosis in some gout cases–notably the use of colchicine in cases of clinically defined gout attacks. However, this is by no means a universal finding. Here we report on a cutaneous case of gout with AA amyloidosis in a 73-year-old man Included in this case study is a review of the other 16 cases reported within the literature in an attempt to clarify the associated pathophysiological process between these two diseases and the anti-inflammatory treatment regimens employed which may impact the occurrence of AA amyloidosis.

**Keywords: gout, AA (secondary) amyloidosis, urate crystals, amyloid, chronic inflammation**

## INTRODUCTION

Gout is a form of inflammatory arthritis. It commonly affects one joint at a time, often digits, especially the big toe. There is considerable pain and discomfort along with swelling, redness, and tenderness of the surrounding affected tissue. The condition is caused when urate (monosodium) crystals accumulate within the affected joint which subsequently causes inflammation and intense pain [1–4]. The urate crystals accumulate due to a build-up of uric acid in the blood as a result of the breakdown of purines which occur naturally. Uric acid is normally discharged through the kidneys into the urine. However, a build-up of uric acid may occur due to a number of different factors such as dietary issues, i.e., consuming a diet rich in meat and shellfish and drinking sweetened drinks or alcoholic beverages in excess [3, 4]. Underlying medical conditions such as high blood pressure, diabetes, and heart and kidney diseases are also risk factors as are obesity, family history, and predisposition to gout [1–5]. Gout may also occur following recent surgery or trauma [6] and is generally more prevalent in men than women [1, 2].

Amyloidosis occurs when the normal alpha-helical structure of proteins loses its three-dimensional structure, and, as a result, becomes twisted and clumps together to form a beta-pleated sheet conformation of otherwise termed amyloid fibrils. These accumulate within tissues and organs and effectively cause disruption to normal physiological and biochemical activities within the body [7–9]. AA (secondary or serum A) amyloidosis is a condition that arises when there are high levels of inflammation within the body. As such it is regarded as a serious complication of any

OPEN ACCESS

***Correspondence:***
*G. E. Orchard*
*guy.orchard@synnovis.co.uk,*
*orcid.org/0000-0002-4757-0022*

***Received:*** *05 April 2023*
***Accepted:*** *24 May 2023*
***Published:*** *13 June 2023*

***Citation:***
*Orchard GE (2023) Gout With Associated Cutaneous AA Amyloidosis: A Case Report and Review of the Literature. Br J Biomed Sci 80:11442. doi: 10.3389/bjbs.2023.11442*

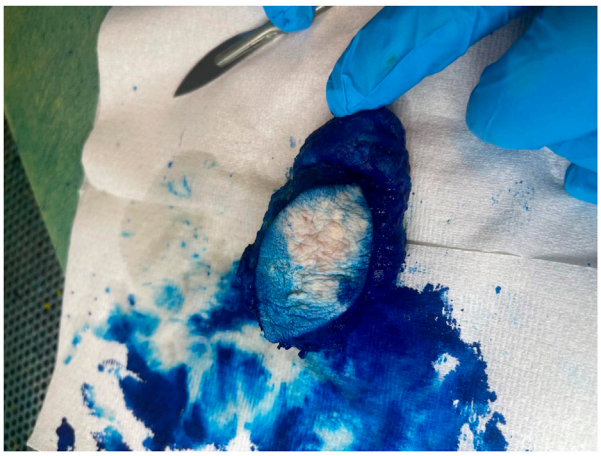

**FIGURE 1 |** Macroscopic appearance of the gout tophus removed from the right elbow of a 73-year-old man.

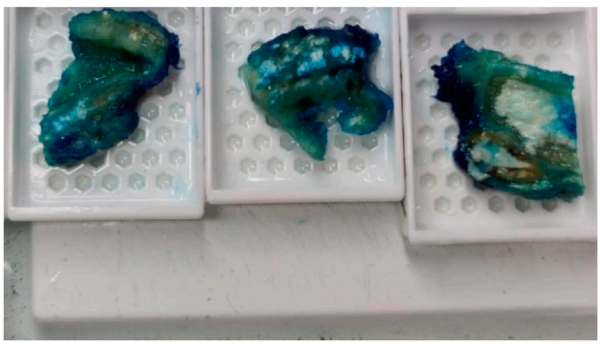

**FIGURE 2 |** On grossing the sample amorphous deposits of white material were seen predominantly within the reticular dermal area and extended down to the subcutaneous fat.

chronic inflammatory conditions such as rheumatoid arthritis, Crohn's disease, or ulcerative colitis [10]. The association of AA amyloidosis with gouty arthritis is however unusual and rare [11–15]. Here we report a case of a 73-year-old man with renal disease, with gout and cutaneous AA amyloidosis from a tophus removed from the right elbow.

## CASE STUDY

A 73-year-old man with impaired renal function and a previous history of gout presented with a gout tophus on his right elbow. Physical examination showed extensive inflammation of the right elbow area. The laboratory findings included an abnormal renal profile with creatinine level 179 (reference 64–104 μmol/L), sodium level 140 (reference 133–146 mmol/L) which is within the normal range, and potassium level 5.4 (reference 3.5–5.3 mmol/L). The urea level was 11.6 (reference 2.5–7.8 mmol/L) and the Erythrocyte sedimentation rate was 100 mm/h. Histopathological examination

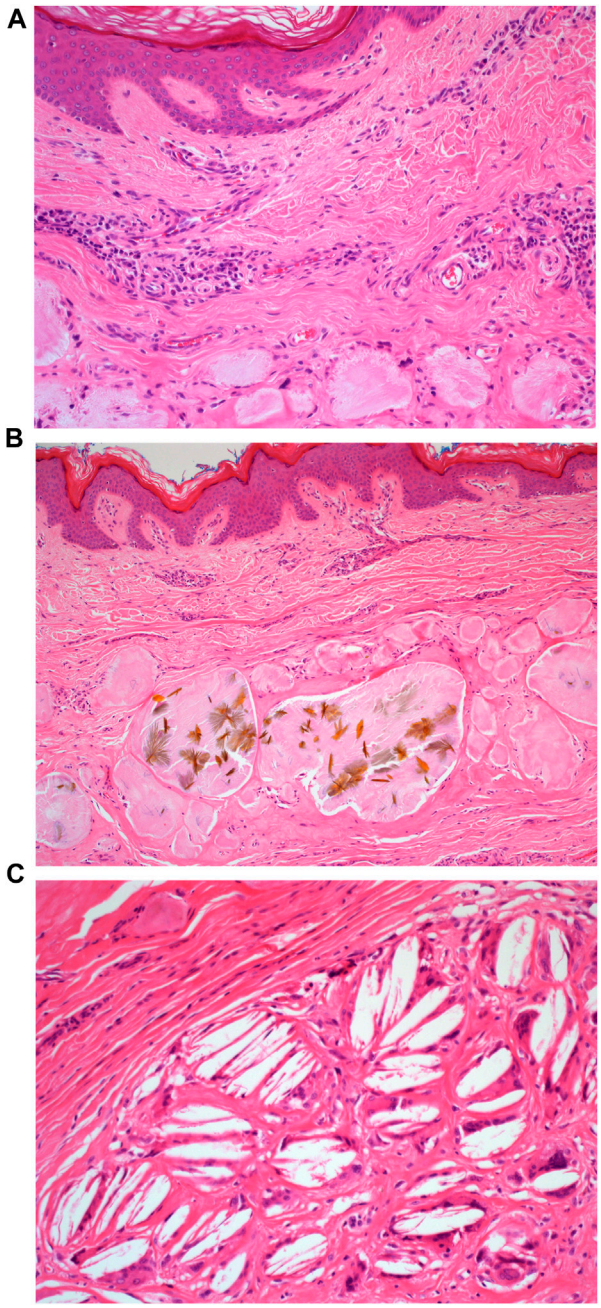


**FIGURE 3 | (A)**: H&E staining of the microscopic appearance of the dermal amorphous eosinophilic deposits. Mag ×20. **(B)**: H&E staining of the microscopic appearance of the crystalloid structures. Mag ×20. **(C)**: H&E staining demonstrating the appearance of cholesterol clefts. Mag ×40.

of the removed gout tophus from the right elbow demonstrated a fibrofatty mass measuring 70 × 46 × 22 mm (**Figure 1**). Macroscopically on slicing the tophus, areas of amorphous crystalloid material were seen and identified predominantly within the reticular dermal area (**Figure 2**). Macroscopically, sections revealed an epidermis with hyperkeratosis and regular acanthosis. Within the reticular and subcutaneous tissue there

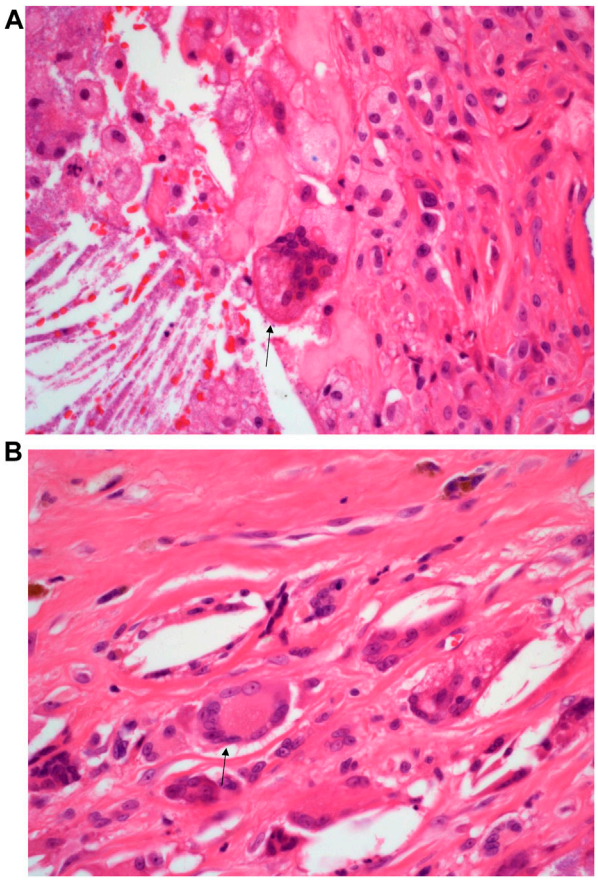


**FIGURE 4 | (A)**: H&E staining of the inflammatory infiltrate composed of foreign body multi-nucleated giant cells (black arrow). Mag ×40. **(B)**: H&E staining of the inflammatory infiltrate composed of Touton type multi-nucleated giant cells (black arrow) Mag ×40.

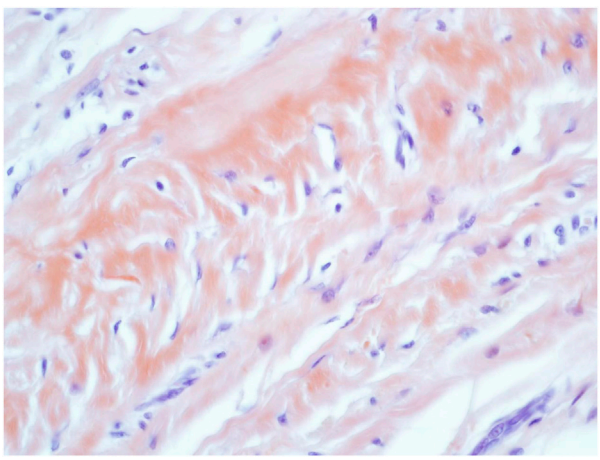

**FIGURE 5 |** Congo Red (CR) staining of the amorphous AA amyloid deposits within the reticular dermal area Mag ×40.

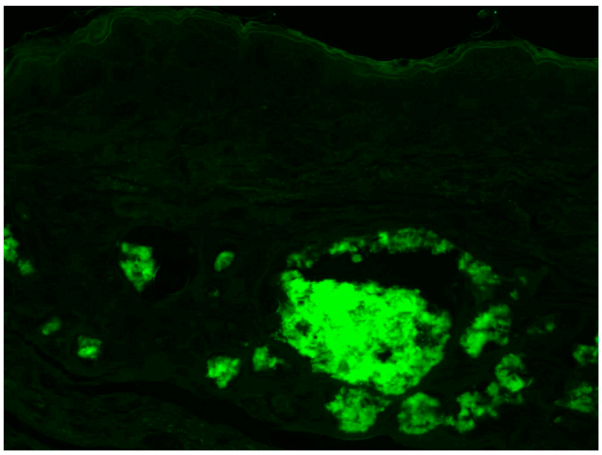

**FIGURE 6 |** Fluorescent microscopy of Thioflavin-T (Thio-T) staining of the AA amyloid deposits found within the dermal area. Mag ×40.

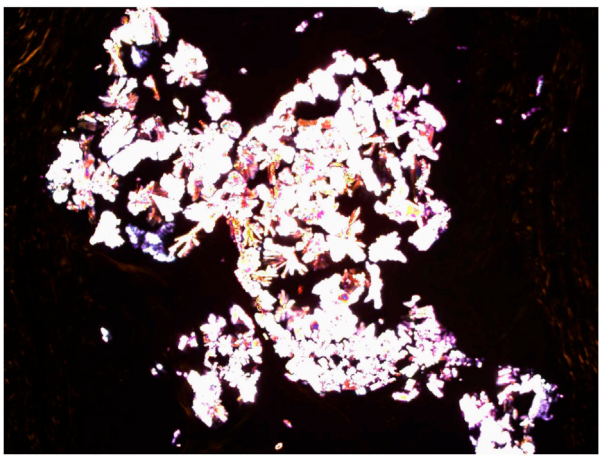

**FIGURE 7 |** Congo Red (CR) staining with cross polarisers demonstrating the Uric acid crystalloid structures. Mag ×30.

were areas of amorphous pale eosinophilic material with associated crystalloid structures (**Figures 3A, B**) displaying a feathery appearance with characteristic needle-shaped spaces (Cholesterol clefts) (**Figure 3C**). There were also areas of calcification seen. Of note was the presence of granulomatous inflammation with the presence of histiocytes, giant cells (foreign body and Touton types) (**Figures 4A, B** arrowed), plus the presence of fibrosis. The amorphous material extended to the papillary dermis and special stains for amyloid were conducted which included Congo Red (CR) (**Figure 5**) and Thioflavine–T (Thio-T) (**Figure 6**). Using cross-polarized light the crystalloid structures (**Figure 7**) within the amorphous material located within the papillary and reticular dermal areas exhibited birefringence in the CR-stained sections and was positive with Thio T confirming the presence of amyloid.

**TABLE 1 |** Key features of patients with gout and AA amyloidosis from the literature including our case (patient 16).

| Case number and references | Age | Sex | Type of gout and duration | Site of amyloid deposition | Family history | Treatment and associated possible causes of amyloid |
|---|---|---|---|---|---|---|
| Levo et al. [8] | 46 | Male | Chronic Tophaceous gout 32 years | Kidneys, adrenals | Yes | Colchicine |
| Levo et al. [8] | 39 | Male | Monoarthritis gout 1 year | Kidneys | No | Colchicine |
| Lens et al. [9] | 49 | Male | Chronic Tophaceous gout 20 years | Kidneys, liver, and subcutaneous fat | No | No Colchicine |
| Guma et al. [12] | 46 | Male | Chronic Tophaceous gout 20 years | Rectum and kidneys | No | No Colchicine |
| Vernerova et al. [14] | 56 | Male | Chronic Tophaceous gout 15 years | Kidneys | Yes | Allopurinol |
| Vernerova et al. [14] | 44 | Male | Chronic Tophaceous gout 10 years | Rectum, Kidneys | Yes | Allopurinol and colchicine (after diagnosis of AA amyloidosis) |
| Rubinow and Sonnemblick [11] | 85 | Male | Chronic Tophaceous gout 10 years | Rectum and kidneys | No | Colchicine (after diagnosis AA amyloidosis) |
| Talbott and Terplan [7] | 42 | Male | Chronic Tophaceous gout 25 years | Widespread | No | Azathioprine (Pyelonephritis) |
| Talbott and Terplan [7] | 23 | Male | Chronic Tophaceous gout 9 years | Kidneys | Yes | No Colchicine Probenecid dialysis (tuberculosis) |
| Talbott and Terplan [7] | 32 | Male | Monoarthritis 4 years | Kidneys | No | Tuberculosis meningitis No colchicine |
| Talbott and Terplan [7] | 72 | Male | Chronic Tophaceous gout 37 years | Kidneys | No | High-dose salicylates and on allopurinol dialysis |
| Gaviria et al. [16] | 47 | Female | Monoarthritis gout 1 year | Kidneys and liver | No | Allopurinol and Colchicine |
| Gromova and Tsurko [15] | 62 | Male | Chronic Tophaceous gout 36 years | Kidneys GI tract, adrenal glands | No | Colchicine, prednisone, allopurinol |
| Jacobelli et al. [13] | 61 | Male | Chronic Tophaceous gout | Kidneys | No | Unknown |
| Ter-Borget al. [10] | 57 | Male | Chronic Tophaceous gout | Kidneys | No | Colchicine after gout attack |
| *Last case* | 73 | Male | Chronic Tophaceous gout 10 years | Kidneys and skin | No | Colchicine after gout attack |

## DISCUSSION

Gout is a fairly common disease and an ancient one, being described by the Egyptians in 2640 BC as lesions compromising the first metacarpophalangeal joints [16]. To give an idea of how common the occurrence of gout is–an estimated 6.1 million adults within the United States (approximately 2.5%) of the adult population are diagnosed with gout [16]. However, gout with associated amyloidosis is rare in comparison [10] (**Table 1**). AA amyloidosis causes complications in chronic infections and inflammatory diseases like rheumatoid arthritis. Since the pathophysiological connection between gout and amyloidosis is not understood there have been variable approaches to treatment regimens [10, 15]. Some of these could control either the gout or the amyloidosis, but there is no evidence that describes the successful treatment of both conditions [15]. The large majority of the cases reported in the literature had tophaceous gout for at least a period of 10 years [10–14] and were not using colchicine (Colcrys, Gloperba, Mitigare) on a regular basis. Colchicine is an anti-inflammatory drug that reduces the effects of gout and is often preferred over nonsteroidal anti-inflammatory drugs ibuprofen or naproxen or more powerful options such as indomethacin or celecoxib, or corticosteroids such as prednisone.

Amyloid deposits are due to an elevation in acute-phase reactants or proteins, which often occur in and around gout tophi. However, not all of the reactant proteins share the amyloidogenic profile thus in part explaining why so few cases are perhaps reported [15]. AA amyloid results from the extracellular deposition of the sub–acute-phase reactant serum amyloid A (SAA) protein as insoluble amyloid fibrils. When this process is prolonged the liver will produce high levels of SAA resulting in the trigger that drives the development of AA amyloidosis [15]. It is also possible that the inflammatory mediators that trigger and accentuate the inflammatory response may differ between gout and associated amyloid conditions like rheumatoid arthritis. Rheumatoid arthritis is a long-term chronic inflammatory condition whereas gout, although also a chronic inflammatory condition is generally a more active and florid inflammatory response in keeping with the clinical spectrum of progressive inflammation which suggests perhaps the difference between the respective inflammatory pathways could also account for the absence of amyloid deposits within the majority of gout cases [1, 10].

Finally, since the routine treatment for patients with gout is the use of colchicine and many of the cases reported within the literature for clinically defined reasons did not have colchicine administered, it is thus that one could speculate that the lack of administration of colchicine is a contributing factor in the development of amyloid in this case as in others reported [10, 17]. It is known that colchicine does prevent casein-induced amyloidosis in mice [18]. However, conversely, it is also the case that the majority of patients with gout are only

administered colchicine during a gout attack and not as an ongoing regular treatment option. Cumulatively this may suggest that the low incidence of amyloidosis in gout may not be directly associated with the administration of this drug, but may be related to a number of clinical and pathological multifactorial issues. Further studies are therefore required to understand the pathophysiological relationship between gout with AA amyloidosis.

Summarising the data in the literature along with the evidence from this case study, there are only 16 reported cases of amyloidosis associated with gout. The incidence is rare. This case is also unusual as most cases of chronic gout with amyloidosis occur in the kidney or rectum. Investigations of kidney AA in this case are under review. It is unusual to find cases of gout with AA amyloidosis within the skin [16].

## SUMMARY TABLE

- The association of gout with AA amyloidosis is rare. There are currently only 15 reported cases within the literature. In most cases, the AA amyloid is found within the kidneys. The presence of AA amyloid in these cases appears to be associated with the anti-inflammatory drug treatment given to these patients, most notably during a gout attack. However, the physiological and clinical-pathological correlation between gout and AA amyloidosis is not fully understood.
- Here we report an unusual case of gout with AA amyloidosis occurring in a 73-year-old man and affecting the skin, in which the amyloid presented whilst the patient had been previously treated with the anti-inflammatory drug colchicine. The association between these two disease processes needs further elucidation, as most publications to date are of isolated case reports.
- This work represents an advance in biomedical science because it demonstrates that the association between these two disease processes affects multi-organ sites and that the simultaneous occurrence in the skin is unusual.

## DATA AVAILABILITY STATEMENT

The original contributions presented in the study are included in the article/supplementary material, further inquiries can be directed to the corresponding author.

## ETHICS STATEMENT

The case study: "Gout with associated cutaneous AA Amyloidosis A case report and review of the literature" is registered centrally with Synnovis. Ethical review and approval was not required for the study on human participants in accordance with the local legislation and institutional requirements. The patients/participants provided their written informed consent to participate in this study. Written informed consent was obtained from the individual(s) for the publication of any potentially identifiable images or data included in this article.

## AUTHOR CONTRIBUTIONS

The author confirms being the sole contributor of this work and has approved it for publication.

## CONFLICT OF INTEREST

The author declares that the research was conducted in the absence of any commercial or financial relationships that could be construed as a potential conflict of interest.

## ACKNOWLEDGMENTS

Miss Paige Cole for her technical assistance with Congo Red (CR) and Thioflavin-T (Thio-T) staining.

## REFERENCES

1. Suresh E. Diagnosis and Management of Gout: a Rational Approach. *Postgrad Med J* (2005) 81:572–9. doi:10.1136/pgmj.2004.030692
2. McGill NW. Gout and Other crystal-associated Arthropathies. *Baillieres Best Pract Res Clin Rheumatol* (2000) 14:445–60. doi:10.1053/berh.2000.0087
3. Zhang Y, Chen C, Choi H, Chaisson C, Hunter D, Niu J, et al. Purine –rich Foods Intake and Recurrent Gout Attacks. *Ann Rheum Dis* (2012) 71:1448–53. doi:10.1136/annrheumdis-2011-201215
4. Zhang Y, Woods R, Chaisson CE, Neogi T, Niu J, McAlindon TE, et al. Alcohol Consumption as a Trigger of Recurrent Gout Attacks. *Am'J.Med.* (2006) 119: e13–8. doi:10.1016/j.amjmed.2006.01.020
5. Dalbeth N, Gosling AL, Gaffo A, Abhishek A. Gout. *Lancet* (2021) 397(10287): 1843–1855. doi:10.1016/S0140-6736(21)00569-9
6. Simman R, Kirkland B, Jackson S. Post Traumatic Tophaceous Gout: A Case Report and Literature Review. *J Am Col Certif Wound Spec* (2009) 1:114–6. doi:10.1016/j.jcws.2009.11.001
7. Talbott JH, Terplan KL. The Kidney in Gout. *Medicine (Baltimore)* (1960) 39: 469–526. doi:10.1097/00005792-196012000-00001
8. Levo Y, Shalev O, Rosenmann E, Eliakim M. Gout and Amyloidosis. *Ann Rheum Dis* (1980) 39:589–91. doi:10.1136/ard.39.6.589
9. Lens XM, Rosello R, Montoliu J, Solé M, Darnell A, Rotés J, et al. Amyloidosis Secondary to Gout. *J Rheumatol* (1985) 12:1024–6.
10. Ter-Borg EJ, Wegewijs MA, de Bruin P. Gout and AA Amyloidosis a Case Report and Review of the Literature. *J Clin Rheumatol* (2017) 23(4):233–4. doi:10.1097/RHU.0000000000000518
11. Rubinow A, Sonnemblick M. Amyloidosis Secondary to Polyarticular Gout. *Arthritis Rheum* (1981) 24:1425–7. doi:10.1002/art.1780241115
12. Guma M, Bayes B, Bonet J, Olivé A. Gout and Secondary Amyloid. *Clin Rheumatol* (1999) 18:54–5. doi:10.1007/s100670050053
13. Jacobelli S, Vial S, Rosenberg H, Benson MD, Scheinberg MA. Amyloidosis Secondary to Gout. Identification with a Monoclonal Antibody to Amyloid Protein A. *Clin Rheumatol* (1988) 7:534–7.
14. Vernerova Z, Rychlik I, Brunerova L, Dvoráková L, Pavelková A, Sebesta I. An Unusual Cause of Renal Amyloidosis Secondary to Gout: the First Description

of Familial Occurrence. *Nucleosides Nucleotides Nucleic Acids* (2006) 25: 1305–8. doi:10.1080/15257770600893941
15. Gromova MA, Tsurko VV. Gout and AA –Amyloidosis: A Case –based Review. *Mediterr J Rheumatol* (2020) 32(1):74–80. doi:10.31138/mjr.32.1.74
16. Gaviria JL, Ortega VG, Gaona J, Motta A, Medina Barragán OJ. Unusual Dermatological Manifestations of Gout: Review of Literature and a Case Report. *Plast Reconstr Surg Glob Open* (2015) 3(7):e445. doi:10.1097/GOX.0000000000000420
17. Brunger AF, Nienhuis HLA, van Rheenen RWJ. Obesity-induced AA Amyloidosis: A Diagnosis of Exclusion. *Int J Clin.Rheumatol* (2020) 15(2): 26–32.
18. Shtrasburg S, Pfras M, Gal R, Salai M, Livneh A. Inhibition of the Second Phase of Amyloidogenesis in a Mouse Model by a Single-Dose Colchicine Regimen. *J Lab Clin Med* (2001) 138:107–11. doi:10.1067/mlc.2001.116488

IBMS Institute of Biomedical Science | BJBS

REVIEW
published: 07 June 2023
doi: 10.3389/bjbs.2023.11314

# Dermatopathology and the Diagnosis of Fungal Infections

*S. A. Howell**

*Mycology, St John's Specialist Dermatology Laboratories, Synnovis, London, United Kingdom*

Diagnosis of superficial/cutaneous fungal infections from skin, hair and nail samples is generally achieved using microscopy and culture in a microbiology laboratory, however, any presentation that is unusual or subcutaneous is sampled by taking a biopsy. Using histological techniques a tissue biopsy enables a pathologist to perform a full examination of the skin structure, detect any inflammatory processes or the presence of an infectious agent or foreign body. Histopathological examination can give a presumptive diagnosis while a culture result is pending, and may provide valuable diagnostic information if culture fails. This review demonstrates how histopathology contributes to the diagnosis of fungal infections from the superficial to the life threatening.

**Keywords: dermatopathology, fungal infection, tissue biopsy, histopathology, mycoses**

## INTRODUCTION

The prevalence of fungal infection is far greater than might be thought. Fungal infections of skin, hair and nail have been estimated to affect one to two billion people worldwide, mucosal *candida* infections affect tens of millions of people, and serious fungal infections affect 150 million people (1, 2). Mortality from the serious fungal infections has been estimated to be similar to the number of deaths from tuberculosis (1). Superficial fungal infections have been reported to affect 20%–25% of the world's population with dermatophyte infections predominating (3). Global estimation of the prevalence of subcutaneous infections is difficult as these infections are less common, some are more prevalent in certain areas or regions, and are not notifiable diseases. Therefore, subcutaneous fungal infections are under reported and are considered to be Neglected Tropical Diseases by the World Health Organisation (4). Systemic infections involve the internal organs and may disseminate to the skin *via* the blood. Many systemic infections occur in immune compromised patients and the prevalence of these infections varies according to patient risk factors, country or region, and availability of surveillance data (1).

The diagnosis of cutaneous fungal infections requires laboratory testing with microscopic examination of tissue to detect the presence of a fungus, and culture to enable the identification of the pathogen. The diagnosis of systemic infections is complex and involves clinical imaging, serology, and molecular tests in addition to microscopy and culture, and has been reviewed elsewhere (5).

OPEN ACCESS

***Correspondence:**
*S. A. Howell,*
*via Guy Orchard*
*Guy.Orchard@viapath.co.uk*

***Received:** 27 February 2023*
***Accepted:** 20 April 2023*
***Published:** 07 June 2023*

***Citation:***
*Howell SA (2023) Dermatopathology and the Diagnosis of Fungal Infections. Br J Biomed Sci 80:11314. doi: 10.3389/bjbs.2023.11314*

**TABLE 1** | Types of fungal infections.

| Type of mycosis | Tissue type | Tissue involvement | Sources, route/risks of infection |
|---|---|---|---|
| Superficial and cutaneous | Skin, hair and nail | Skin infections confined to epidermis | Human, animal, soil<br>For mould and environmental yeasts—contact with infected material, minor abrasion<br>For commensal yeast species—changes in host susceptibility, underlying disease |
| Subcutaneous | Skin | Penetration of the dermis and subcutaneous tissue | Traumatic inoculation, fungi are environmental |
| Systemic | Blood, lungs, internal organs, dissemination possible | Dissemination from internal infection into the skin may be possible | Opportunistic infections—major risk is immune suppression, underlying disease, hospitalisation<br>Endemic dimorphic infections—inhalation of fungal spores, immune suppression |

This review outlines the different types of fungal infections that manifest in the skin, how cutaneous fungal infections are identified in a microbiology laboratory, and the role of dermatopathology in the diagnosis of fungal skin infection.

## LABORATORY DETECTION OF FUNGAL INFECTION

The traditional methods to detect fungal infection in a microbiology laboratory are microscopy and culture (6). The presence of a fungal infection can be confirmed by the observation of fungal structures in tissue by microscopic examination. This process involves placing a piece of skin, nail or tissue in a potassium hydroxide solution on a slide to soften. Once soft the preparation is squashed to make it as thin as possible as it is easier to detect fungal elements in a thin sample. Samples of hair or scalp are not squashed prior to initial microscopic examination as the arrangement of fungal elements within the hair can give useful information. A fluorescence stain such as calcofluor can be added to the sample to enhance visualization under filtered UV light (7, 8). The identity of the causative organism is determined following growth on culture plates (9). Although molecular diagnostics are available for life threatening infections and to detect specific panels of fungi (mainly used in larger laboratories), the microscopic detection of fungal structures in tissue remains a gold standard in diagnosis (6).

## TYPES OF FUNGAL INFECTION

Fungal infections can be divided into three categories: superficial and cutaneous, subcutaneous, and systemic (see **Table 1**). Superficial and cutaneous infections may occur following contact with an infectious source, or from a change in the host or the skin flora. These infections are unsightly, uncomfortable, some are contagious, and they can affect anyone (10).

Subcutaneous infections result from penetrating traumatic inoculation deep into the skin by objects contaminated with fungi from the environment. They can progress slowly and can cause significant disfigurement if left untreated (10).

There are two types of systemic fungal infections: opportunistic infections are caused by fungi that have a worldwide distribution which can cause significant illness in debilitated hosts, particularly the immune suppressed. These infections can be caused by commensal flora (such as *Candida* species) or from the environment. In contrast the endemic dimorphic fungi are highly virulent, are mostly acquired by the inhalation of fungal spores, and can cause disease in immune competent and immune compromised people (10).

## SUPERFICIAL/CUTANEOUS MYCOSES

Superficial and cutaneous mycoses are fungal infections of the skin, hair, and nails and are generally confined to the epidermis of the skin (10). These infections can have characteristic clinical presentations (11–15) which enable diagnosis with the aid of microscopy and culture (**Table 2**; **Figures 1**, **2**). Rare deeper infections can arise when infection penetrates *via* infected follicles presenting as pustules, papules or nodules, as occurs in Majocchi's granuloma (4, 11).

Infections that can arise from the host commensal flora are caused by *Candida* and *Malassezia* yeasts, therefore risks for infection include changes in the host susceptibility, underlying disease, and integrity or damage of the tissue (12, 14). *Candida albicans* is a commensal of the gastrointestinal tract and is the commonest cause of *candida* skin and nail infection. Superficial *candida* skin infection tends to occur where the skin is moist such as the axillae, groin, perineum, web spaces, and other skin folds where the conditions permit the yeast to colonise and proliferate (14) (**Figure 2**).

*Malassezia* species are common skin commensal yeasts that prefer regions with greater skin lipid content such as the chest, back, face and scalp. The genus contains 17 species, 10–12 have been identified from the human skin flora, and many have been associated with skin infections (16). One of the commonest skin infections is pityriasis versicolor and microscopic examination of the infected skin shows characteristic broad short hyphae, which have been described as having an appearance resembling spaghetti and meatballs (6) (**Figure 2**).

**TABLE 2 |** Superficial/cutaneous mycoses, causative organisms, and common clinical features (4, 10, 11, 15).

| Tissue | Infection | Cause | Clinical features |
|---|---|---|---|
| Hair | Black Piedra | *Piedraia hortae* | Dark hard nodules on the hair shaft |
| | White Piedra | *Trichosporon* yeasts | Soft white nodules on the hair shaft |
| | Tinea capitis | Dermatophytes mostly *Trichophyton* and *Microsporum* species | Scaling, itch, erythema, hair loss, broken hair at or just above the scalp surface, can lead to an inflammatory kerion lesion |
| Nail | Tinea unguium | Dermatophytes—mostly *Trichophyton* and Epidermophyton species | Discolouration, streaking, hyperkeratosis |
| | Onychomycosis | Generic term for any fungal cause—mould or yeast | Discolouration, streaking, hyperkeratosis, paronychia, onycholysis |
| | *Candida* | *Candida* species | Paronychia, onycholysis, discolouration |
| Skin | Tinea | Dermatophyte species | Scaling, erythema, presence of a raised leading edge with some healing behind. Itch |
| | *Candida* | *Candida* species | Scaling, erythema, maceration, satellite lesions forming away from lesion edge, may be sore |
| | Pityriasis versicolor | *Malassezia* species | Scaling, hypo/hyper pigmentation. Itch |
| | Tinea nigra | *Hortea werneckii* | Scaling, dark discolouration |

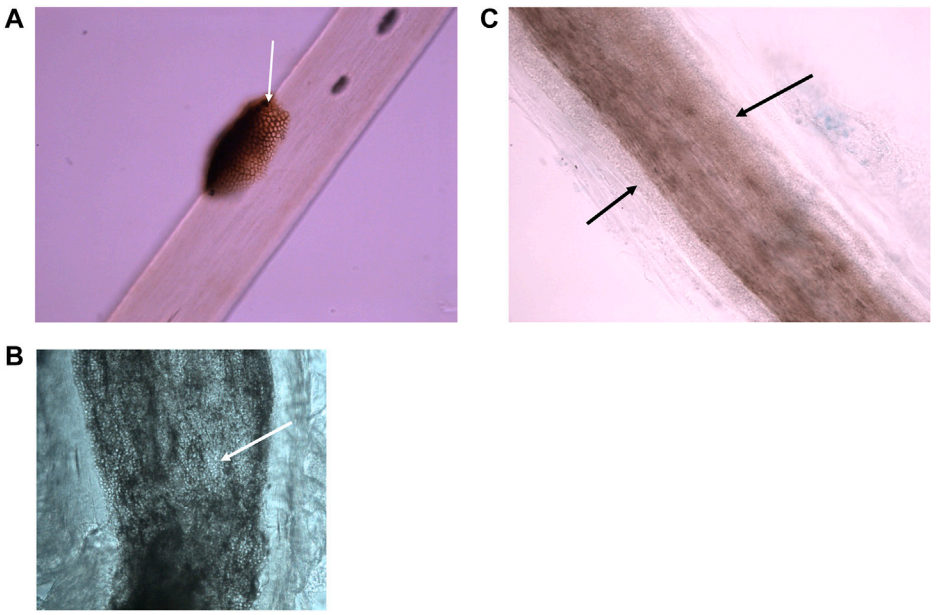


**FIGURE 1 |** Microscopic appearance of superficial fungal hair infections using bright field microscopy. **(A)** Black piedra—a dark nodule containing pigmented hyphae is located on the surface of a hair shaft. (Photographed with a ×40 lens). **(B)** Endothrix dermatophyte infection—hyphae and arthroconidia (spores) found within the borders of the hair shaft (photographed using a ×40 lens). **(C)** Small spored ectothrix dermatophyte infection—hyphae and arthroconidia found surrounding the hair shaft forming a sheath. (Photographed using a ×40 lens).

Dermatophyte moulds cause infections known as ringworm or tinea and these can be contagious. Dermatophytes are found worldwide and there are species that have evolved to live on humans, on specific animals, and in soil, so infection requires contact with a source and probably mild abrasion or prolonged contact to initiate the infective process (17). Microscopic examination cannot determine the causative species so identification relies on growth of the fungus on culture. Knowledge of the identity of the fungus can indicate a likely source of infection and any actions that can be taken to reduce the risk of re-infection. If a scalp sample contains intact infected hairs it can be possible to determine the type of dermatophyte infection: for example, endothrix infections are passed person to person and are caused by *Trichophyton* species, whereas ectothrix infections can be from a human, animal or soil sources (8) (**Figure 1**).

Dermatophytes are considered to be pathogens as their isolation from tissue is associated with the presence of clinical infection, however, common environmental fungi can be isolated from skin, hair and nail as contaminants of culture plates (17). Interpretation of the isolation of an environmental fungus from a non-sterile site is complex and requires the detection of fungal

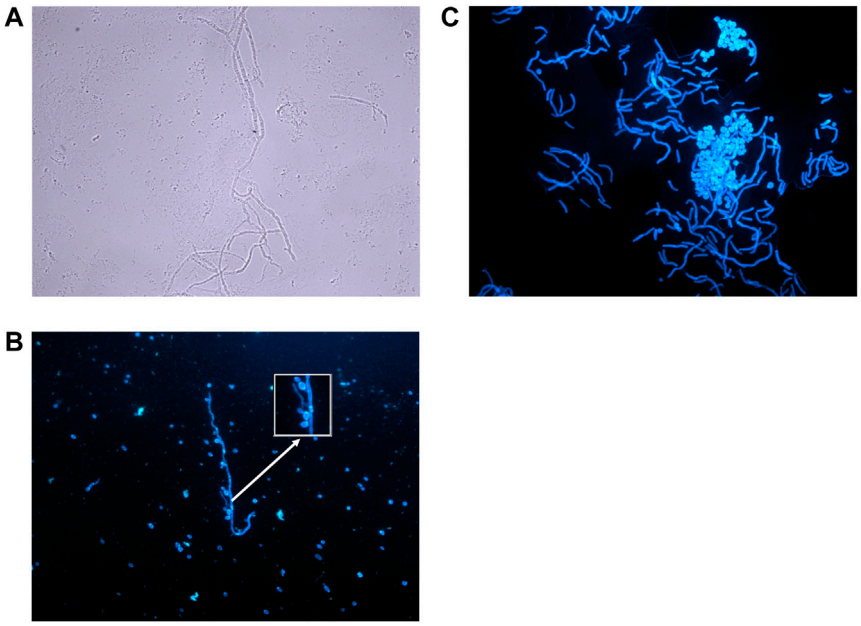


**FIGURE 2 |** Microscopic appearance of fungal skin and nail infections. **(A)** Mould hyphae—Colourless (hyaline), septate, even sided, branching hyphae. (Photographed using a ×40 lens). **(B)** *Candida* species—Small budding yeasts (3–5 μm) that bud from any point on the cell. In this diagram budding yeasts are also attached to a hypha/pseudohypha (stained with calcofluor and photographed using ×40 lens). **(C)** Pityriasis versicolor—Thin walled, short hyphal filaments that fragment. Thick walled, round to oval budding yeasts with prominent bud scars (stained with calcofluor, photographed using ×40 lens).

structures in the tissue by microscopic examination for the fungus to be considered for significance (7).

The fungi that cause the hair infections known as black and white piedra are more common in hot humid environments. Risk factors for infection in these environments are colonisation of the hair, particularly if it is kept tied or braided (18). The infection presents as a nodule on the hair shaft and the nodule colour and hardness form part of the clinical description of the condition. Microscopic examination confirms the type of infection while culture enables the pathogen to be identified (**Figure 1**).

## IMPORTANCE OF HISTOLOGY FOR THE DIAGNOSIS OF SUPERFICIAL AND CUTANEOUS FUNGAL INFECTION

A failure to diagnose a superficial mycosis can be due to the quality and amount of material provided for testing (4). Many factors can alter the clinical appearance of a fungal infection making diagnosis difficult. For example, a history of treatment with steroids can alter the clinical appearance by reducing scaling and itch, a condition known as tinea incognito (10). Similarly partial treatment with an antifungal can prevent good samples being taken for microbiology assessment by reducing the scaling of the lesion. Patients with underlying diseases can present with an atypical appearance or an atypical distribution of lesions (4). In these circumstances biopsy samples taken for histopathology analysis should provide a diagnosis, although the causative species cannot be determined by this process.

For histological examination skin, hair and nail samples are routinely embedded, sectioned, and stained with Hematoxylin and Eosin (H&E) (19). H&E provides a background stain and highlights the presence of nucleic acids within cells by staining nucleic acids blue and the cytoplasm pink (20). Fungal structures that lack pigment (hyaline) can be difficult to detect as the stain does not bind to the cell wall, therefore, special stains can be used to highlight the presence of fungal cells: Periodic Acid-Schiff (PAS), Grocott and Gomori Methenamine Silver (GMS), and Fontana-Masson stain (**Table 3**). These stains can highlight the presence of non-fungal materials as well, so a histopathology diagnosis of a fungal infection requires careful inspection of the morphology, surrounding tissue reactions, and interpretation of clinical information (20).

The appearance of mould and yeast structures in tissue are similar when observed in wet preparations and in histology sections, however, there are some conditions where histological examination is superior. For example, skin folliculitis caused by *Malassezia* yeasts is diagnosed using clinical criteria and histological examination of a biopsy (12). The condition is caused by an accumulation of these yeasts within follicles which are surrounded by inflammation. A potassium hydroxide mount would not demonstrate the location of the yeasts as the process is destructive and the skin structures would be destroyed, and only histopathology can demonstrate the presence of inflammation around the follicles.

**TABLE 3 |** Histology stains used in the diagnosis of fungal infections (20).

| Stain | Appearance of fungus in tissue | Reaction in tissue |
|---|---|---|
| H & E | Cytoplasm pink<br>Nucleus blue<br>Cell wall colourless | Stains nucleic acids blue/purple. Stains proteins in cytoplasm, membranes, etc., pink. Useful to highlight inflammatory processes in tissue |
| PAS | Cell wall pink to red to purple | Stains carbohydrates, polysaccharides, glycogen, mucoproteins, and mucins in tissue |
| GMS | Cell wall dark brown to black | Primarily used to bind to carbohydrate in cell walls of fungi. Tissue usually stained green |
| Fontana Masson | Stains melanin deposits brown to black | Stains melanin deposits in tissue |

**TABLE 4 |** Subcutaneous fungal infections (4, 10, 15, 21, 22).

| Disease | Common causes | Clinical presentation | Histology |
|---|---|---|---|
| Mycetoma | *Madurella mycetomatis Trematosphaeria grisea*, *Falciformispora senegalensis, Phialophora, Scedosporium*, *Fusarium species*, *Aspergillus nidulans, Sarocladium*, (*Acremonium*) | Chronic infection of skin, subcutaneous tissue and bone. Nodule forms an abscess and drains to the surface *via* sinus, discharge contains grains. Deformity and disability considerable. Important to distinguish bacteria from fungal cause | Presence of a grain surrounded by an inflammatory reaction. Eumycetoma grains contain narrow hyphae—pigmented (dark grain) or hyaline (pale grain) |
| Sporotrichosis | *Sporothrix schenckii, S. brasiliensis*, *S. mexicana*, *S. globose, S. luriei* | Cutaneous infection: initial nodule forms a granuloma or ulcer with satellite lesions at the edges, secondary nodules appear along course of draining lymphatics, commonly limbs | Oval to elongated (cigar shaped) yeasts with budding from a narrow base, asteroid bodies |
| Chromoblastomycosis | *Fonsecaea pedrosoi*, *F. compacta*, *Cladophialophora carrionii*, *Phialophora verrucosa* | Chronic, slow growing warty nodule to plaque, autoinoculation results in satellite lesions. Elephantitis | Epidermal hyperplasia, granulomatous response, transepidermal elimination of debris, presence of round thick walled fungal cells (muriform bodies) |
| Phaeohyphomycosis | *Exophiala jeanselmei, E. dermatitidis, E. spinifera, Phaeoacremonium parasiticum, Phialophora verrucosa, Alternaria alternata, Bipolaris* species, *Scedosporium* species, *Lomentospora prolificans, Curvularia lunata* | Subcutaneous cysts, abscess, verrucous plaque. Immune suppression and transplant are risk factors<br>Some species can cause systemic infections | Pseudoepitheliomatous hyperplasia, inflammatory infiltrate, presence of septate pigmented hyphae or hyphal fragments |
| Hyalohyphomycosis | *Aspergillus* species<br>*Fusarium* species<br>*Scedosporium* species<br>*Acremonium* species<br>*Paecilomyces/Purpureocilllium* species | Varied: verrucous, erythematous macules, papules and indurated nodules, ulceration<br>Some species can cause systemic infections | Inflammation, granulomatous reactions, narrow, regularly septate hyphae |
| Mucormycosis | *Rhizopus* species<br>*Lichtheimia corymbifera*<br>*Rhizomucor* species<br>*Mucor* species | Necrosis, ulceration, swelling, inflammation, rapid progression | Wide, thin walled, pauciseptate hyphae, Branching may be at right angles. Hyphae may appear distorted. Little inflammation surrounding hyphae |
| Entomophthoromycosis | *Basidiobolus ranarum Conidiobolus coronatus* | Slowly progressing subcutaneous swelling:<br>*Conidiobolus* mainly affects the face and nasal passages<br>*Basidiobolus* mainly affects limbs | Wide, thin walled, pauciseptate hyphae, Branching may be at right angles. Hyphae may appear distorted. Surrounded by granulomatous inflammatory reaction |
| Lobomycosis | *Lacazia loboi* | Papule slowly progresses to form nodules or plaques with keloid like appearance. Older lesions can be crusted | Oval yeast-like cells connected in short chains by a tubular structure |

## SUBCUTANEOUS INFECTIONS

Subcutaneous fungal infections result from traumatic inoculation deep into the skin and are mostly due to environmental moulds. Identification of the pathogen requires culture, but histology can provide important diagnostic information, especially when routine microscopy and culture are negative (**Table 4**; **Figure 3**) (4, 19).

Mycetoma can be caused by filamentous bacteria (actinomycetoma) or by fungi (eumycetoma) (4, 23). Pieces of the infective organisms become encased in an inflammatory matrix that forms grains and these can be expressed from subcutaneous abscesses *via* a sinus tract, or can be seen in the tissue from a deep subcutaneous biopsy. Analysis of the grains distinguishes the type of mycetoma and enables appropriate

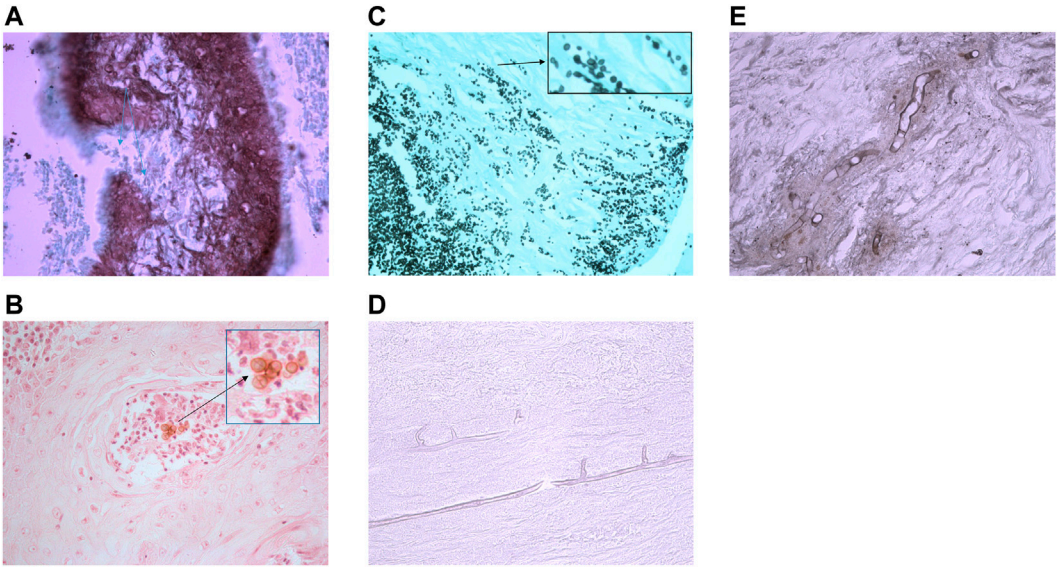


**FIGURE 3 |** Histology sections of subcutaneous fungal infections demonstrating characteristic morphology for each disease type. **(A)** Eumycetoma grain in tissue stained with GMS. Interior of grain contains brown/stained hyphae that have been sectioned longitudinally and horizontally resulting in various shaped fungal structures (photographed using a ×40 lens). **(B)** Pigmented muriform bodies in a biopsy from a chromoblastomycosis lesion stained with H&E. (Photographed using a ×40 lens). **(C)** Sporotrichosis stained with GMS. In tissue *Sporothrix* produces yeast-like budding with characteristic elongated buds. (Photographed using a ×40 lens). **(D)** Mucormycosis of tissue stained with PAS shows wide, thin-walled hyphae with few septa. (Photographed using a ×40 lens). **(E)** *Conidiobolus* infection stained with GMS shows wide, thin-walled hyphae with few septa, but these are surrounded by inflammatory material (photographed using a ×40 lens).

empirical antifungal or antibacterial therapy to be commenced. The simple distinction between actinomycetoma from eumycetoma is important as culture of the grains may fail or yield fungi that lack typical features making them difficult to identify unless there is access to a centre that performs molecular diagnostic testing (24, 25).

*Sporothrix* species cause a subcutaneous infection following traumatic inoculation. Subcutaneous infection in immune competent patients can have a low fungal load, making detection of the characteristic elongated budding yeasts difficult by direct microscopy (26). Histology is more sensitive as it detects the areas of inflammation where the fungus might reside, and with the use of serial sections and special stains can detect the presence of scanty yeast-like cells and asteroid bodies which are present in many sporotrichosis infections (20).

Chromoblastomycosis is a slowly progressing, chronic, pigmented fungal infection. This is characterised by the presence of pigmented, multiseptate, round, thick-walled cells sometimes referred to as muriform bodies (4, 19, 27). These cells are not detected in other subcutaneous pigmented fungal infections which are grouped under the heading of phaeohyphomycosis, and are more hyphal (19).

Hyalohyphomycosis is the subcutaneous (or systemic) infection with a non-pigmented fungus. Many species can cause hyalohyphomycosis but the species cannot be determined by histology. All species would demonstrate narrow, regularly septate branching hyphae (20).

Mucormycosis is a subcutaneous infection that follows trauma to the skin from penetrating injuries, scratches, or by contamination of burns or injuries, and can cause systemic infection following inhalation of spores mainly in immune compromised patients (28). The main causes of this infection belong to a group known as the mucoraceous moulds, and these fungi grow rapidly in the tissue and have a predilection for blood vessel invasion. These moulds exist worldwide in the environment and differ from other types of moulds as they have broader hyphae and far fewer septa within the hyphae. As a result they often have rather distorted appearances when sectioned and appear creased or with an unusual shape.

Although the Entomophthorales moulds may appear similar in appearance in the tissue to the mucoraceous moulds, they cause clinically very different infections (subcutaneous swellings, not angioinvasive) and histologically the broad aseptate hyphae are surrounded by an inflammatory reaction (28).

Lobomycosis is a cutaneous to subcutaneous infection caused by the *Lacazia loboi* and this environmental fungus is found in the tropical climates of Central and South America, and most often affects people in rural communities. The fungus does not grow on culture so diagnosis is based only on clinical suspicion and histology (29).

## SYSTEMIC FUNGAL INFECTIONS THAT CAN DISSEMINATE TO THE SKIN

Systemic opportunistic fungal infections occur in significantly debilitated hosts including those with immune suppression, transplant recipients, surgery, hospitalization, broad spectrum

**TABLE 5 |** Types of systemic infection and their features on histology sections (19, 20, 21, 22).

| Disease | Causative organism | Clinical features | Histological features |
|---|---|---|---|
| Candidiasis | *Candida albicans, Candida* species | Invasive and disseminated infection occurs in seriously ill and immune compromised patients | Budding yeast cells (3–5 μm), hyphae and pseudohyphae (constriction occurs where there are septa). *C. glabrata* does not produce hyphae |
| Cryptococcosis | *Cryptococcus neoformans, Cr. gatii* | Pulmonary infection, dissemination in the immune compromised, meningitis in AIDS. | Small yeasts (4–10 μm) budding from a narrow base, mucopolysaccharide capsule stains well with mucicarmine. Fontana Masson stain useful for acapsular variants |
| Histoplasmosis | *Histoplasma capsulatum, H. capsulatum var. duboisii* | Pulmonary disease, dissemination in immune compromised. *H. duboisii* disseminates to skin and bone, Africa | Small (2–4 μm) round to oval yeasts, budding from a narrow base, may be clustered intracellularly. *H. duboisii* are larger (8–15 μm) budding yeasts |
| Blastomycosis | *Blastomyces dermatiditis, B. gilchristii* | Pulmonary disease. Dissemination possible | Large thick walled yeasts (8–15 μm) that bud from a broad base |
| Paracoccidioidomycosis | *Paracoccidioides brasiliensis, P. lutzii* | Pulmonary disease. Dissemination especially mucocutaneous | Large yeast cells (15–30 μm) with multiple budding—ship's wheel appearance |
| Coccidioidomycosis | *Coccidioides immitis, C. posadasii* | Acute or chronic pulmonary disease, lung cavities form, dissemination possible in immune competent and immune compromised | Thick walled spherules (10–100 μm) containing endospores (2–5 μm) in different stages of development, granulomatous reaction |
| Talaromycosis | *Talaromyces marneffei* | Pulmonary infection, mainly immune compromised. Dissemination | Small oval or curved yeast like cells that divide by transverse fission forming a thick septum. May be clustered inside macrophages |
| Emergomycosis (Emmonsiosis) | *Emergomyces (Emmonsia) p*asteurianus, *Es. africanus, Es. canadensis, Es. orientalis, Es. europaeus* | Pulmonary infection with dissemination, immune compromised hosts | Yeast-like cells (2–7 μm) |

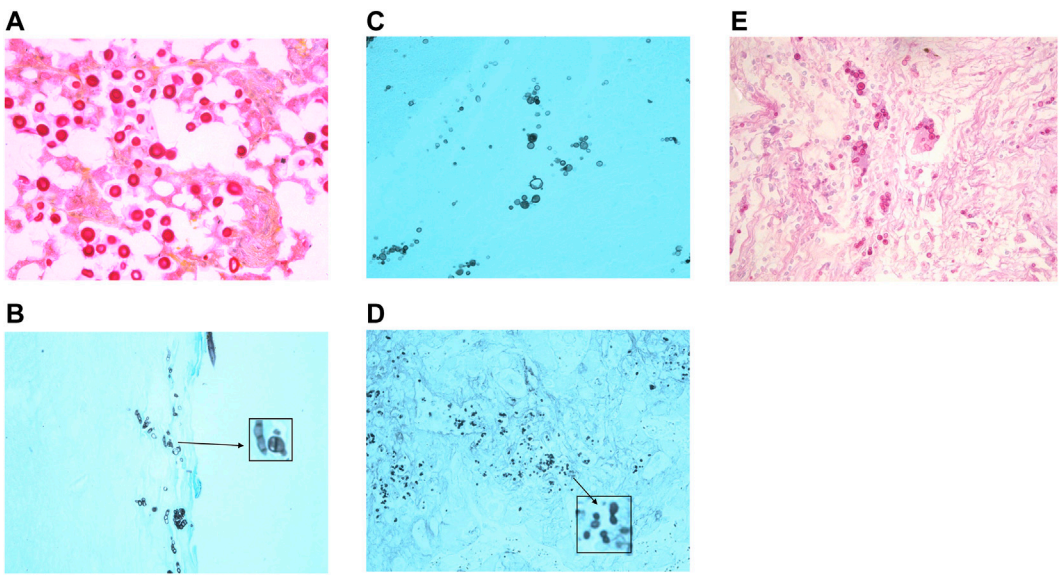


**FIGURE 4 |** Histology images of some causes of systemic fungal infection. **(A)** *Cryptococcus* yeasts in tissue stained with mucicarmine to demonstrate the presence of the red stained mucopolysaccharide capsule. (Photographed using a ×40 lens). **(B)** Talaromycosis histology section stained with GMS shows yeast cells with a central division, as these cells divide by fission and not by budding. (Photographed using a ×40 lens). **(C)** Paracoccidioidomycosis (stained with GMS) is characterised by the presence of multipolar budding yeast cells. (Photographed using a ×40 lens). **(D)** Histoplasmosis stained with GMS to show the small budding yeasts. (Photographed using a ×40 lens). **(E)** Blastomycosis stained with PAS shows large thick walled yeasts that bud from a broad base. (Photographed using a ×40 lens).

antibiotic treatment, or in patients with other significant underlying disease (10). It is possible for systemic fungal infections to disseminate *via* the bloodstream and produce lesions in the skin (4). Histology of a biopsy can detect the presence of a fungal cause and provide information on the type of underlying infection (**Table 5**; **Figure 4**).

**TABLE 6 |** Locations of endemic dimorphic fungal infections (4, 21, 33, 34, 35).

| Disease | Organism | Location |
|---|---|---|
| Histoplasmosis | *H. capsulatum* | States around the Mississippi and Ohio river valleys (eastern to central USA), smaller foci in Central (Mexico) + South America (e.g., Venezuala to Argentina), Africa, Asia (Thailand) and India, not in northern Europe |
| | *H. duboisii* | Found in Africa and between Tropics of Cancer and Capricorn, and also on Madagasgar |
| Coccidioidomycosis | *C. immitis* | California, USA |
| | *C. posadasii* | Texas, Arizona, Mexico, central and south America |
| Blastomycosis | *B. dermatitidis* | Areas prone to flood, USA, Canada, small foci in North and Central Africa and in India |
| Paracoccidioidomycosis | *P. brasiliensis, P. lutzii* | Central and South America, not Chile. Moist subtropical forested areas with high rainfall |
| Talaromycosis | *T. marneffei* | Southeast Asia, Thailand, Hong Kong, China |
| Emergomyces | *Es. p*asteurianus, | Europe (Italy, Spain, France, the Netherlands), Asia (China and India), Uganda, and South Africa |
| | *Es. africanus* | South Africa and Lesotho |
| | *Es. canadensis* | Canada (Saskatchewan), USA (Colorado and New Mexico) |
| | *Es. orientalis* | China |
| | *Es. europaeus* | Germany |

*Candida* species are commensal to the human gastrointestinal tract, and are found in low numbers on the skin, mouth and vaginal tract. *C. albicans* is the commonest cause of human infection, although there has been a rise in systemic infections caused by non- *C. albicans* species (1). Superficial infection occurs when there is a disturbance in the competing bacterial flora allowing the yeasts to proliferate, such as the use of broad spectrum antibiotics or occlusion, or due to underlying disease, for example, diabetes or HIV. Systemic infection occurs in patients where the yeasts escape from their normal location by the colonisation of indwelling lines or other implants, or due to the effects of broad spectrum antibiotics, immune suppression, neutropenia, cancer, or surgery (14, 30). *Candida* infection in tissue can present with a variety of morphologies: budding yeasts, hyphae, and pseudohyphae (6, 8, 19) (**Table 5**).

*Aspergillus* and *Fusarium* species are common environmental moulds that can cause systemic infection in patients with neutropenia, haematological malignancies, and in immune suppressed patients usually by inhalation of airborne spores. These moulds can disseminate *via* the bloodstream and can cause skin lesions (20). It is not possible to distinguish the species by microscopic appearance in tissue (19, 31) (**Table 4**). As there can be important differences in the treatment of infections caused by different species histology reports generally describe the type of fungal structures seen, for example, hyalohyphomycosis, rather than suggesting a causative organism (19, 31).

*Cryptococcus neoformans* and *Cr. gatii* are environmental yeasts that can cause pulmonary infection by inhalation of spores or yeasts, and in immune suppressed patients dissemination can occur to skin and other tissue (32). Cryptococcal meningitis is a significant risk in AIDS patients when their CD4 count falls below 100 cells per µl (32). A major characteristic of these yeasts is the presence of a mucopolysaccharide capsule which on microscopy gives the appearance of a clear halo surrounding the small budding yeasts in tissue (6). The capsule can be highlighted in microbiology wet preparations using India ink, and in histology sections using the mucicarmine stain. Acapsular variants can be confused with *Histoplasma* or *Candida* yeasts, but use of mucicarmine to detect remnants of capsule, or staining with Fontana Masson to detect melanin in the cryptococcal cell walls, will assist in differentiation of these organisms in tissue (20, 32).

The diseases histoplasmosis, paracoccidiodomycosis, blastomycosis, coccidioidomycosis, and talaromycosis are caused by highly infectious endemic dimorphic moulds. These fungi are limited in location geographically and environmentally and exist in the environment as a mould, however, when they infect the human host they demonstrate a different more yeast-like appearance (33). The areas where infections are endemic are listed in **Table 6**, and people who have a travel history to these regions may become infected. All of these infections are acquired by inhalation of spores that leads to a pulmonary infection. Dissemination to the skin is possible in some patients, usually those that have not received treatment or have immune suppression (4, 33). Histology sections of these fungi may demonstrate a distinctive morphology, but culture of the pathogen and serology is always recommended to confirm the diagnosis. Detailed descriptions of the histological appearance of these infections and how to distinguish them from unusual presentations of other infections can be found in the review by Guarner and Brandt (20).

Emergomyces (previously Emmonsia) infections usually start with a pulmonary infection and many disseminate to the skin (33). These fungi infect immunocompromised patients such as solid organ transplant recipients, HIV, and those receiving corticosteroid treatment and have been reported from South Africa, Canada, Germany, Israel, Italy, China (33–35). Dissemination to the skin occurs in 92%–96% of the patients examined (34, 35). Skin lesions were often clinically misdiagnosed as Karposi sarcoma, varicella infection or drug reactions, but the visualisation of the yeast-like cells on histology sections confirmed the presence of a fungal infection and that a systemic source should be investigated. Culture is required to confirm the cause of infection and distinguish it from other dimorphic fungal infections such as histoplasmosis which also presents as small budding yeasts in the skin (34, 35).

## ADVANCED DIAGNOSTIC HISTOLOGICAL TECHNIQUES

Immunohistochemistry (IHC) is used to detect protein antigens in histology sections and is widely employed in the diagnosis of melanoma, other skin cancers, a variety of other skin diseases, and to detect the presence of some infections (36). To detect systemic fungal infection IHC stains are commercially available to detect *Aspergillus* species, *Candida* species and Mucormycete moulds, but the potential of cross-reaction with other fungi means this cannot be used to identify a specific organism (20, 37).

*In situ* hybridisation (ISH), uses a species-specific probe to detect fungal nucleic acids in tissue sections. This should be highly specific, but there are no commercially validated protocols and there have been reports of cross-reactions (37). The advantage of both IHC and ISH is that they maintain the structure of the tissue and the localisation of the fungal antigen or nucleic acid for histopathological examination. Both tests have greatest sensitivity when applied to samples where GMS or PAS staining has already demonstrated the presence of fungal infection and a panel of tests can be performed to indicate the likely genus of the infecting agent (20, 37).

Amplification of fungal DNA directly from a sample potentially provides a sensitive and specific method to diagnose fungal infection. Amplification from non-embedded fresh tissue is more reliable than from FFPE tissue due to the difficulties with extraction, DNA concentration and integrity, and the presence of inhibitors (20). The choice of target sequence for amplification requires careful consideration to ensure it can distinguish between many different species, and that there are sufficient sequences in public validated databases that are available for comparison (37). The internal transcribed spacer (ITS) regions have been used for fungal DNA barcoding and the ISHAM database has sequences for 421 fungal species, however, there are some fungi that cannot be adequately identified using this target alone and so additional genetic markers would need to be used (38). Amplification directly from FFPE tissue would also have to consider the possible presence of environmental contamination of histology laboratory materials, for example, the wax used for embedding is not stored or used under sterile conditions (37). Despite these difficulties the importance of histology in the diagnosis of fungal infections is recognised. Recent guidelines for the diagnosis of invasive fungal infections permit the use of PCR and sequencing to identify the fungus from tissue where fungal structures have been seen on histology (37). By following the ten criteria explained in the revised guidelines samples with histopathology evidence of fungal infection and a fungal identification using PCR and sequencing would fulfil the diagnosis of a proven invasive infection, and would be especially important in cases where culture fails to grow a pathogen. The guidelines also recommend this molecular approach where an endemic dimorphic fungal infection has been detected by histopathology and the microbiology laboratory has little experience with these pathogens.

## CONCLUSION

Histology provides a gold standard for the diagnosis of fungal infections from biopsies. Special stains such as PAS and GMS greatly enhance the detection of fungal elements making this a highly sensitive technique. Careful morphological examination of the tissue, in combination with a clinical history can indicate the type of fungal infection, but it cannot identify the causative species. Identification of the fungal species can indicate the most appropriate choice of treatment for the patient. Currently fungal identification still relies on culture, but molecular diagnostics are developing for the detection of subcutaneous and systemic pathogens directly from tissue samples.

## AUTHOR CONTRIBUTIONS

The author confirms being the sole contributor of this work and has approved it for publication.

## CONFLICT OF INTEREST

The author declares that the research was conducted in the absence of any commercial or financial relationships that could be construed as a potential conflict of interest.

## REFERENCES


1. Bongomin F, Gago S, Oladele RO, Denning DW. Global and Multi-National Prevalence of Fungal Diseases-Estimate Precision. *J Fungi* (2017) 3:57. doi:10.3390/jof3040057
2. Urban K, Chu S, Scheufele C, Giesey RL, Mehrmal S, Uppal P, et al. The Global, Regional, and National burden of Fungal Skin Diseases in 195 Countries and Territories: A Cross-Sectional Analysis from the Global Burden of Disease Study 2017. *J Am Acad Dermatol Int* (2021) 2:22–7. doi:10.1016/j.jdin.2020.10.003
3. Ameen M. Epidemiology of Superficial Fungal Infections. *Clin Dermatol* (2010) 28:197–201. doi:10.1016/j.clindermatol.2009.12.005
4. Hay RJ. Fungal Infections of the Skin and Subcutaneous Tissue. In: CC Kibbler, R Barton, NAR Gow, S Howell, DM MacCallum, RJ Manuel, editors. *Oxford Textbook of Medical Mycology*. Oxford, UK: Oxford University Press (2018). p. 145–53. Chapter 23.
5. Mendonça A, Santos H, Franco-Duarte R, Sampaio P. Fungal Infections Diagnosis - Past, Present and Future. *Res Microbiol* (2022) 173(3):103915. doi:10.1016/j.resmic.2021.103915
6. Shankland GS. Microscopy and Culture of Fungal Disease. In: CC Kibbler, R Barton, NAR Gow, S Howell, DM MacCallum, RJ Manuel, editors. *Oxford Textbook of Medical Mycology*. Oxford, UK: Oxford University Press (2018). p. 283–8. Chapter 39.
7. Ellis DH, Watson AB, Marley JE, Williams TG. Non-dermatophytes in Onychomycosis of the Toenails. *Br J Dermatol* (1997) 136:490–3. doi:10.1046/j.1365-2133.1997.d01-1222.x
8. UK Standards for Microbiology Investigations. Investigation of Dermatological Specimens for Superficial Mycoses. Issued by the

Standards Unit, Microbiology Services. *PHE Bacteriol* (2016) B 39(3.1):1–26.
9. Campbell CK, Johnson EM, Warnock DW. *Identification of Pathogenic Fungi*. 2nd ed. New Jersey, US: Wiley-Blackwell (2013).
10. Midgley G, Clayton YM, Hay RJ. *Medical Mycology*. London: Moseby-Wolfe (1997).
11. Degreef H. Clinical Forms of Dermatophytosis (Ringworm Infection). *Mycopathologia* (2008) 166:257–65. doi:10.1007/s11046-008-9101-8
12. Saunte DML, Gaitanis G, Hay RJ. *Malassezia*-Associated Skin Diseases, the Use of Diagnostics and Treatment. *Front Cel Infect Microbiol* (2020) 10:112. doi:10.3389/fcimb.2020.00112
13. Gaitanis G, Magiatis P, Hantschke M, Bassukas ID, Velegraki A. The *Malassezia* Genus in Skin and Systemic Diseases. *Clin Microbiol Rev* (2012) 25(1):106–41. doi:10.1128/CMR.00021-11
14. Talapko J, Juzbaši´c M, Matijevi´c T, Pustijanac E, Beki´c S, Kotris I, et al. *Candida Albicans*—The Virulence Factors and Clinical Manifestations of Infection. *J Fungi* (2021) 7(2):79. doi:10.3390/jof7020079
15. Montalván Miró E, Sánchez NP. Cutaneous Manifestations of Infectious Diseases. In: NP Sánchez, editor. *Atlas of Dermatology in Internal Medicine*. Berlin, Germany: Springer Science + Business Media LLC (2012). p. 77–119. doi:10.1007/978-1-4614-0688-4_7
16. Theelen B, Cafarchia C, Gaitanis G, Bassukas ID, Boekhout T, Dawson TL, Jr. *Malassezia* Ecology, Pathophysiology, and Treatment. *Med Mycol* (2018) 56: S10–S25. doi:10.1093/mmy/myx134
17. Weitzman I, Summerbell RC. The Dermatophytes. *Clin Microbiol Rev* (1995) 8(2):240–59. doi:10.1128/CMR.8.2.240-259.1995
18. Bonifaz A, Badali H, de Hoog HGS, CruzAraizaCruz MJMA, Fierro L, Ponce RM. Tinea Nigra by *Hortaea werneckii*, a Report of 22 Cases from Mexico. *Stud Mycol* (2008) 61:77–82. doi:10.3114/sim.2008.61.07
19. Lucas SB. Histopathology of Fungal Disease. In: CC Kibbler, R Barton, NAR Gow, S Howell, DM MacCallum, RJ Manuel, editors. *Oxford Textbook of Medical Mycology*. Oxford, UK: Oxford University Press (2018). p. 283–8. Chapter 39.
20. Guarner J, Brandt ME. Histopathologic Diagnosis of Fungal Infections in the 21st Century. *Clin Microbiol Rev* (2011) 24(2):247–80. doi:10.1128/CMR.00053-10
21. The University of Adelaide. *Mycology Online*. Available at: https://www.adelaide.edu.au/mycology/ (Accessed April 14, 2023).
22. DermNet. *DermNet*. Available at: https://dermnetnz.org/ (Accessed April 14, 2023).
23. Ameen M, Arenas R. Developments in the Management of Mycetoma's. *Clin Exp Dermatol* (2009) 34(1):1–7. doi:10.1111/j.1365-2230.2008.03028.x
24. Karrakchou B, Boubnane I, Senouci K, Hassam B. *Madurella mycetomatis* Infection of the Foot: a Case Report of a Neglected Tropical Disease in a Non-endemic Region. *BMC Dermatol* (2020) 20:1. doi:10.1186/s12895-019-0097-1
25. Ahmed SA, González GM, TiradoSánchez A, Moreno-López LM, de Hoog S, Bonifaz A. *Nigrograna mackinnonii*, Not *Trematosphaeria grisea* (syn., *Madurella Grisea*), Is the Main Agent of Black Grain Eumycetoma in Latin America. *J Clin Microbiol* (2018) 56:e01723–17. doi:10.1128/JCM.01723-17
26. Barros MB, de Almeida Paes R, Schubach AO. *Sporothrix Schenckii* and Sporotrichosis. *Clin Microbiol Rev* (2011) 24(4):633–54. doi:10.1128/CMR.00007-11
27. Ameen A. Chromoblastomycosis: Clinical Presentation and Management. *Clin Exp Dermatol* (2009) 34:849–54. doi:10.1111/j.1365-2230.2009.03415.x
28. Prabhu RM, Patel R. Mucormycosis and Entomophthoramycosis: a Review of the Clinical Manifestations, Diagnosis and Treatment. *Clin Microbiol Infect* (2004) 10:31–47. doi:10.1111/j.1470-9465.2004.00843.x
29. Arajo MG, Cirilo NS, Barbosa dos Santos SNM, Aguilar CR, Guedes ACM. Lobomycosis: a Therapeutic challenge. *Bras Dermatol* (2018) 93(2):279–81. doi:10.1590/abd1806-4841.20187044
30. Lopes JP, Lionakis MS. Pathogenesis and Virulence of *Candida albicans*. *Virulence* (2022) 13:89–121. doi:10.1080/21505594.2021.2019950
31. Sabino R, Wiederhold N. Diagnosis from Tissue: Histology and Identification. *J Fungi* (2022) 8:505. doi:10.3390/jof8050505
32. Maziarz EK, Perfect JR. Cryptococcosis. *Infect Dis Clin North Am* (2016) 30(1): 179–206. doi:10.1016/j.idc.2015.10.006
33. Restrepo A, Gonzalez A, Gomez BL. Endemic Dimorphic Fungi. In: CC Kibbler, R Barton, NAR Gow, S Howell, DM MacCallum, RJ Manuel, editors. *Oxford Textbook of Medical Mycology*. Oxford, UK: Oxford University Press (2018). p. 98–106. Chapter 16.
34. Schwartz IS, Govender NP, Corcoran C, Dlamini S, Prozesky H, Burton R, et al. Clinical Characteristics, Diagnosis, Management, and Outcomes of Disseminated Emmonsiosis: A Retrospective Case Series. *Clin Infect Dis* (2015) 61(6):1004–12. doi:10.1093/cid/civ439
35. Schwartz IS, Kenyon C, Feng P, Govender NP, Dukik K, Sigler L, et al. 50 Years of *Emmonsia* Disease in Humans: The Dramatic Emergence of a Cluster of Novel Fungal Pathogens. *PLoS Pathog* (2015) 11(11):e1005198. doi:10.1371/journal.ppat.1005198
36. Palit A, Inamadar AC. Immunohistochemistry: Relevance in Dermatology. *Ind J Dermatol* (2011) 56(6):629–40. doi:10.4103/0019-5154.91818
37. Lockhart SR, Bialek R, Kibbler CC, Cuenca-Estrella M, Jensen HE, Kontoyiannis DP. Molecular Techniques for Genus and Species Determination of Fungi from Fresh and Paraffin Embedded Formalin-Fixed Tissue in the Revised EORTC/MSGERC Definitions of Invasive Fungal Infection. *Clin Infect Dis* (2021) 72(S2):S109–13. doi:10.1093/cid/ciaa1836
38. Irinyi L, Serena C, Garcia-Hermoso D, Arabatzis M, Desnos-Ollivier M, Vu D, et al. International Society of Human and Animal Mycology (ISHAM)-ITS Reference DNA Barcoding Database–The Quality Controlled Standard Tool for Routine Identification of Human and Animal Pathogenic Fungi. *Med Mycol* (2015) 53:313–37. doi:10.1093/mmy/myv008

BJBS

The British Journal of Biomedical Science is the official journal of the Institute of Biomedical Science

Since January 2022, the journal began publishing under a Gold Open Access model. All articles will be immediately, permanently, and freely available to read, download, and access for people everywhere. Authors will retain copyright on all new articles published and the journal will be compliant with Plan S.

---

## Discover more of our Special Issues

See more →

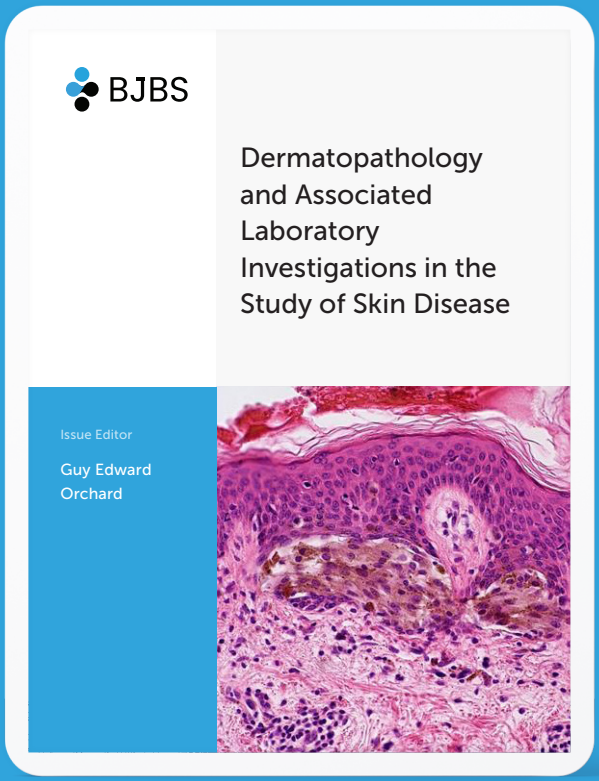


fro.ntiers.in/dermatopathology
frontierspartnerships.org

Contact

bjbs.office@frontierspartnerships.org